



Defence Research and  
Development Canada

Recherche et développement  
pour la défense Canada



# Joint Biological Standoff Detection System increment II: Field demonstration

*SINBAHD performances*

*Sylvie Buteau, Jean-Robert Simard, Pierre Lahaie, Gilles Roy, Pierre Mathieu  
DRDC Valcartier*

*John McFee, Jim Ho.  
DRDC Suffield*

**Defence R&D Canada – Valcartier**

Technical Memorandum

DRDC Valcartier TM 2006-140

December 2007

Canada



# **Joint Biological Standoff Detection System increment II: Field demonstration**

*SINBAHD performances*

Sylvie Buteau, Jean-Robert Simard, Pierre Lahaie, Gilles Roy, Pierre Mathieu  
DRDC Valcartier

John McFee, Jim Ho.  
DRDC Suffield

**Defence Research & Development Canada Valcartier**

Technical Memorandum

DRDC Valcartier TM 2006-140

December 2007

Author

---

Sylvie Buteau

Approved by

---

J.-M. Garneau  
Section Head

Approved for release by

---

C. Carrier  
Chief Scientist

© Her Majesty the Queen as represented by the Minister of National Defence, 2007

© Sa majesté la reine, représentée par le ministre de la Défense nationale, 2007

## Abstract

---

By the end of the 90s, Defence Research and Development Canada (DRDC) initiated the investigation of a novel LIDAR concept which open the possibility of collecting all at once the detailed spectral information contained in the return signals. This 3-year project called SINBAHD (Stand-off INtegrated Bioaerosol Active Hyperspectral Detection) aimed at evaluating the capability of using UV LIF with intensified range-gated spectrometry to detect and characterize bioaerosol from stand-off position. Essentially, the LIDAR system monitors atmospheric volumes in which specific spectrally wide fluorescence signal can be generated from inelastic interactions with complex molecules forming the building blocks of most bioaerosols. This LIF signal is collected by the combination of a dispersive element and a range-gated ICCD that limits the spectral information within the selected volume. This technique has showed an important potential of detecting and discriminating different bioaerosol agent simulants in real time. Through the Standoff Biodetection Working Group (SBWG) under the CANUKUS CBR MOU, SINBAHD was invited to participate in the Joint Biological Standoff Detection System (JBSDS) increment II field demonstration trial. The purpose of this international trial, which took place at Dugway Proving Ground (DPG), Utah in June 2005, was to determine the benchmark sensitivity of different technologies to various biological simulants and interferents. SINBAHD demonstrated its high level of performance and the results made it possible to obtain new spectral signatures.

## Résumé

---

Vers la fin des années 1990, Recherche et développement pour la défense Canada (RDDC) a entrepris l'étude d'un nouveau concept LIDAR qui permet d'obtenir l'ensemble de l'information spectrale détaillée contenue dans un signal de retour. Ce projet de trois ans appelé SINBAHD (Stand-off INtegrated Bioaerosol Active Hyperspectral Detection) avait pour but d'évaluer les capacités d'une technologie utilisant la détection spectrométrique de la fluorescence induite par laser (FIL) et l'intensification à crénelage en distance pour détecter et caractériser en retrait les bioaérosols. Essentiellement, le système LIDAR permet de surveiller des volumes atmosphériques ciblés dans lesquels des signaux spécifiques de fluorescence, distribués spectralement, peuvent être générés par des interactions inélastiques avec des molécules complexes présentes dans les particules des bioaerosols. Ce signal FIL est recueilli par la combinaison d'un élément dispersif et d'une caméra intensifiée (ICC) à crénelage en distance qui limite l'information spectrale au volume atmosphérique d'intérêt. Cette technique a démontré son important potentiel pour la détection et la discrimination en temps réel de différents simulants d'agents biologiques en aérosols. SINBAHD a été invité à participer au 'Joint Biological Standoff Detection System (JBSDS) increment II field demonstration' par le groupe de travail international sur la détection biologique à distance (SBWG) dans le cadre du CANUKUS CBR MOU. Ces essais, qui ont eu lieu au Dugway Proving Ground (DPG) en Utah, en juin 2005, avaient pour but de déterminer les sensibilités de différentes technologies à divers simulants/interférents biologiques. SINBAHD a alors démontré son niveau élevé de performance et les résultats obtenus ont permis d'obtenir de nouvelles signatures spectrales.

This page intentionally left blank.

## Executive summary

---

The biological threat has emerged as one of today's primary security challenges due to the increased accessibility to biological warfare technology and the limited efficiency of detection and protection measures against such a menace. Defence Research and Development Canada (DRDC) has investigated various methods, including the improvement of atmospheric bioaerosol monitoring, to increase readiness against such a threat. By the end of the 90s, DRDC developed a standoff bioaerosol sensor based on intensified range-gated spectrometric detection of Laser Induced Fluorescence (LIF). The LIDAR system that monitors atmosphere volumes from a standoff position induces specific spectrally wide fluorescence signals originating from inelastic interactions with complex molecules forming the building blocks of the bioaerosols. This LIF signal is spectrally collected by the combination of a dispersive element and a range-gated ICCD that records spectral information within a range-selected atmospheric volume. This technique has showed an important potential of detecting and discriminating in several bioaerosol agent simulants real-time. In 2005, the BioSense TDP, which is a standoff bioaerosol sensing, mapping, tracking and classifying system based on SINBAHD technology, was selected to go in its definition year. BioWarn is sponsored by the Director Joint Capability Production for Chemical Biological Radiological Nuclear and Explosive (DJCP-5).

Through the Standoff Biodetection Working Group (SBWG), under the CANUKUS CBR MOU, SINBAHD was invited to participate in the Joint Biological Standoff Detection System increment II field demonstration trial (JBSDS Demo II). This international trial took place at Dugway Proving Ground (DPG), Utah, USA, in June 2005 and regrouped 12 systems using different technologies. The purpose of this field demonstration was to determine the benchmark sensitivity of the participant systems to various biosimulants/interferents and to demonstrate other capabilities (daytime, on the move operation and simulant/interferent discrimination). The data collected from each system would also be independently analyzed by the Johns Hopkins University Applied Physics Laboratory (JHU-APL) in order to validate technology models and perform virtual integration.

SINBAHD participation in this field trial made it possible to assess further its potential of detection and also to obtain new spectral signatures to be added to its library. SINBAHD participated in 34 cross wind open air releases at Target S. From those, 19 signatures could be extracted, nine did not have any fluorescence signal and one was lost due to a PC crash. The five releases left, from which no fluorescence signal could be visually observed in real time, were processed with SINBAHD virtual multivariate analysis (MA) tool. In all these five cases, a detection signal could be extracted but with a fairly low signal-to-noise ratio. All the results, once processed with the MA, were correlated with the data of DPG West Desert LIDAR (WDL) reference system. From this correlation, the 4 sigma sensitivity was evaluated for a given cloud depth and range. The obtained signatures of two bioaerosol agent simulants, *Bacillus subtilis var globiggi* (BG) and *Erwinia herbicola* (EH) were compared with those acquired in Suffield in 2001 in order to underline the robustness of the spectral signature of a particular biomaterial but of different origin, preparation and dispersion methods.

Buteau, S., Simard, J.R., McFee, J., Ho, J., Lahaie, P., Roy, G., and Mathieu, P., 2007. Joint Biological Standoff Detection System increment II: Field demonstration –SINBAHD performances. DRDC Valcartier TM 2006-140, Defence R&D Canada.

This page intentionally left blank.

## Sommaire

---

La menace biologique a émergé comme l'un des principaux défis en matière de sécurité aujourd'hui en raison de l'accessibilité croissante des technologies de guerre biologique et l'efficacité limitée de la détection et des mesures de protection contre de telles menaces. Recherche et développement pour la défense Canada (RDDC) a examiné différentes méthodes, incluant l'amélioration de la surveillance des bioaérosols atmosphériques, afin d'augmenter la disponibilité opérationnelle contre une telle menace. Vers la fin des années 90, RDDC a développé un détecteur en retrait de bioaérosols basé sur la détection spectrométrique de la fluorescence induite par laser (FIL). Le système LIDAR permet de surveiller à distance la fluorescence produite dans des volumes atmosphériques présélectionnés. Cette fluorescence spécifique et étendue spectralement provient des interactions inélastiques avec les molécules complexes formant le corps des bioaérosols. Ce signal FIL est recueilli par un élément dispersif combiné à une caméra intensifiée (ICCD) à crénelage en distance qui limite l'information spectrale à ce volume atmosphérique. Cette technique a démontré son important potentiel pour la détection et la discrimination en temps réel de différents simulants d'agents biologiques en aérosols. En 2005, le PDT BioSense, consistant en un système de détection, de cartographie, de poursuite et de classification en retrait de bioaérosols basé sur la technologie de SINBAHD, a reçu l'autorisation d'entrer en année de définition. Le client de BioSense est le 'Director Joint Capability Production for Chemical Biological Radiological Nuclear and Explosive' (DJCP-5).

SINBAHD a été invité à participer aux essais du 'Joint Biological Standoff Detection System increment II field demonstration (JBSDS Demo II)' par le groupe de travail international sur la détection biologique à distance (SBWG) dans le cadre le CANUKUS CBR MOU. Cet essai international a eu lieu au Dugway Proving Ground (DPG) en Utah aux É.-U. en juin 2005 et regroupait 12 systèmes basés sur différentes technologies. Le but poursuivi de ces essais était de déterminer les sensibilités de référence des systèmes participants à divers simulants/interférents biologiques et de démontrer certaines autres capacités (opération de jour, en mouvement, discrimination simulants/interférents). Les données obtenues par chaque système seront également analysées de façon indépendante par le Laboratoire de physique appliquée de l'Université Johns Hopkins (JHU-APL) afin de valider les modèles des différentes technologies et d'effectuer leur intégration virtuelle.

La participation de SINBAHD à ces essais a permis d'évaluer, une fois de plus, son potentiel de discrimination ainsi que d'obtenir de nouvelles signatures spectrales qui seront ajoutées à sa bibliothèque. SINBAHD a participé à 34 disséminations à l'air libre avec vent de travers au site 'Target S'. De ces disséminations, 19 signatures ont été extraites, neuf n'avaient aucun signal de fluorescence et un a été perdu en raison d'un trouble d'ordinateur. Les cinq acquisitions restantes desquelles aucun signal de fluorescence n'était visuellement observé, ont été traitées avec l'outil basé sur la méthode d'analyse multivariée (AM) de SINBAHD virtuel. Dans ces cinq cas, la détection a pu être mise à jour avec un faible rapport signal à bruit. Tous les résultats, une fois traités avec l'AM, ont été corrélés avec les données du système de référence de DPG, le 'West Desert LIDAR (WDL)'. À la suite de cette corrélation, la sensibilité à 4 sigma (4 fois l'écart type) a été évaluée pour chaque type d'aérosol pour des distances et des épaisseurs de nuages données. Les signatures obtenues de

deux simulants de bioagents en aérosol, *Bacillus subtilis var globiggi* (BG) et *Erwinia herbicola* (EH), ont été comparées à celles acquises à Suffield en 2001 afin de constater le degré de robustesse des signatures spectrales provenant d'échantillons de différentes origines avec différentes méthodes de préparation et de dispersion.

Buteau, S., Simard, J.R., McFee, J., Ho, J., Lahaie, P., Roy, G., and Mathieu, P., 2007. Joint Biological Standoff Detection System increment II: field demonstration – SINBAHD performances. DRDC Valcartier TM 2006-140. R et D pour la défense Canada.

# Table of contents

---

Abstract/Résumé.....	i
Executive summary .....	iii
Sommaire.....	v
Table of contents .....	vii
List of figures .....	xi
List of tables .....	xv
Acknowledgements .....	xvii
1 Introduction .....	1
1.1 Bio-Defence.....	1
1.2 Standoff versus Point Detection .....	1
1.3 LIDAR Techniques .....	1
1.4 Canadian Standoff Bio-Detection Effort.....	2
2 Objectives .....	4
2.1 JBSDS Increment II: Field Demonstration Trial, 2005.....	4
2.2 SINBAHD Participation to JBSDS Demo II trial .....	4
3 System description.....	5
3.1 Hardware .....	5
3.2 Software.....	7
3.2.1 SINBAHD Control Software .....	7
3.2.2 ‘SINBAHD Virtual’ Software .....	9
4 JBSDS Demo II trial, 2005.....	10
4.1 Standoff Ambient Breeze Tunnel (sABT) trial phase .....	10
4.2 Crosswind Testing .....	12
5 Data Processing .....	15

5.1	Normalized Fluorescence Spectral Signature.....	15
5.1.1	Spectral range.....	15
5.1.2	Spectral filtering.....	16
5.1.3	Normalisation.....	16
5.1.4	Acquisition summation .....	17
5.1.5	Background spectral signature .....	18
5.1.6	Detector artefact.....	20
5.2	Normalized Raman Spectral Signature.....	23
5.3	Multivariate Analysis Tool.....	24
6	Results .....	26
6.1	Normalized Spectral Signature, JBSDS Demo II, 2005 .....	26
6.1.1	Spectral signature robustness during dissemination.....	28
6.1.2	Normalized spectral signature discrepancy.....	29
6.1.3	Spectral signature robustness with different origin, preparation or dissemination method .....	31
6.1.4	Sensor correction.....	33
6.2	Multivariate Analysis results.....	35
6.3	West Desert LIDAR referee data correlation .....	35
7	Bug and Issues.....	61
7.1	Weather monitoring.....	61
7.2	PC Bug .....	61
7.3	Laser power stability .....	62
8	Conclusion.....	63
9	Recommendations .....	64
10	References .....	65
	Annex A: Crosswind tests during JBSDS Demo II, 2005 .....	67
	Annex B: SINBAHD general alignment procedure .....	72
	Annex C: Normalized signature construction (1 acq) .....	73
	Annex D: Normalized signature construction (many acq) .....	74

List of symbols/abbreviations/acronyms/initialisms ..... 76

Distribution list..... 78

This page intentionally left blank.

## List of figures

---

Figure 1. SINBAHD integrated prototype in Suffield 2001.....	5
Figure 2. Schematic representation of SINBAHD prototype. ....	6
Figure 3. SINBAHD virtual software user interface. ....	9
Figure 4. Standoff Ambient Breeze Tunnel (sABT), DPG, Utah, June 2005 and its dissemination mechanism. ....	10
Figure 5. Particle size distributions of different simulant/interferent, sABT, JBSDS Demo II, 2005.....	12
Figure 6. Target S grid for JBSDS Demo II trial, 2005.....	13
Figure 7. Crosswind testing dissemination mechanisms, JBSDS Demo II, 2005. ....	13
Figure 8. Impact of the three filtering methods on fluorescence spectra.....	16
Figure 9. Normalized (dashed) and un-normalized (solid lines) fluorescence spectra for four materials, JBSDS Demo II. ....	17
Figure 10. Summation and normalization (black) of many weak fluorescence acquisitions of BG (red, rescaled) with SINBAHD with a 600m-gate at 800 m range.....	18
Figure 11. Background fluorescence Signature: offset shifted (pale blue line) or not (black). 19	
Figure 12. Evolution of the spectrally integrated background LIF with time, DPG, June 13 <sup>th</sup> 2005.....	20
Figure 13.A) SINBAHD measurement of background LIF (red) and measured naturally occurring radiance (blue) for a gate width of 600 m and a range of 800 m; B) result from the subtraction of the naturally occurring radiance from background LIF.....	21
Figure 14. Naturally occurring radiance acquired between laser shots subtracted from the same signal acquired during laser shot (beam blocked). ....	22
Figure 15. Normalized spectral signature for Raman lines A) N <sub>2</sub> , B) H <sub>2</sub> O and C) 2N <sub>2</sub> .calculated from 90 acquisitions of background3.acq file (June 13 <sup>th</sup> , 2007, 600m gate at 800m range) ....	23
Figure 16. Normalized signatures selection table: example for TDA015:BA detection. ....	25
Figure 17. Normalized fluorescence signatures obtained at JBSDS Demo II trial, 2005.....	26
Figure 18. Yellow smoke normalized signature obtained with a 600m-gate at 800 m range... 28	

Figure 19. Spectral signature for the vegetative cells EH and irradiated Yp obtained by SINBAHD with a 600m-gate at 800 m range. ....	29
Figure 20. Normalized spectral signature for killed-Ba, BG, MS2, OV, diesel and burning brushes obtained with SINBAHD. ....	30
Figure 21. Normalized spectral signature for different type of BG and dissemination method obtained with SINBAHD at Suffield in 2001 and during JBSDS Demo II trial in 2005. ....	32
Figure 22. Normalized spectral signature for EH of different origin and preparation method obtained with SINBAHD at Suffield in 2001 and during JBSDS Demo II trial in 2005. ....	33
Figure 23. Spectral probability distributions and normalized spectral signature for killed-Yp, EH and BG from one single acquisition with SINBAHD during JBSDS Demo II trial at DPG. ....	34
Figure 24. SINBAHD Virtual interface showing the multivariate analysis results for a release of killed-Ba at 1.2 km range with a gate of 600 m (June 13 <sup>th</sup> , 2007, TDA015_Ba). ....	35
Figure 25. WDL calibrated concentration (solid blue line) and SINBAHD multivariate analysis results (dashed pink for Killed Ba; green triangles for background) for TDA015-Ba at 1.2 km. ....	37
Figure 26. WDL calibrated concentration (solid blue line) and SINBAHD multivariate analysis results (solid pink line for Killed Ba; green triangles for background) for TDA021-Ba at 2.6 km. ....	38
Figure 27. WDL calibrated concentration (solid blue line) and SINBAHD multivariate analysis results (dashed pink for Killed Yp; green triangles for background) for TDA017-Yp at 1.2 km. ....	39
Figure 28. WDL calibrated concentration (solid blue line) and SINBAHD MA results (dashed pink for Killed Yp; green triangles for background) for TDA027- Yp at 1.45 km. ....	40
Figure 29. WDL calibrated concentration (solid blue line) and SINBAHD multivariate analysis results (dashed pink for BG; green triangles for background) for TDA013-BG at 1.2 km. ....	41
Figure 30. WDL calibrated concentration (solid blue line) and SINBAHD multivariate analysis results (dashed pink for BG; green triangles for background) for TDA019-BG at 2.0 km. ....	42
Figure 31. WDL calibrated concentration (solid blue line) and SINBAHD multivariate analysis results (dashed pink for BG; green triangles for background) for TDA024-BG at 2.5 km. ....	43

Figure 32. WDL calibrated concentration (solid blue line) and SINBAHD multivariate analysis results (dashed pink for BG; green triangles for background) for TDA033-BG at 3.2 km. ....	44
Figure 33. WDL calibrated concentration (solid blue line) and SINBAHD multivariate analysis results (dashed pink for BG; green triangles for background) for TDA034-BG at 2.0 km. ....	45
Figure 35. WDL calibrated concentration (solid blue line) and SINBAHD multivariate analysis results (dashed pink for EH; green triangles for background) for TDA016-EH at 1.2 km. ....	46
Figure 36. WDL calibrated concentration (solid blue line) and SINBAHD multivariate analysis results (dashed pink for EH; green triangles for background) for TDA025-EH at 2.5 km. ....	47
Figure 37. WDL calibrated concentration (solid blue line) and SINBAHD multivariate analysis results (dashed pink for MS2; green triangles for background) for TDA026-MS2 at 1.55 km. ....	48
Figure 38. WDL calibrated concentration (solid blue line) and SINBAHD multivariate analysis results (dashed pink for OV; green triangles for background) for TDA011-OV at about 1.2 km. ....	49
Figure 39. WDL calibrated concentration (solid blue line) and SINBAHD MA results (dashed pink for OV; green triangles for background) for TDA020-OV at 2.3 km. ....	50
Figure 40. WDL calibrated concentration (solid blue line) and SINBAHD MA results (dashed pink for Yellow Smoke; green triangles for background) for TDA010-Yellow Smoke at 1.2 km. ....	51
Figure 41. WDL calibrated concentration (solid blue line) and SINBAHD MA results (dashed pink for Yellow smoke; green triangles for background) for TDA028-Yellow Smoke at around 1.5 km. ....	52
Figure 42. WDL calibrated concentration (solid blue line) and SINBAHD MA results (dashed pink for fog oil; green triangles for background) for TDA032-fog oil at 1.5 km. ...	53
Figure 43. WDL calibrated concentration (solid blue line) and SINBAHD multivariate analysis results (dashed pink for diesel; green triangles for background) for TDA006-diesel at 1.2 km. ....	54
Figure 44. WDL calibrated concentration (solid blue line) and SINBAHD multivariate analysis results (dashed pink for diesel; green triangles for background) for TDA018-Diesel at 1.2 km. ....	55

Figure 45. WDL calibrated concentration (solid blue line) and SINBAHD multivariate analysis results (dashed pink for diesel; green triangles for background) for TDA023-diesel at 2.35 km..... 56

Figure 46. WDL calibrated concentration (solid blue line) and SINBAHD MA results (dashed pink for diesel; green triangles for background) for TDA008-tires at 1.2 km. .... 57

Figure 47. WDL calibrated concentration (solid blue line) and SINBAHD MA results (dashed pink for burning brush; green triangles for background) for TDA007-burning brush at 1.2 km..... 58

Figure 48. WDL calibrated concentration (solid blue line) and SINBAHD MA results (dashed pink for burning cotton; green triangles for background) for TDA007-burning brush at 1.2 km..... 59

Figure 49. WDL calibrated concentration (solid blue line) and SINBAHD multivariate analysis results (dashed pink for top soil; green triangles for background) for TDA005-top soil at 1.2 km. .... 60

## List of tables

---

Table 1. SINBAHD Software parameters used during JBSDS Demo II trial. ....	8
Table 2. simulants/interferents used during JBSDS Demo II trial. ....	11
Table 3. Crosswind tests performed by SINBAHD (except 1 and 2) during JBSDS Demo II trial. ....	14
Table 4. Overview of SINBAHD results during JBSDS Demo II trial. ....	27
Table 5. Specific information on BG and EH samples studied at Suffield in 2001 and at DPG during the JBSDS Demo II field trial in 2005.....	31
Table 6. Overview of SINBAHD/WDL correlation results during JBSDS Demo II trial.....	36
Table 7. Suggested trial data sheet. ....	64

This page intentionally left blank.

## **Acknowledgements**

---

Different peoples have helped either directly or indirectly for the actual achievements of SINBAHD. They should be mentioned and acknowledged. In no particular order their names and affiliation follows: Vincent Larochelle, Denis Vincent, Denis Dubé, Sgt. Marc Grenier, David Comeau and Jacques Tremblay, all from DRDC Valcartier.

This page intentionally left blank.

# 1 Introduction

---

## 1.1 Bio-Defence

Bioaerosol threats have been around for centuries and mostly associated with war activities, and more lately to terrorist organizations. However, with the recent political developments that altered the image and dynamics of the international order and security, the importance of these bioaerosol threats have considerably increased in the past few years. Consequently, Canada has adopted different measures to increase its readiness facing this potential menace, one of which is the improvement of atmospheric bioaerosol monitoring.

## 1.2 Standoff versus Point Detection

Point and standoff detection are the two main approaches to monitor the bioaerosol contents of the atmosphere. Remote detection is, herein, considered as a remotely controlled point detector. Technologies associated with point detection systems have progressed rapidly mainly due to their relatively lower complexity and unit cost. Direct contact between the bioaerosols and the point detectors facilitates the extraction of different types of information such as the size and the spectral signature of fluorescence that increases their monitoring capability [1-5]. However, they must be positioned within the bioaerosol cloud in order to detect it and the information gathered is only relevant for a single location (or multiple discrete locations for a network of point detectors). Alternatively, standoff detection does not have these drawbacks but the information produced by those sensors is degrading as a function of range and bioaerosol concentration. Nevertheless, similar types of information, such as fluorescent spectra [6-9] and aerosol size statistics [10], can also be obtained from a standoff sensor approach.

## 1.3 LIDAR Techniques

Light Detection And Ranging (LIDAR) systems have proven to be efficient to monitor the atmosphere from a standoff position. Those systems can be separated into two main categories: elastic and inelastic LIDARs, which are defined herein, as applications in which the monitored returned signals are at the same wavelength as and at different ones than the source signal, respectively. Elastic LIDAR produces strong return signal located in a narrow spectral interval, which eases the detection process and makes possible demanding applications like cloud mapping [11], long-range low-concentration aerosol detection [12], or multiple field of view LIDAR [13]. The main limitation of an elastic LIDAR is its inability to distinguish clouds having similar distributions in aerosol size but of different material compositions. This is not the case for an inelastic LIDAR, which can procure specific information on the scatterers following the absorption and emission of a photon of a different frequency either through a virtual energy level in the case of Raman LIDARs or through a real excited state for the resonant LIDARs. The former is characterized by a spectrally narrow return signal independent of the irradiation wavelength. The return signal of the resonant LIDAR, which is called Laser Induced Fluorescence (LIF), can either be spectrally narrow or

distributed over a wide spectral interval, depending on the complexity of the illuminated species atomic structure [6, 14]. Since this technique implies a resonant effect, the irradiating wavelength is, in this particular case, critical and must be chosen in relation with the types of aerosols to be detected. More recently, with the introduction of efficient photon counting instruments based on intensified charge coupled device (ICCD) technology, it is possible, with the insertion of dispersive elements, to collect simultaneously the detailed spectrum of complex return signals [15-16].

## 1.4 Canadian Standoff Bio-Detection Effort

In the spring of 1999, DRDC initiated a 3-year program, called SINBAHD (Standoff Integrated Bioaerosol Active Hyperspectral Detection), to assess the potential of detecting and characterizing bioaerosol by laser-induced fluorescence and intensified range-gated spectrometric detection techniques. First, a model was built to predict the performance of such a device as a function of its numerous design parameters [17]. This model, derived from the classical LIDAR equation for multi-spectral returns and a proposed expression for the bioaerosol fluorescence cross-section, constituted one of the bases of this work. Following this initial modeling, an exploratory prototype was completed by December 2000. After extensive optical characterization, SINBAHD was tested at DRDC Suffield (May and September 2001) during open-air releases of two different simulants of biological agents: *Bacillus Globiggi* (BG), a spore-like bioaerosol, and *Erwinia herbicola* (EH), a vegetative celltype bioaerosol, [9]. The results of these tests show an excellent agreement with the proposed model and a very good correlation with the point detectors located near the investigated atmospheric cell. At these occasions, sensitivities of about 6 and 1 living Agent Containing Particles per Litre of Air (or ACPLA) of BG and EH, respectively, was derived for a range of 1.4 km (10-second integration, 5-metres range-gate and night time). Furthermore, the exploitation of the spectral information contained in the fluorescence signatures with multivariate analysis has demonstrated the capability of differentiating fluorescence from the disseminated BG and EH, and *Coleoptera* (beetle-like insect present in the probed atmospheric volume) with high probability from standoff positions as far as 1.4 km. Since then, other significant trials were conducted on biosimulants/interferents at Dugway Proving Ground (DPG), Utah, USA, (July 2002 and June 2005) and on natural bioaerosols at DRDC Valcartier (August 2004 and September 2005). The goal behind all these field campaigns is to assess further its potential of discrimination, to evaluate the robustness of the obtained spectral information and also to acquire new spectral signatures in order to construct a reference spectral signature library. The BioSense project consisting in a standoff bioaerosol sensing, mapping, tracking and classifying system, was submitted to the 2005 Technology Demonstration Program (TDP). BioSense was selected to go into its definition year in May 2005 and the first Senior Review Board (SRB) of March 2006 has decided (Mai 2006) that the project could proceed to the implementation phase.

This memorandum is intended to gather all the pertinent information related to SINBAHD participation in the Joint Biological Standoff Detection System increment II field demonstration trial (JBSDS Demo II), which took place at Dugway Proving Ground (DPG), Utah, USA, in June 2005. The objectives behind this participation will be first stated followed by a system overview. The trial site and procedures will then be briefly described. SINBAHD

testing procedures, data processing algorithms, results and issues will follow and finally, a conclusion and some recommendations for future field trials will be stated.

## **2 Objectives**

---

The pursued objectives expressed herein for the JBSDS Demo II as well as for SINBAHD participation to this trial are the ones behind the action initiative and do not include subsequent benefits, which there are no doubt there is.

### **2.1 JBSDS Increment II: Field Demonstration Trial, 2005**

The fundamental objective of this field demonstration was to determine the benchmark sensitivity of the participant systems to various biosimulants/interferents and to demonstrate other capabilities like interferent rejection, daytime and on the move operations. The data collected from each participant system will also be independently analyzed by the Johns Hopkins University Applied Physics Laboratory (JHU-APL) in order to validate technology models and perform virtual integration.

### **2.2 SINBAHD Participation to JBSDS Demo II trial**

The objective behind SINBAHD participation to the JBSDS field Demo II trial was first to obtain spectral fluorescence signatures of different bioaerosol agent simulants and interferents at the excitation wavelength of 351 nm. The obtained results will be used in the algorithm development process for the spectral information data exploitation of the BioSense TDP. Indeed, the more acquired data available there is and the most efficient will be the data exploitation strategy development. It was also an additional opportunity to assess SINBAHD detection potential and its discrimination capabilities between simulant and interferent bioaerosols.

### 3 System description

The exploratory SINBAHD prototype was built and delivered in December 2000. The entire LIDAR system, which includes the transmitter, receiver, electronics and cooling systems, is integrated within a 12 m-long modified towable trailer and, with a diesel-electric generator, constitutes a completely self-sufficient system (Figure 1). The selection of the different components of the prototype was based mainly on maximizing the LIDAR output power and collection sensitivity while staying within the available budget allocation.



*Figure 1. SINBAHD integrated prototype in Suffield 2001.*

#### 3.1 Hardware

SINBAHD prototype is schematized in Figure 2. The laser source is a UV Xenon-Fluoride excimer laser (GSI Lumonix, model PM-848) emitting about 150 mJ per pulse at 351 nm. A 15.1-ns pulses emitted at a pulse repetition frequency (PRF) of 125 Hz (limited by the acquisition camera), exits the unstable optical cavity of the laser and pass into a 3.65x beam expander providing a final measured Full Width Half Maximum (FWHM) beam divergence (including pointing stability) of 147  $\mu$ rad (width) x 308  $\mu$ rad (height). A visual channel is

inserted between the laser and the beam expander with the Visual Beam Splitter (VBS). With the help of a CCD camera equipped with a zoom lens and an optical high-pass filter, this visual channel allows the laser beam to be directed precisely towards the target of interest. The expanded laser beam is then made co-axial with the collecting optical axis using an adjustable 45-degree square folding mirror (FM) placed at the center of the telescope-collecting aperture. The combined emitter and collector optical axes are directed at the monitored atmospheric volume using a 50 cm by 33 cm elliptical steering mirror mounted on motorized gimbals providing 10  $\mu$ rad pointing accuracy (model AOM130M-400-2-41 made by Industrial Automation).

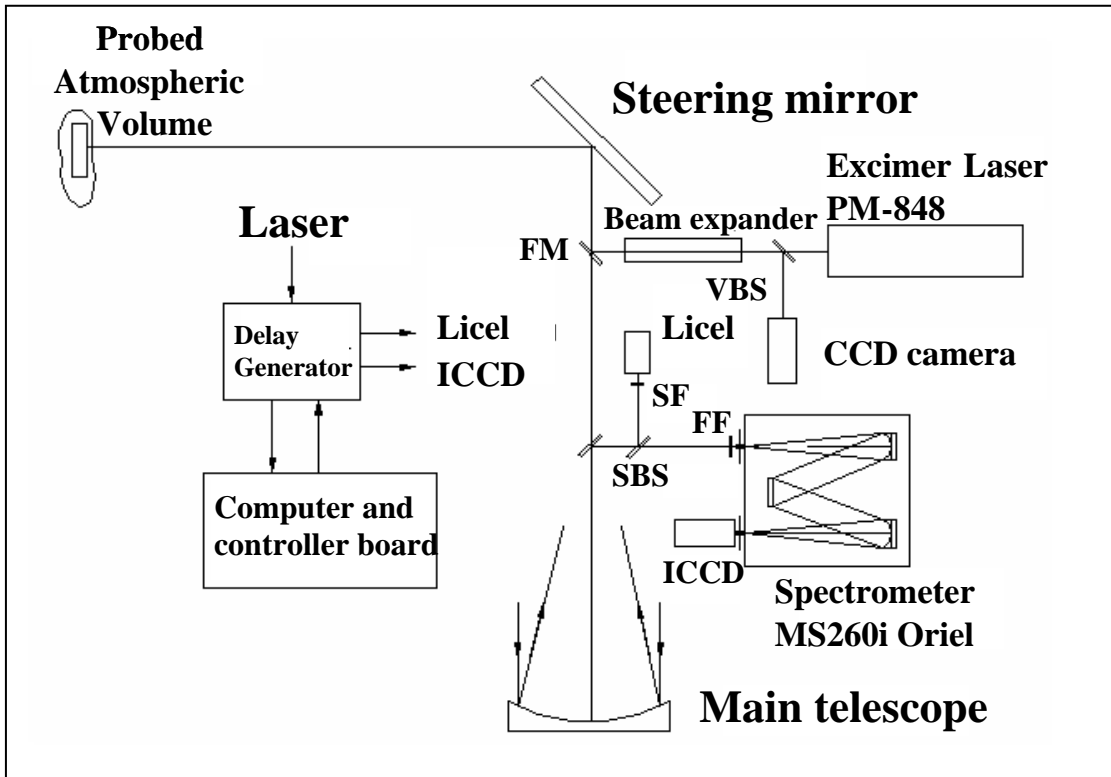


Figure 2. Schematic representation of SINBAHD prototype.

A 30-cm diameter, 127-cm focal length, Newtonian telescope (custom made by Space Optics Research Labs) collects the radiation returned by the monitored volume and focuses it at the entrance slit of the imaging spectrometer (Oriel, model MS260i), after passing through two UV high-pass filters (fluorescence filter: FF) to block the elastic scattered radiation. The 300 line/mm grating of this spectrometer in combination with a 200  $\mu$ m wide entrance slit confers a spectral resolution of 4.8 nm and a span of 230 nm, optimized between 300 and 600 nm. The entrance slit defines a 157  $\mu$ rad wide collecting field of view (FOV). However, the height of the slit, which has no impact on the spectral resolution but fixes the background contribution, is 3.3 mm (2.6 mrad FOV in height). An intensified CCD camera (Andor model

DH501-18F-01, option W) detects the dispersed radiation at the exit window of the spectrometer. The 128×1024-pixel CCD array is binned vertically (over the 128-pixel column) to keep only the spectrally dependent signal. From the 1024 pixel array, 675 pixels are in the intensified region and define the 230-nm spectral span of the inelastic scattering collector. The intensifier gate is synchronized with each fired laser pulse with a delay defining the range of the probed atmospheric cell. Furthermore, the natural radiant contribution present in the atmospheric cell, and collected simultaneously with the laser scatter, is sampled between each laser pulse. This requires operating the intensifier gate and the CCD readout at a frequency twice the laser PRF (250 Hz). The combination of the intensifier sensitivity, the 16-bit dynamic range of the camera, and the spectral distribution of the collected signal over the CCD columns give this detector configuration the capability of counting individual detected photons while keeping a very large dynamic range. This makes the actual sensor very attractive for detecting very low signal levels while retaining the spectral information. In parallel with the fluorescence channel, the elastic scattering is sampled from the collector axis with an anti-reflection (AR) coated quartz beam splitter (SBS) and is directed at a photo-multiplier tube (Licel) after being filtered by a 10 nm-wide band pass filter centered at 350 nm (SF). This photo-multiplier is connected to a transient recorder and provides elastic scatter returns as a function of range. This information is used to configure the width and position of the intensified range-gate. More information and calibration data for the SINBAHD system can be found in Simard *et al*, 2002 [17] and the final report of SINBAHD project from the prime contractor, 2000 [18].

## **3.2 Software**

SINBAHD LIDAR system is controlled by the custom software named SINBAHD, and an other equivalent software called SINBAHD Virtual allows to re-play performed acquisition and to perform multivariate analysis (MA) processing in order to exploit the data.

### **3.2.1 SINBAHD Control Software**

The ‘SINBAHD’ software installed in a primary computer controls all the instruments except the steering mirror which is controlled via a secondary computer and/or a joystick. The software assures proper synchronization between all instruments acquires the data and performs pre-processing in a probed atmosphere cell defined by the gate width and range. The general software operation is discussed in details in the Software User Manual [19]. Table 1 presents the values of different parameters that need to be chosen before performing an acquisition.

*Table 1. SINBAHD Software parameters used during JBSDS Demo II trial.*

<b>MENU</b>	<b>PARAMETER</b>	<b>VALUES</b>
Main	Operation mode	Multiple acquisitions
OpMode	Number of laser pulse	1 000
	Max. number of acquisition	200
	Pulse energy	Vary for each acquisition and even during an acquisition
	ICCD gain	8
	BG subt	Checked (√)
	Background subtraction	Checked (√)
	Range	Vary for each acquisition
	Width	Vary for each acquisition
	All other parameters in this menu	Default settings and checkbox not checked
	ICCD	Shift speeds
Exposure time		0.004 s
External trigger level		2.5 V
All other parameters in this menu		Default settings
Spectrometer	Central wavelength (position)	485 nm (from 370 to 600 nm)
	Grating	#2 (300 lines/mm)
BackScatter	Threshold	Low
	Input range	500 mV
	Discriminator	8
Weather	All parameters	Default; no choices

### 3.2.2 'SINBAHD Virtual' Software

SINBAHD virtual is a tool to replay and analyze the acquired data on the base of the multivariate analysis [17]. Section 5 will briefly overlook the procedure used to exploit the data acquired during the JBSDS Demo II trial, 2005. All the results presented in this memorandum were obtained from this software. Figure 3 presents the user interface of SINBAHD virtual software [19]. IN the first portion of the interface, different information and setting parameters are displayed. The second portion of the interface includes three windows: 1) the spectral window showing the acquired spectral signature obtained from the pre-selected volume in green and the best fit calculated from the MA in red; 2) the backscatter window showing the elastic return in the line of sight of the LIDAR and the pre-selected volume bounds with the two red lines; and 3) the time logged window showing the amplitude evolution of pre-selected signatures used in the MA.

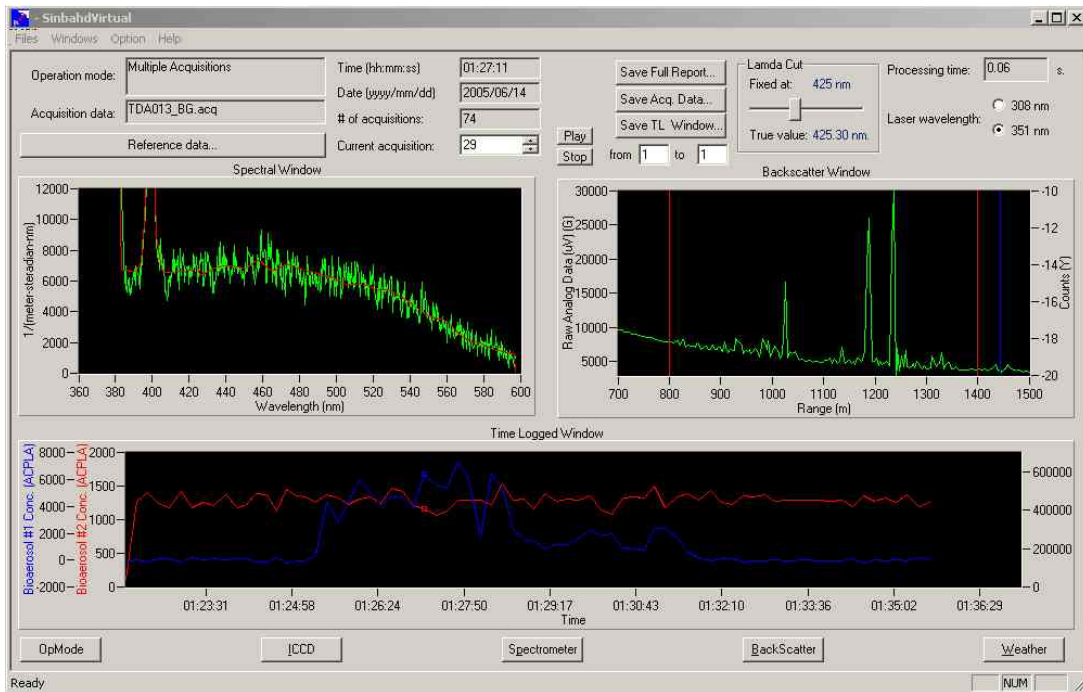


Figure 3. SINBAHD virtual software user interface.

## 4 JBSDS Demo II trial, 2005

The trial sites and their respective testing procedures will be briefly introduced in the present section. This trial was separate in three phases: 1) Standoff Ambient Breeze Tunnel (sABT) 2) crosswind testing and, 3) excursion testing/on the move. The last testing type won't be mentioned further since SINBAHD did not participate to this part of the trial. Annex A gives different parameters for each releases during the crosswind testing portion of the trial.

### 4.1 Standoff Ambient Breeze Tunnel (sABT) trial phase

This phase, which took place from June 6<sup>th</sup> to the 10<sup>th</sup> at the Tower Grid (sABT), is the absolute measurement portion of the trial. The sABT consist in a tunnel in which bioaerosols are released and the evolution of their concentration with time is measured by 6 calibrated Aerosol Particle Seizer (APS) placed at even increments in sequential order with APS1 at the release point and APS 6 at the outlet (Figure 4).



*Figure 4. Standoff Ambient Breeze Tunnel (sABT), DPG, Utah, June 2005 and its dissemination mechanism.*

An overall of 63 releases of simulants/interferents were performed, for which DPG West Desert LIDAR (WDL) acquired data. Those concentration calibrated reference data will be used to evaluate SINBAHD sensitivity limit. Information on the disseminated materials (sABT and/or Target S) can be found in Table 2. For each material disseminated in the sABT, a particle size distribution obtained from one APS is presented in Figure 5.

**Table 2.** simulants/interferents used during JBSDS Demo II trial.

<b>TYPE</b>	<b>MATERIAL</b>	<b>INFORMATIONS</b>
Bacteria spore	Ba ( <i>Bacillus anthracis</i> )	Dry killed vaccine strain, <i>Bacillus anthracis</i> Sterne
	BG ( <i>Bacillus subtilis</i> var. <i>niger</i> )	Dry, new BG (Denmark) milled at the same size as the old BG
Vegetative cell	Yp ( <i>Yersinia pestis</i> )	Wet killed vaccine strain KIM of <i>Yersinia pestis</i> ( $5 \times 10^9$ cfu/ml)
	EH ( <i>Erwinia herbicola</i> )	Wet unwashed EH in the spent media, from ATCC #33243
Protein (toxin simulant)	OV (ovalbumin)	Dry, the white of an egg
Virus simulant	MS2	Wet male-specific bacteriophage type 2 ( $1 \times 10^{10}$ pfu/ml)
Interferent	Kaolin (Hydrocil or Glowmax)	Hydrated Aluminum silicate ( $H_2Al_2Si_2O_8H_2O$ )
	Cabosil	Anti-caking agent
	Diesel	Exhaust from a 100-KW generator and release from HMMWV
	Yellow smoke	M18 colored smoke grenade (for signalling and screening)
	HC smoke	AN-M8 grenade (white smoke for signalling and screening)
	Pollen, Top soil, Burning brush, Burning tires, Burning cotton	

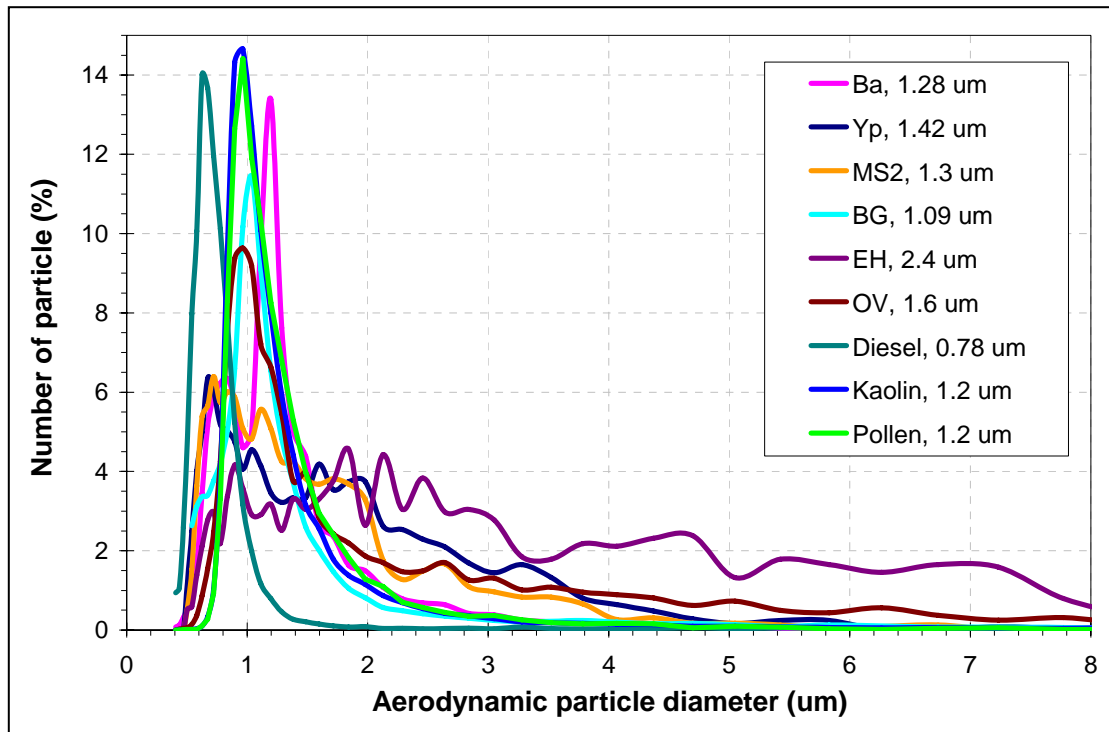


Figure 5. Particle size distributions of different simulants/interferent, sABT, JBSDS Demo II, 2005.

## 4.2 Crosswind Testing

This phase consisted in open-air releases in a given predefined target location. These crosswind testing took place on the 9, 12-17 of June 2005 at the Target S Grid (Figure 6). An overall of 48 crosswind trials, some with multiple releases of simulants/interferents were performed and in most cases, the WDL provided reference data. Three different dissemination mechanisms were used for this type of testing: point, puff or aerial (Figure 7). The location of the point and puff mechanisms, which are mounted on a mobile platform, is determined in function of wind direction and speed in order to obtain the bio-cloud on the target location.

SINBAHD was at Target S site for 5 nights during the cross-wind testing period. Table 3 presents the different trials attendant by SINBAHD with the exception of TDA001 and TDA002, which ones were dedicated for passive systems. Annex A presents some more details for those trials. The testing procedure was fairly constant over the trial period. First of all, an alignment/testing period was planned at the beginning of each testing night during which all systems, one after the other, was asked to verify its alignment with the target location (see Annex B for SINBAHD general alignment procedure). After a ‘time hack’ (time synchronization) and if the wind was cooperative, the dissemination team could go into position. The detection systems were asked to begin recording at a certain time and the release started 4 minutes later. In most cases, the dissemination was ramped down for the last portion of the release (see comments in Annex A).

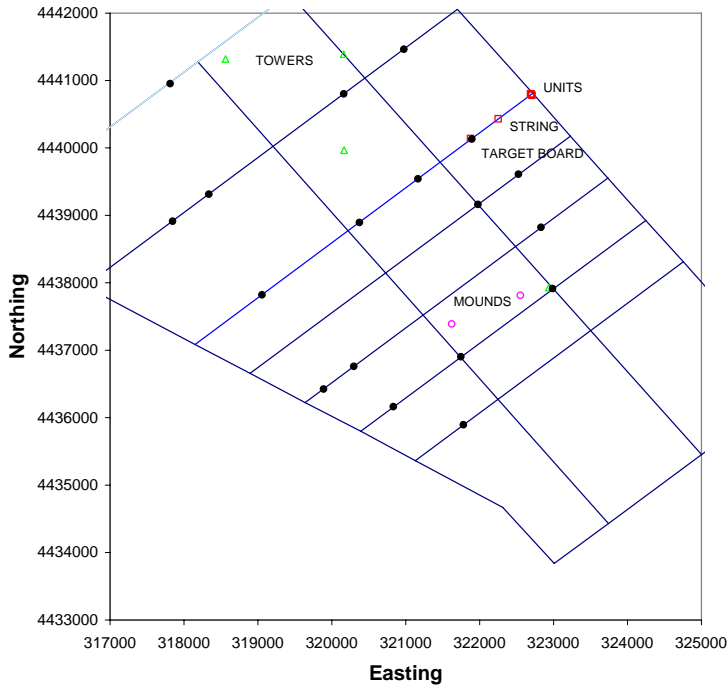


Figure 6. Target S grid for JBSDS Demo II trial, 2005.



Figure 7. Crosswind testing dissemination mechanisms, JBSDS Demo II, 2005.

*Table 3. Crosswind tests performed by SINBAHD (except 1 and 2) during JBSDS Demo II trial.*

Beginning Date (YYYYM MDD)	Release Number	Time (hh:mm:ss)				Aerosol type	Quantity (g or L)
		Start Record	Start Release	Stop Release	Stop Record		
20050609	TDA001	23:48:00	23:52:00	23:57:00	00:00:00	Road dust	N/A
	TDA002	00:14:00	00:18:00	00:18:40	00:26:30	Kaolin	19.5 g
	TDA003	00:43:00	00:47:00	00:53:00	00:58:00	Kaolin	96 g
	TDA004	01:06:00	01:10:00	01:17:00	01:23:00	BG	106 g
	TDA005	02:51:00	02:55:00	03:01:00	03:05:00	Top soil	178 g
	TDA006	03:52:00	03:56:00	04:02:00	04:07:00	Diesel	N/A
	TDA007	04:18:00	04:22:00	04:29:30	04:34:00	Burning brush	N/A
	TDA008	04:45:00	04:49:00	05:00:00	05:06:00	Burning tire	N/A
20050612	TDA009	22:37:00	22:41:00	22:49:45	22:57:00	Burning cotton	N/A
	TDA010	23:44:00	23:28:00	23:33:00	23:43:00	Yellow smoke	2ea
20050613	TDA011	00:23:00	00:27:00	00:31:30	00:35:00	OV	133 g
	TDA012	00:50:00	00:54:00	00:59:15	01:09:00	Kaolin(H)	56 g
	TDA013	01:21:00	01:25:00	01:31:00	01:36:00	BG	77 g
	TDA014	01:47:00	01:51:00	01:57:00	02:00:00	Kaolin(G)	24 g
	TDA015	02:28:00	02:32:00	02:35:30	02:40:00	BA	20 g
	TDA016	03:27:00	03:31:00	03:40:00	03:43:00	EH	7 L
	TDA017	04:08:00	04:12:00	04:18:00	04:22:00	YP	3.5 L
	TDA018	04:33:00	04:37:00	04:43:00	04:51:00	Diesel	N/A
20050614	TDA019	01:25:00	01:25:00	01:31:00	01:44:00	BG	85.5 g
	TDA020	01:51:00	01:51:00	01:57:00	02:05:00	OV	133.5 g
	TDA021	02:30:00	02:30:00	02:34:00	02:44:00	BA	20 g
	TDA022	02:57:00	02:57:00	03:03:00	03:13:00	Kaolin(G)	33 g
	TDA023	03:22:00	03:22:00	03:28:00	03:40:00	Diesel	N/A
	TDA024	04:16:00	04:16:00	04:16:05	04:32:00	BG	400 g
	TDA025	04:48:00	04:48:00	04:54:00	05:02:00	EH	5 L
20050615	TDA026	23:39:00	23:41:00	23:49:00	23:54:00	MS2	13 L
	TDA027	00:05:00	00:07:00	00:13:00	00:19:00	YP	7 L
	TDA028	00:28:00	00:33:00	00:36:09	00:46:00	Yellow Smoke	2 ea
	TDA029	00:57:00	01:02:00	01:02:10	01:20:00	Kaolin(G)	1750 g
	TDA030	01:30:00	01:36:03	01:36:15	01:53:00	Kaolin(G)	1750 g
	TDA031	02:07:00	02:08:00	02:13:26	02:20:00	HC Smoke	2ea
	TDA032	02:31:00	02:36:00	02:40:00	02:46:00	Fog Oil	N/A
	TDA033	02:59:00	03:04:00	03:04:14	03:12:00	BG	2700 g
	TDA034	03:24:00	03:35:31	03:35:45	03:48:00	BG	2700 g
	TDA035	04:24:00	04:27:00	04:30:00	04:32:00	Cabosil	0.5 g
	TDA036	04:43:00	04:46:00	04:50:00	04:52:00	Cabosil	51 g

## 5 Data Processing

---

The numerous data acquired during JBSDS Demo II trial had to be processed before any final conclusion, on the presence of a detection signal, could be drawn. In order to do so, the first step was to obtain the fluorescence and Raman normalized spectral signature. Then, the multivariate analysis tool of SINBAHD Virtual was used to evaluate if a fluorescent signal was present or not.

### 5.1 Normalized Fluorescence Spectral Signature

The Laser-induced fluorescence (LIF) emitted by the different studied species must be adequately characterized in order to use these fluorescence signature subsequently in the multivariate analysis. The two chosen acquisitions (with and without specific fluorescence), which are saved as a *txt* file via SINBAHD Virtual, have been pre-processed based on the choices made in the *OpMode* menu (Table 1). In the present case, only the background subtraction box was checked, which consist in subtracting the signal obtain while the laser is not shooting to the one when it actually is. It consists in subtracting the fluorescence occurring naturally in the selected atmosphere window. The first step, once the two files have been read is to subtract the LIF background from the simulat/interferent specific signal. This step permits to get rid of the background LIF while no specific materials are present and most of the intense Raman signals. Then a local smoothing is performed around the maxima of single Raman scattering from N<sub>2</sub> and H<sub>2</sub>O with the help of two local polynomial filters. Finally, some filtering (5.1.2) and a normalization (5.1.3) is performed before obtaining the final normalized spectral signature of the specie. Annex C presents the *matlab* subroutine used to perform these steps in order to econstruct the fluorescence spectral bases from LIF signal acquired with SINBAHD. Section 5.1.4 will show how the signal to noise ratio can be maximized by summing many acquisition signals; the related sub-routine can be found in Annex D. The special case of the background fluorescence signature will follow in section 5.1.5. Finally, detector specific artifacts will be discussed in 5.1.6.

#### 5.1.1 Spectral range

The CCD camera has 128x1024 pixels, which are binned vertically (over the 128-pixel column) and only 675 over the 1024 pixels are in the intensified region. The spectral intensified region ranges from 373.5 to 597.2 nm (pixel #165 to #839). This spectral interval can be segmented in two regions delimited by the 425nm wavelength cut-off: the Raman and fluorescence spectral regions. Indeed, all the Raman signals (section 5.2) have their maxima at wavelength shorter than 425nm. The fluorescence signal is not however confined to wavelength longer than 425 nm. So, even though the multivariate analysis tool of SINBAHD Virtual proceeds with its data exploitation algorithm after segmenting the spectral region (section 5.3), the fluorescence spectral signature presented in this report will cover the entire collected spectral range. It must be kept in mind that the obtained fluorescence signatures can be highly disrupted by Raman signals in the spectral region from 373 to 425 nm.

### 5.1.2 Spectral filtering

The noisy part of the signal consists in photon shot noise increased by a multiplicative random noise from the amplifier. The output noise is white and can be modeled using a Gaussian distribution. In order to reduce this noise, three type of linear filtering were tested: Lee filter, moving average and hyperspectral-Gaussian filter. The last two are more aggressive than the former one and the Gaussian filter is much less efficient in the tails sections (beginning and end). Figure 8 presents the background corrected signal from acquisition #35 of trial TDA013\_BG (black) and the results from the three different filtering methods (blue, red, green). Even though the moving average option (sliding mean) is slightly longer to process, it was the filtering method retained.

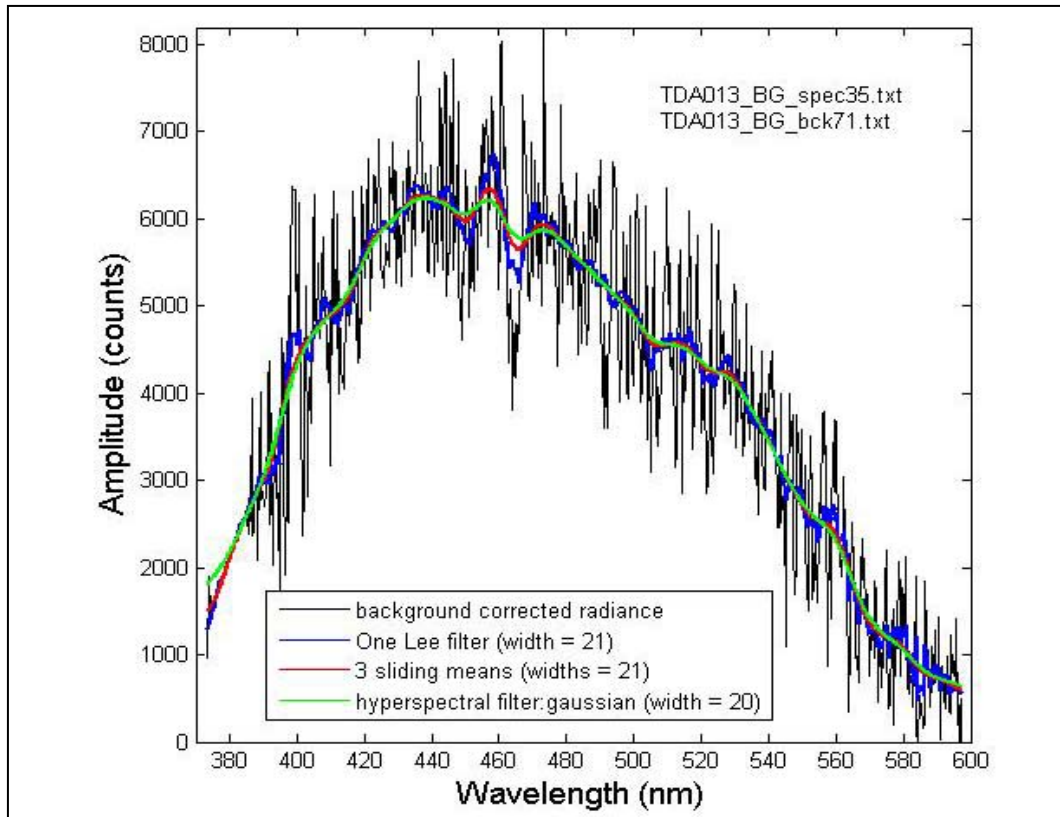


*Figure 8. Impact of the three filtering methods on fluorescence spectra.*

### 5.1.3 Normalisation

The spectral normalization (from 373 to 597 nm) process consists in finding the normalizing constant and dividing the fluorescence spectra by its value. This constant is defined as the value by which an everywhere nonnegative function must be multiplied in order that the area under its graph is 1 (such as a probability density function). Figure 9 presents fluorescence un-normalized (left axis, solid lines) and corresponding normalized (right axis, dashed lines) spectral signatures for four different materials: BG, EH, Yellow smoke and Fog oil.

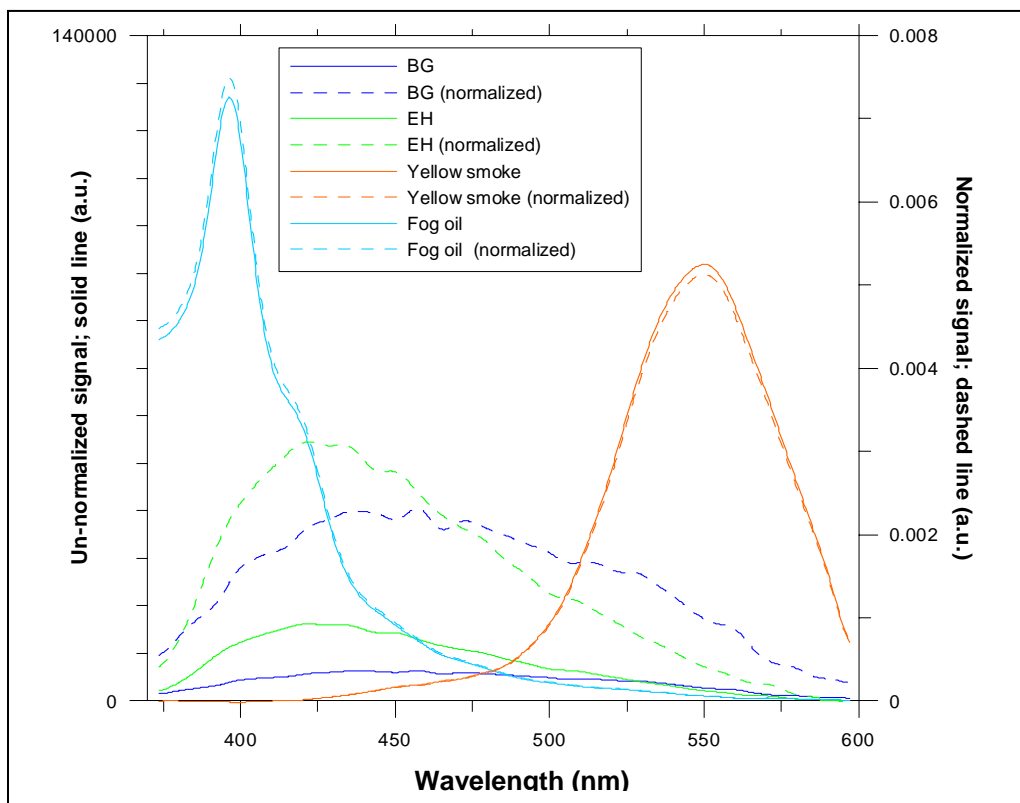


Figure 9. Normalized (dashed) and un-normalized (solid lines) fluorescence spectra for four materials, JBSDS Demo II.

### 5.1.4 Acquisition summation

Each acquisition acquired during a measurement, results from the summation of 1000 laser pulse (Table 1) that maximizes the intensity of the detected signal. The same technique can be used during the processing. Indeed, all acquisition demonstrating a significant specific fluorescent signal can be added before normalization to maximize the signal to noise ratio (S/N). Figure 10 shows this improvement while summing 17 weak fluorescence acquisitions of BG (TDA013).

The *matlab* sub-routine used to perform this processing is presented in Annex D. The fluorescence and background acquisitions of interest must be selected and extracted from the raw data files (ReadSNBDVersion2File sub-routine). The naturally occurring radiance in the selected atmosphere window (acquired between laser shots) is then subtracted from the LIF signal. All the background acquisitions are averaged and Gaussian filtered before being subtracted from all fluorescence signal acquisitions selected, which removes the background LIF and most of the Raman signals. Then, local smoothing is performed with polynomial filters around the maxima of single Raman scattering from  $N_2$  and  $H_2O$  and the 586nm-detector artifact, followed by a triple sliding mean filtering (5.1.2). The resulting fluorescence signatures are finally all spectrally summed before being normalized (5.1.3).

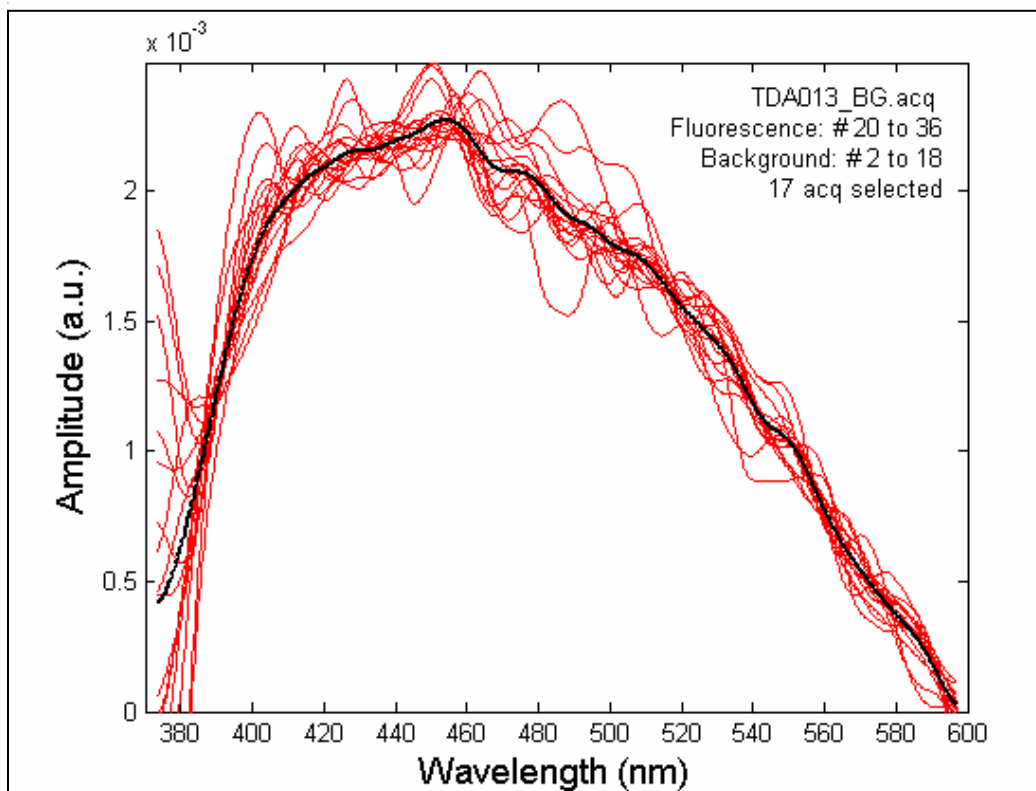
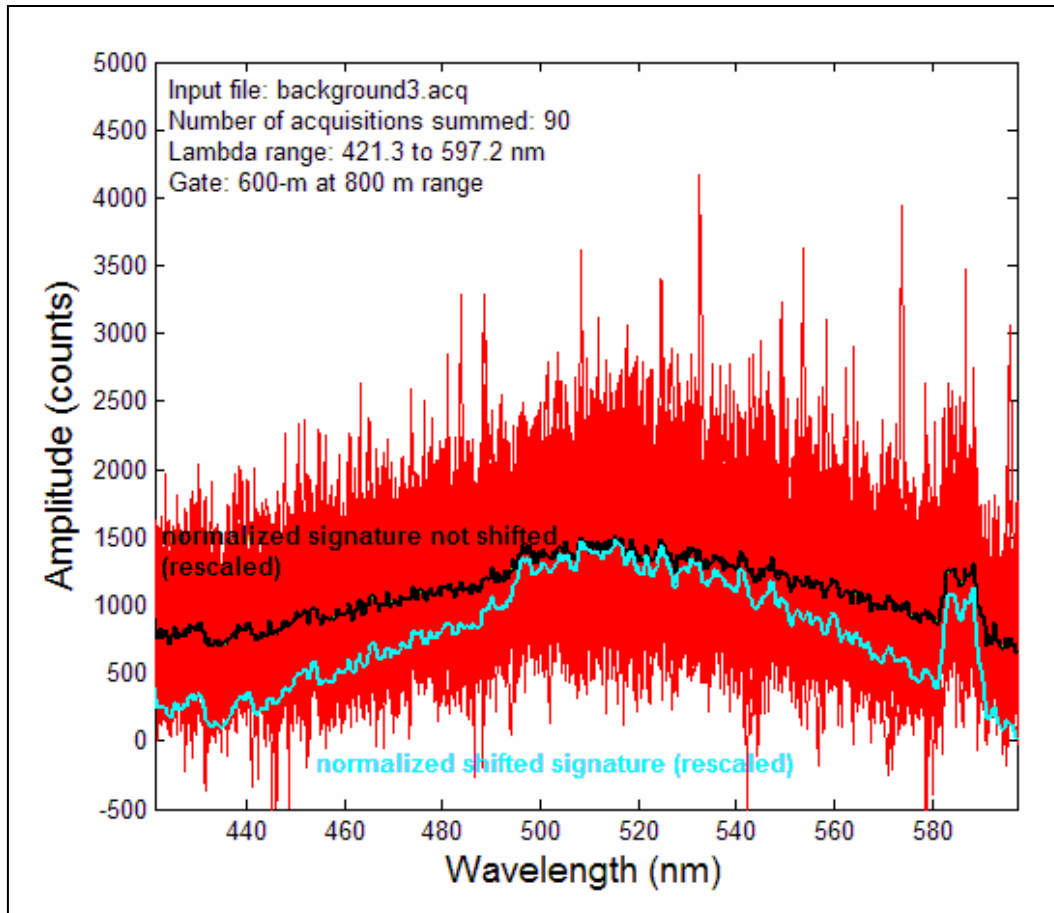


Figure 10. Summation and normalization (black) of many weak fluorescence acquisitions of BG (red, rescaled) with SINBAHD with a 600m-gate at 800 m range.

### 5.1.5 Background spectral signature

The background LIF must also be characterized since this fluorescent component is present in all acquisition and must be included into the multivariate analysis. The background normalized spectral signature was obtained by filtering and normalizing the spectral average of many background LIF acquisitions, from which the naturally occurring radiance signal was subtracted. Figure 11 presents the 90 background fluorescence acquisitions (red) that were averaged (black) and from which the background normalized signature was calculated (blue). The spectral feature around 585 nm is related to the detector (section 5.1.6). After utilizing this spectral signature in the multivariate analysis tool of SINBAHD Virtual, it appeared to be not fully adequate. Indeed, the signature amplitude calculated by the multivariate tool was in some cases, negative. The origin of the problem comes from the zero-offset of the calculated mean fluorescence spectra. In order to overcome this problem, a new background normalized signature was constructed by the exact same process as the former one but including a shift of the mean signal before normalizing the function (dark red in Figure 11). Depending on the multivariate analysis results, the un-shifted or shifted background fluorescence spectral signature was used. For all other signatures, this zero-offset do not have a significant impact since these offset amplitudes are fairly small compared to the signal maximum due to the LIF background subtraction and the higher signal intensity.



*Figure 11. Background fluorescence Signature: offset shifted (pale blue line) or not (black).*

The spectral shape and level of the LIF originating from the background depends on many factors such as the specific nature of this background, illumination conditions and gate width. Figure 12 shows the spectrally summed background LIF, corrected for the naturally occurring radiance with respect of the acquisition number; representing a time step of about 11 sec (1000 laser pulses at 125Hz + downloading time). This result is either related to the varying output power of the laser or to the diminution of illumination condition. It must be mentioned that the laser is always used with the STABILASE option selected, which assures that the laser stays at a certain energy level but this feature has a given precision, which has not yet been characterized. The surrounding illumination condition should not radically influence LIF intensity since range gated technique is used and the natural radiance contribution found in the pre-selected volume is systematically subtracted from the LIF signal. However, the lowering of the background LIF signal (Figure 12) seems to correlates with the ambient illumination conditions. Indeed, the acquisition started at 21h21 and ended at 21h38 on June 13 2005, and for most of the acquisition (up to #82; 21:35), the sun was in the civil twilight defined as the period during which the sun is  $6^\circ$  below horizon and hence still having a noticeable influence on the ambient illumination conditions. This matter needs further investigation.

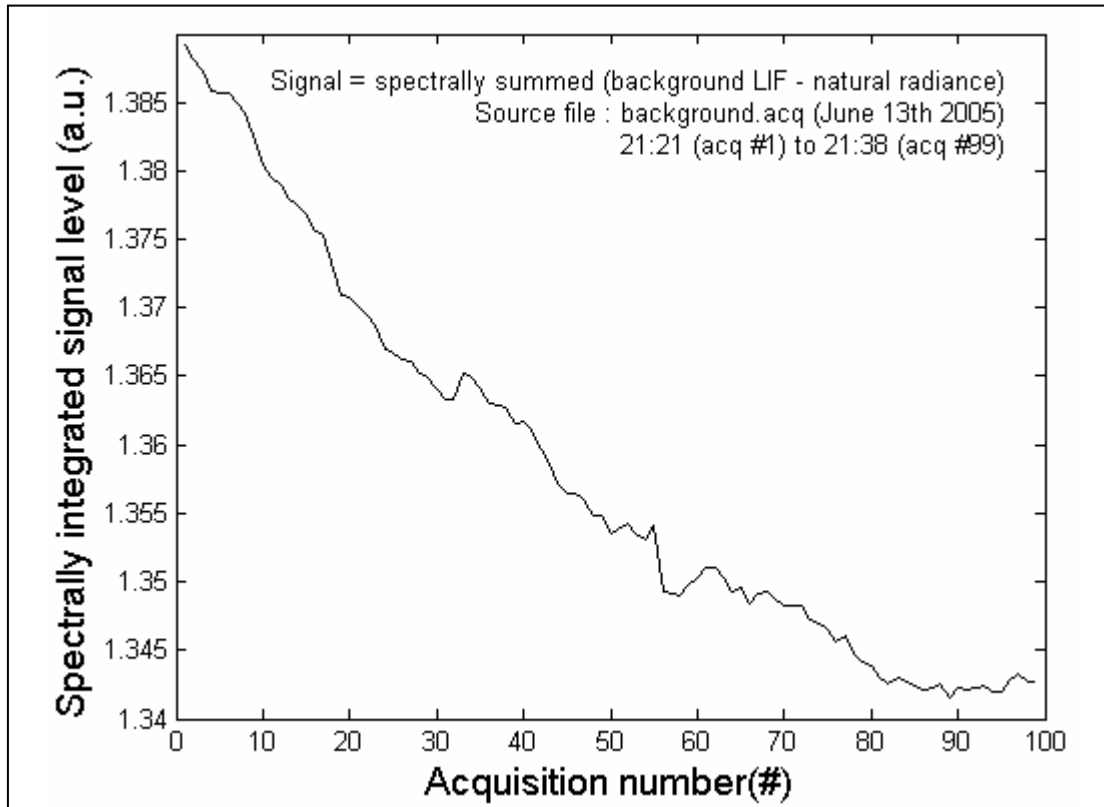


*Figure 12. Evolution of the spectrally integrated background LIF with time, DPG, June 13<sup>th</sup> 2005.*

Since the gate width and range differs between trials and the illumination conditions did change over the trial period (moon phase, setting, astronomical twilight, and clouds), the characterisation of all the various background situations could not be obtained in an acceptable amount of time. A general background LIF signature is hence calculated and used in all cases even though the specific trial conditions are not constant. For the JBSDS Demo II trial, only one background trial was used to construct both the shifted and not shifted normalized background signature (Figure 11).

### 5.1.6 Detector artefact

Each spectral bin signal consists in the integrated signal measured from the 128 pixels of one CCD column of the detector and it is well known that each pixel has its own specificity. Figure 13A tends to represent this fact by showing a close-up (27 nm) of 90 acquisitions of background LIF (red) and its corresponding naturally occurring radiance acquired between laser shot (blue). The spectral features seen in Figure 13A are not exclusively due to the fluorescence (red) and radiance (blue) characteristic of the background but also due to the electronic contribution of the measurement, especially to the specificity of each spectral bin (sum of 128 different pixels).

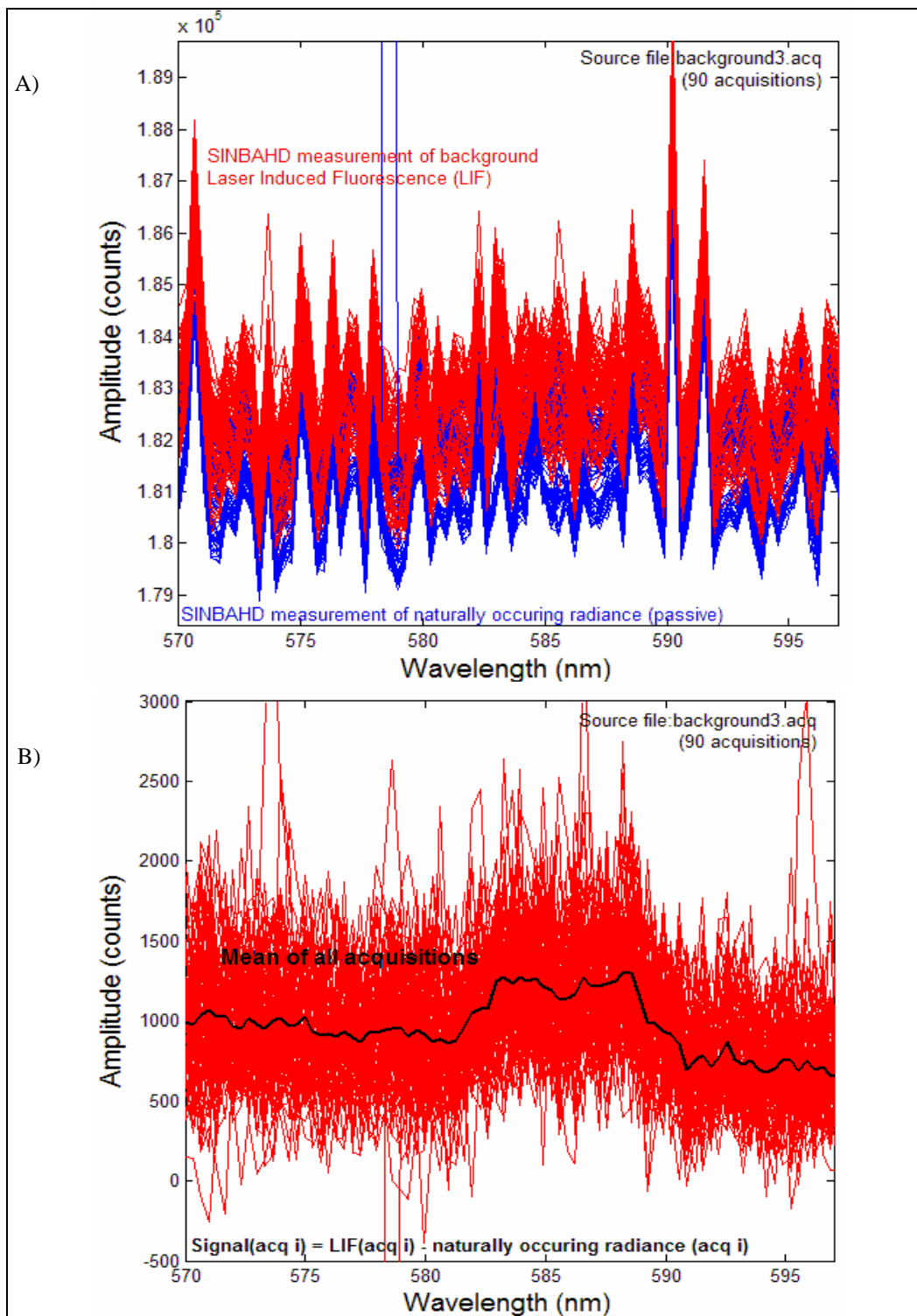


**Figure 13.A) SINBAHD measurement of background LIF (red) and measured naturally occurring radiance (blue) for a gate width of 600 m and a range of 800 m; B) result from the subtraction of the naturally occurring radiance from background LIF.**

By performing the subtraction of the naturally occurring radiance (blue lines) from the background LIF (red lines), most of this bin-to-bin intrinsic variation vanishes but at the expense of possible artefact creation (Figure 13B). This last figure demonstrate this bin specificity lost and also the only noticeable artefact created during the process (from 582 to 589 nm) for the ICCD detector used by SINBAHD. This spectral feature can not be related to any LIF fluorescence process since it is still present in the case of a trial run with the laser blocked (Figure 14). The signals represented in this last figure (red) are the subtraction of naturally occurring background acquired between two laser shots from the same naturally occurring background acquired during the laser shooting but with the laser beam blocked. It seems that the shooting of the laser has the effect of levering-up the electronic signal in the spectral range from 582 to 589 nm. This artefact must hence be related to both the laser system and the detector. Since this artefact is always present in the calculated fluorescence signatures and the systematic subtraction of the measured naturally occurring radiance, this artefact was included in the background normalized fluorescence signature (Figure 11).

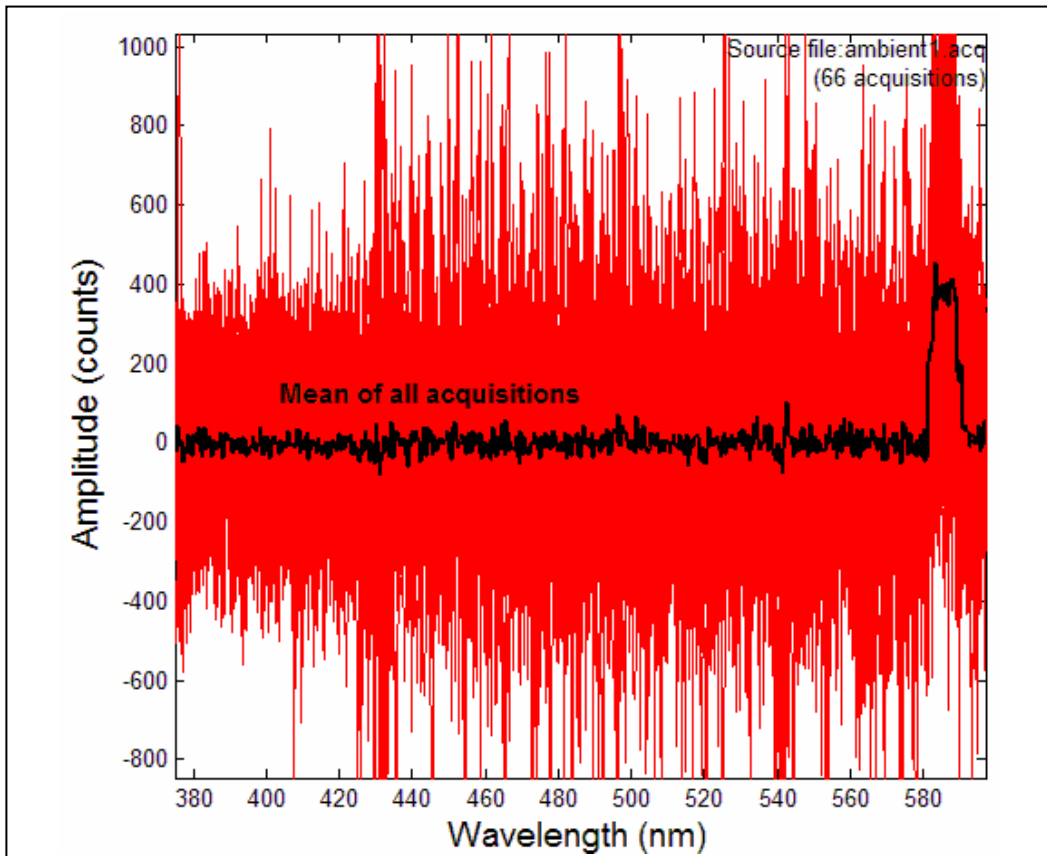


*Figure 14. Naturally occurring radiance acquired between laser shots subtracted from the same signal acquired during laser shot (beam blocked).*

## 5.2 Normalized Raman Spectral Signature

The single Raman scattering from O<sub>2</sub>, N<sub>2</sub> H<sub>2</sub>O and the double Raman scattering from N<sub>2</sub> (denoted 2N<sub>2</sub>) each produces un-resolved doublet Raman lines, which ones must be characterized by proper spectral signatures. For the O<sub>2</sub> Raman line, the calibrated profile found in SINBAHD Virtual software library is used since this line is just partly influencing the spectra by its longer wavelength tail. For the three other lines (N<sub>2</sub>, H<sub>2</sub>O, 2N<sub>2</sub>), their respective normalized signature were obtained by normalizing the shifted mean of 90 spectral acquisitions. The shifted 90 acquisitions are first averaged and then normalized (5.1.3) on the spectral range selected, and set to zero on the rest of the spectral window. Figure 15 A, B and C present respectively the obtained N<sub>2</sub>, H<sub>2</sub>O, 2N<sub>2</sub> normalized signatures.

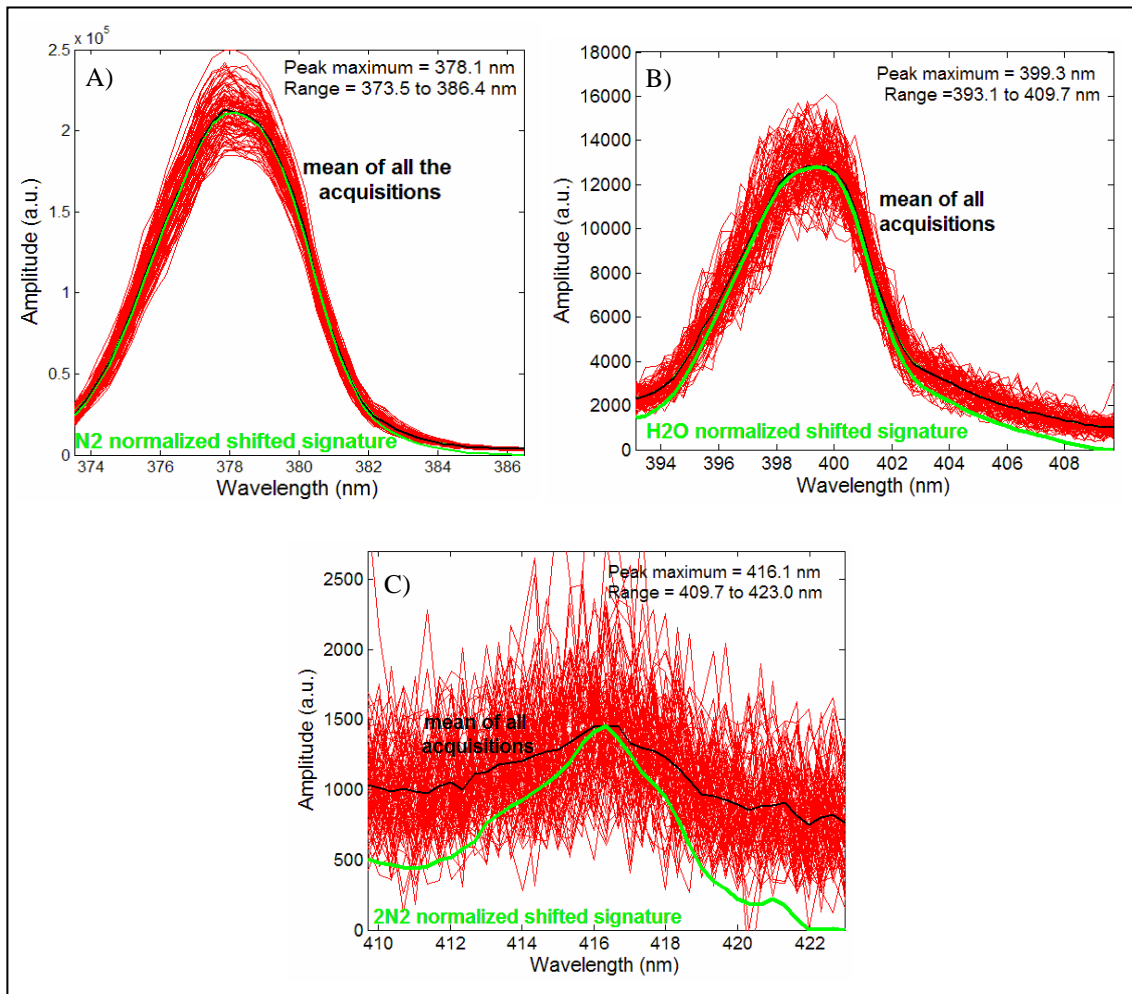


Figure 15. Normalized spectral signature for Raman lines A) N<sub>2</sub>, B) H<sub>2</sub>O and C) 2N<sub>2</sub>, calculated from 90 acquisitions of background3.acq file (June 13<sup>th</sup>, 2007, 600m gate at 800m range).

### 5.3 Multivariate Analysis Tool

The multivariate analysis is used to separate signals associated with different inelastic scatters; biofluorescence scatterer  $E_{is}$ , Raman scatters  $E_{\text{Raman line}}$ , or any other spectrally distributed signals present in the collected spectra. This well-known general mathematical method is well suited for this task. The multivariate analysis technique represents the collected inelastic spectra  $E_\lambda$  as a linear combination of normalized spectral signatures  $\bar{s}_{is}^\lambda$  in the multivariable space from which individual energetic contributions,  $E_{is}$ , can be derived:

$$\bar{E}_\lambda = \overbrace{E_{b1}\bar{s}_{b1}^\lambda + E_{b2}\bar{s}_{b2}^\lambda + \dots}^{\text{Bioaerosols}} + \overbrace{E_{N_2}\bar{s}_{N_2}^\lambda + E_{H_2O}\bar{s}_{H_2O}^\lambda + E_{O_2}\bar{s}_{O_2}^\lambda + E_{2N_2}\bar{s}_{2N_2}^\lambda}^{\text{Ramans}},$$

$$\text{where } \sum_{\lambda} (\bar{s}_{is}^i) = 1. \quad (1)$$

The first steps in order to use the multivariate analysis tool of SINBAHD Virtual, is to select the excitation wavelength (351 nm), the lambda cut (425.3 nm) and the normalized spectral signatures to be considered in the linear combination. This latter will then be fitted in a least-square sense to the acquired fluorescence signal. The signature selection is performed by clicking the ‘*Reference data...*’ tab and by completing the pop-out table entitled ‘load Reference Data Sets’ (Figure 16). The normalized signature used for the Raman lines were in all cases the same (see sec 5.2 and Figure 16). For the fluorescence spectral portion, the proper normalized bioaerosol signature and either shifted or unshifted background signature (sec. 5.1.5) were selected. The second and last step is to extract the calculated data with the ‘*Save TL window*’ from ‘*X*’ to ‘*Y*’ tabs. A txt-file is then created including the different normalized signatures amplitudes (energetic contributions) and the Chi square for both the Raman and the fluorescence spectral section.

For the present work, the goal pursued by performing the multivariate analysis (MA) was to evaluate the minimum possible detection limit. This implies that selected normalized bioaerosol signatures were the ones of the disseminated species when available or some other close signature if not. The choice of the background signature, shifted or not (5.1.5), was made in order to minimise the zero-offset of the specie amplitude before dissemination.

The multivariate analysis tool used by SINBAHD Virtual is not perfect neither than fully optimised but is a powerful tool to obtain for example an evaluation of the amount of given specie versus background and its evolution with time. From the obtained results, the detection limit can be evaluated if a correlation between SINBAHD signals and species concentration are available. This detection limit represents in fact an optimum since: 1) the proper signature was used (not unknown releases), 2) all the releases consisted in unique specie (no mixture or simultaneous interferences) and 3) the background was properly characterized.

**Load Reference Data Sets** [X]

Fit with BioAerosol #1

Fit with BioAerosol #2

Fit with BioAerosol #3

Fit with Raman N2

Use calibration profiles

Use custom profiles

Fit with Raman O2

Use calibration profiles

Use custom profiles

Fit with Raman H2O

Use calibration profiles

Use custom profiles

Fit with Raman X

Use custom profiles

OK

*Figure 16. Normalized signatures selection table: example for TDA015:BA detection.*

## 6 Results

Firstly, the normalized spectral signatures obtained during JBSDS Demo II trial will be presented (6.1). Other interesting fact characterizing these signatures will then be exposed: their robustness during dissemination (6.1.1), their discrepancy (6.1.2), comparison between signatures of the same species (BG and EH) but from different origin, preparation and/or dissemination method (6.1.3), and the sensor correction which must be applied to obtain sensor independent fluorescence spectra (6.1.4). The multivariate analysis results correlated with the West Desert LIDAR (WDL) referee concentration evaluation will finally be presented (6.3).

### 6.1 Normalized Spectral Signature, JBSDS Demo II, 2005

SINBAHD attended to 34 cross-wind releases (TDA003 to TDA036) from which 19 signatures were extracted, 5 multivariate analyses were needed to determine if specific fluorescence was present, 9 did not have any fluorescence and 1 data set was lost. Figure 17 presents typical signatures obtained from multiple SINBAHD acquisitions of simulant and interferent disseminated during JBSDS Demo II trial.

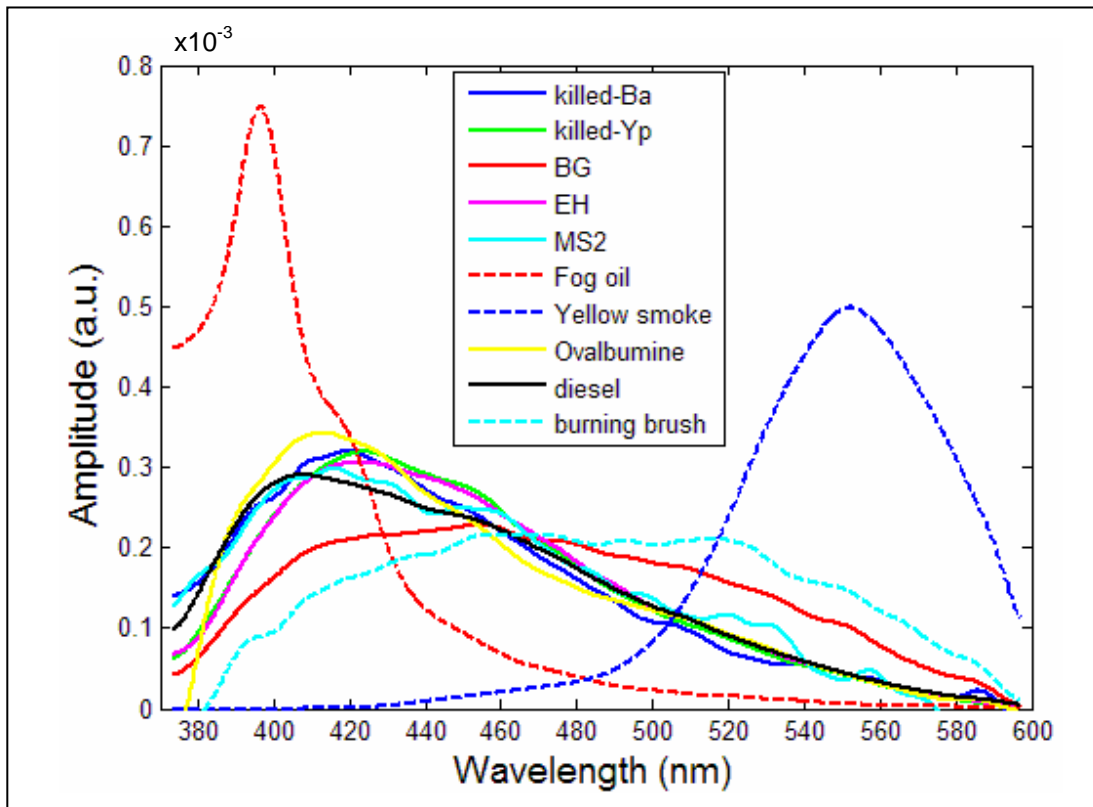


Figure 17. Normalized fluorescence signatures obtained at JBSDS Demo II trial, 2005.

Table 4 gives the details about fluorescence, backscatter signal and the outcome for all the attended trials. When a fluorescence signal was clearly present, a signature could be extracted (light green). When fluorescence was not seen neither than expected and a backscatter response was present, the specie was qualified of having no LIF at 351 nm (clear). In the case of releases showing very weakly or not visually perceptible specific fluorescence but for which fluorescence emissions were expected and for which a backscatter signal is detected, the multivariate analysis tool was used (gray).

*Table 4. Overview of SINBAHD results during JBSDS Demo II trial.*

trial name	target range (km)	fluorescence signal	Backscatter signal	outcome
TDA015_Ba	1.2	X	X	signature
TDA021_Ba	2.6	none visually	X	MA
TDA017_Yp	1.2	X	X	signature
TDA027_Yp	1.5	X	X	signature
TDA004_BG	1.2	X	X	lost data
TDA013_BG	1.2	X	X	signature
TDA019_BG	2.0	X	X	signature
TDA024_BG_puff	2.5	X	X	signature
TDA033_BG_aerial	3.2	X	X	signature
TDA034_BG_aerial_2	2.5	X	X	signature
TDA016_EH	1.2	X	X	signature
TDA025_EH	2.5-2.6	X	X	signature
TDA026_MS2	1.6	weak	X	signature
TDA011_OV	btw 0.8-1.4	X	problem	signature
TDA020_OV	2.3	none visually	X	MA
TDA035_cabosil	1.2	-	-	-
TDA036_cabosil_2	1.2	-	X	-
TDA003_kaolin	1.2	-	X	-
TDA012_kaolin_hydrosil	1.2	-	X	-
TDA014_kaolin_GloMax	1.3	-	X	-
TDA022_kaolin_GloMax	2.6	-	X	-
TDA029_kaolin_aerial	3.1	-	wrong range	-
TDA030_kaolin_aerial_2	3.1	-	X	-
TDA010_yellowsmoke	1.2	X	X	signature
TDA028_yellow_smoke	?	X	problem	signature
TDA031_white_smoke	1.5	-	X	-
TDA032_fog_oil	1.5	X	X	signature
TDA006_diesel	1.2	X	X	signature
TDA018_diesel_exhaust	1.2	none visually	X	MA
TDA023_diesel_exhaust	2.3-2.4	very weak	X	MA
TDA008_tires	1.2	very weak	X	MA (diesel)
TDA007_burningbrush	1.2	X	X	signature
TDA009_cotton	1.2	weak+ short	low + short	signature
TDA005_Topsoil	1.2	weak	X	signature

Over the 16 different studied materials, cabosil, kaolin and HC-white smoke did not show any detectable fluorescence. The burning tires did have some signal but not enough to extract a signature. The burning cotton and top soil releases had sufficient signal to obtain a signature for the MA utility but not enough to clearly characterize them. Finally, clear signatures could be obtained for all the others: Ba, Yp, BG, EH, MS2, OV, yellow smoke, fog oil, burning brushes.

### 6.1.1 Spectral signature robustness during dissemination

During SINBAHD acquisition, 1000 laser pulses are emitted at 125 Hz, the LIF from a selected window is collected and then, the overall spectral signal is downloaded. This process is repeated for a certain time: starting and ending few minutes before and after dissemination respectively in order to measure the LIF signal without the presence of the disseminated specie. One acquisition signal is hence 1000 LIF spectra in which each spectral bin is the result from the 128 pixels binning along the ICCD vertical axis. This stacking and binning process can be seen as pre-processing during which, the signal to noise ratio (S/N) is being raised. In spite of this, the stability of the fluorescence spectra obtained during dissemination is decreasing with the signal level intensity (Figure 10 in sec 5.1.4). Figure 18 presents an example of good spectral signature robustness obtained from the intense yellow smoke signal. In order to obtain robust spectral signatures, high intensity signals are obviously needed.

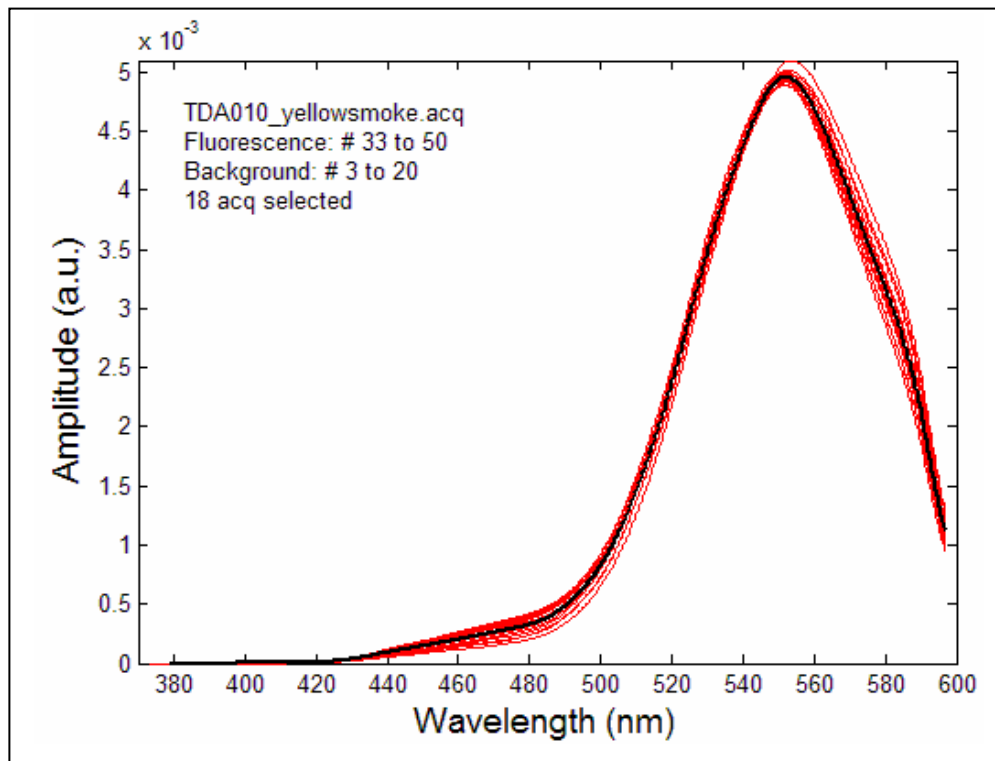


Figure 18. Yellow smoke normalized signature obtained with a 600m-gate at 800 m range.

### 6.1.2 Normalized spectral signature discrepancy

Fluorescence spectral structures were observed for 12 of the 16 disseminated materials during the trial period (sec 6.1). Since the obtained signatures for the burning cotton and top soil are not characterizing clearly their spectral features due to a fairly low signal level, they will not be taken into account in the present section. This leaves 10 signatures (Figure 17) which can be considered as representing, to a different degree depending on the S/N, the specific LIF with an excitation at 355 nm for these materials. The fog oil and yellow smoke signatures are the most easily discernable between the ten signatures. In addition of having clear distinct spectral features, their fluorescence signal level was much higher than the others (high S/N). This implies that these interferences would be easily categorized by a classifier algorithm but could however interfere with bioagents detection following the much higher signal intensity of the former. Signatures of the vegetative cells EH and irradiated Yp have quite similar spectral features (Figure 19). This result shows how difficult the discrimination can be between different materials of the same type.

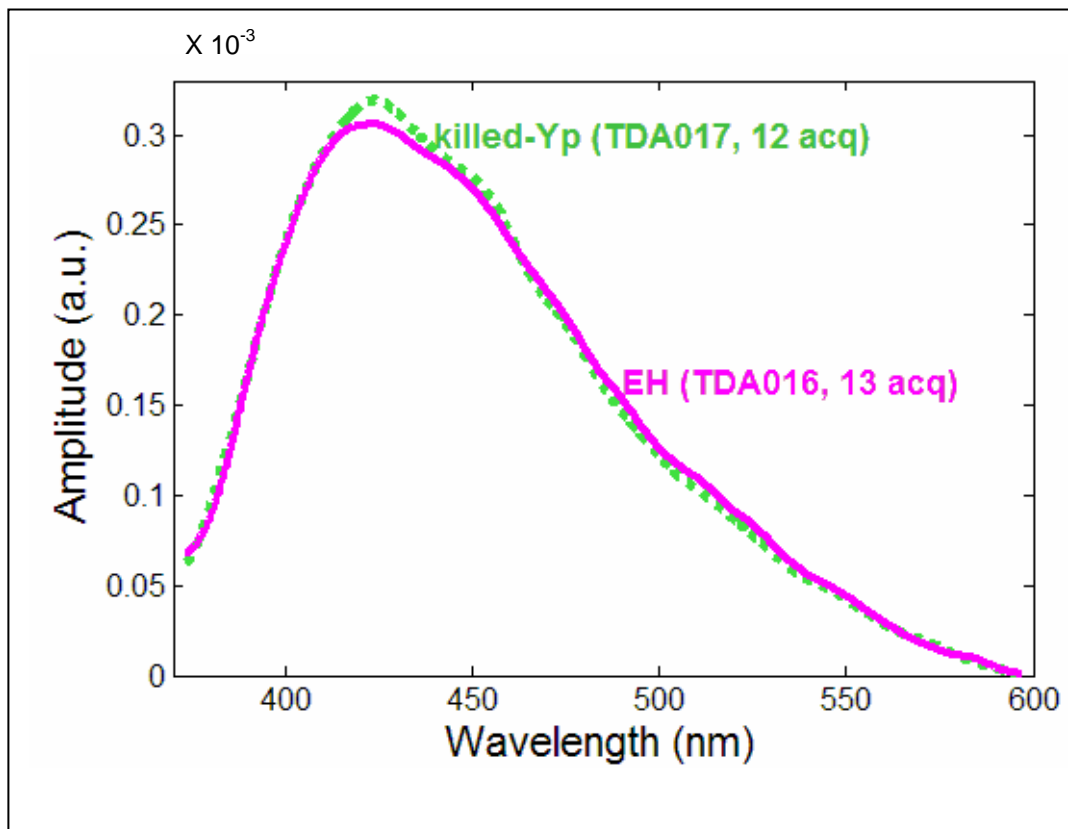
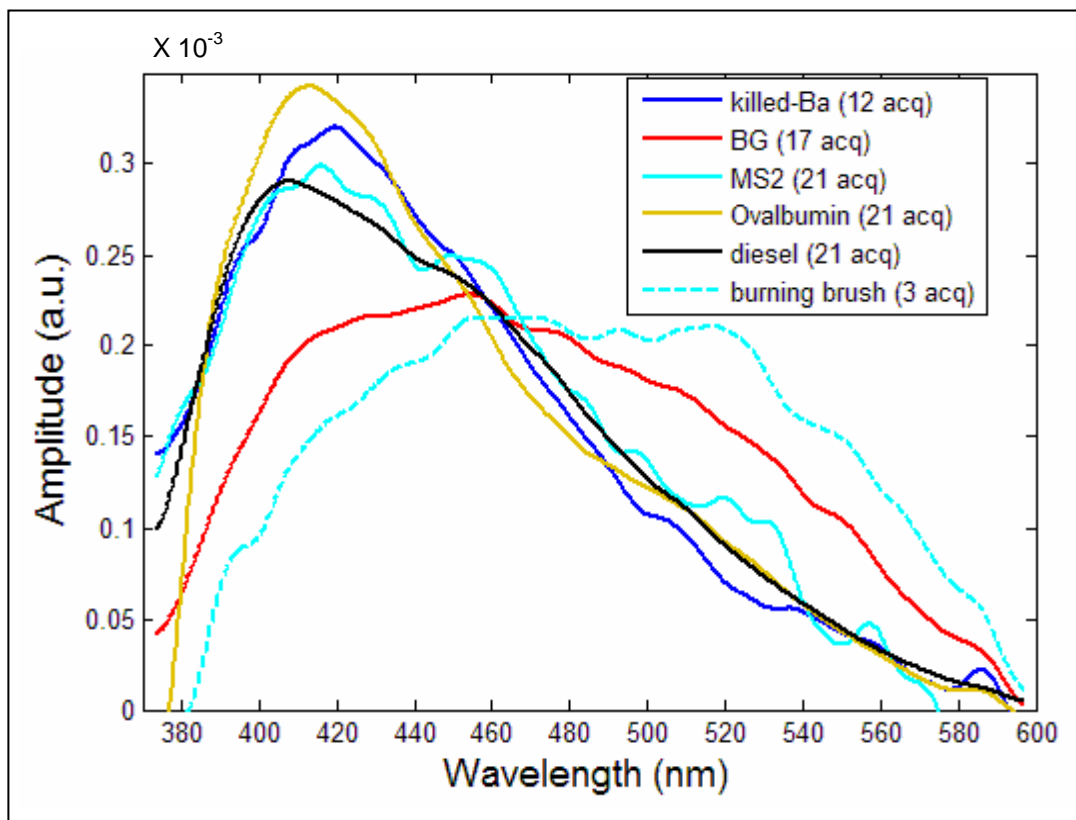


Figure 19. Spectral signature for the vegetative cells EH and irradiated Yp obtained by SINBAHD with a 600m-gate at 800 m range.

The last 6 signatures show discrepancy between them to various degrees (Figure 20). The first interesting fact that must be underlined from these results is the obvious spectral differences between killed-Ba and BG, which are two species of *Bacillus* bacteria spores (rod-shape endospore). In opposition to the vegetative cells studied, the two *Bacillus* species can easily be discriminated even though they are both bacteria spores. It has to be noted that the gamma illumination process performed on both the Ba spores and the YP vegetative cell (killed vaccine strain) had certainly an impact on their LIF signatures. Ovalbumin (OV) and MS2, which are respectively toxin and virus simulants, have spectral features much closer to killed-Ba than BG has. Discrimination between killed-Ba, MS2 and OV would hence not be obvious, especially when the Raman spectral window is removed (see sec 5.1.1). Indeed, when considering only the spectral range from 425 to 600 nm, killed-Ba, MS2, OV, EH, killed-Yp and even diesel have all the same main spectral feature. However, several small spectral differences can also have a significant impact on the efficiency to discriminate fluorescence spectra of various natures.



*Figure 20. Normalized spectral signature for killed-Ba, BG, MS2, OV, diesel and burning brushes obtained with SINBAHD.*

### 6.1.3 Spectral signature robustness with different origin, preparation or dissemination method

The fluorescence signature of a given material can be influenced by several parameters such as its origin, its growth and preparation method, its state (wet or dry), its dissemination process or even the climatic conditions during the dissemination period. This signature variability is annoying since the classification process efficiency depends on the capacity of the signatures in the library to spectrally characterize the material without regard of the origin, preparation, state or dissemination methods. In order to have an appreciation of this potential variability, signatures of BG and EH having different origin, state, preparation or dissemination method were compared. Table 5 presents the different parameters of the studied BG and EH samples.

*Table 5. Specific information on BG and EH samples studied at Suffield in 2001 and at DPG during the JBSDS Demo II field trial in 2005.*

Material name	Origin	Preparation	State	Dissemination	Testing
Old BG	US DPG	Liquid suspension containing 1% BG slurry	Wet	Micronair Blower	Suffield, 2001
New BG	Denmark	Milled at the same size as the old BG	Dry	Skil Blower-point + puff and aerial	DPG, 2005
EH (wild)	Suffield, CAN	Unwashed, in its fermenting spent media Tryptic Soy Broth (TSB)	Wet	Micronair Blower	Suffield, 2001
EH	US (ATCC #33243)	Unwashed, in its fermenting spent media Tryptic Soy Broth (TSB)	Wet	Micronair Blower	DPG, 2005

For the BG, the origin, preparation, state and dissemination method were different at the JBSDS Demo II, DPG 2005 than in the Suffield 2001 trial. For this latter, the only dissemination facility available was the micronair blower, an agricultural sprayer for liquid, which is why the BG was a wet release (see preparation and state in table 5). The old BG came directly from DPG and the new BG, sometimes called super BG, was bought from Denmark and already milled at the same size as the old BG. Figure 21 presents two signatures of the Old BG obtained in May and September 2001, and three signatures of the New BG for three different dissemination processes (point, puff and aerial). Each signature has a particular signal to noise ratio dependent on the type and amount of material released and also the gate width/range for a particular trial. The obtained signatures are fairly consistent with each other even though the samples had major differences (Suffield 2001 versus DPG 2005). From these results, it appears that the dissemination process, the material state (wet/dry) and the

origin/preparation methodology did not have a significant impact on the signatures. The detector artifact around 585 nm can be observed in the two spectra obtained at long range (2.5km) for which signal to noise ratio are much lower. The presence of this artifact can have a slight impact on the normalized signature output due to the normalization process (section 5.1.3) which includes all the spectral features from 373 up to 597 nm.

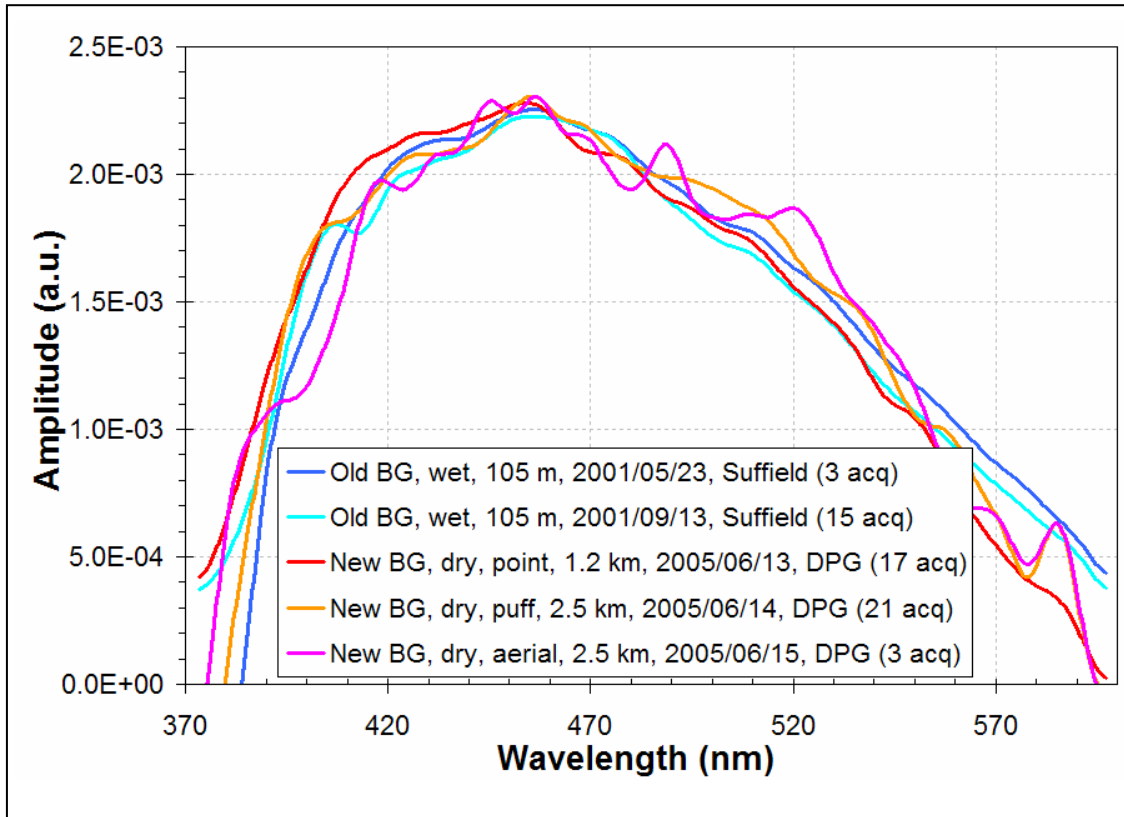


*Figure 21. Normalized spectral signature for different type of BG and dissemination method obtained with SINBAHD at Suffield in 2001 and during JBSDS Demo II trial in 2005.*

For the two EH samples, all the main characteristics of are the same (see table 5) except for their origin. A complete comparison of the preparation method could not be performed since no detailed information were given for the Suffield sample (ex: presence of sucrose, anti-foam, HCL, NaOH). The EH from Suffield was nicknamed ‘wild EH’ or ‘wild type EH’ due to its high degree of resemblance with the EH found in nature. The ATCC EH only denotes that it was purchase from the bioresource center *American Type Culture Collection* (ATCC). Figure 22 presents two signatures of the wild EH obtained at 1.4 km and 105 m, and two signatures of the ATCC EH obtained at 1.2 and 2.5 km. The obtained signatures are consistent with each other. The ATCC EH seems to be slightly more spread spectrally and lower in amplitude around the maxima. Once again the detector artifact (585 nm) can be seen in the two spectra obtained at longer range (2.5 and 1.4 km).

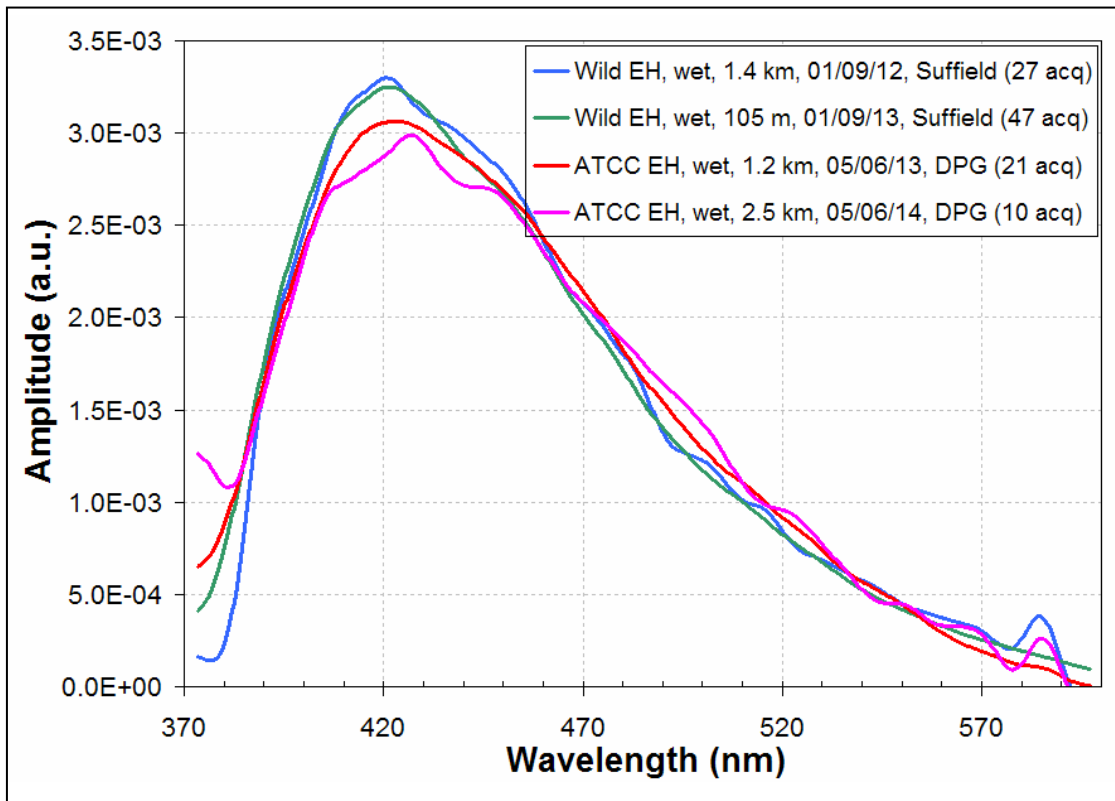


*Figure 22. Normalized spectral signature for EH of different origin and preparation method obtained with SINBAHD at Suffield in 2001 and during JBSDS Demo II trial in 2005.*

From all the obtained results, either BG or EH, the influence of the origin, state, preparation and dissemination methods (Table 5) on a given material signature can sometimes be noticeable but not to the expense of the specific spectral features of that material. The robustness of the spectral signature is hence sufficient to obtain interesting to good classification results with an algorithm based on spectral feature matching and a signature pattern set (library).

#### **6.1.4 Sensor correction**

All signatures presented previously were sensor dependent and hence not exploitable by other sensor than the one used to perform the acquisition. The sensor independent signature is in fact the fluorescence spectral probability distribution of the bioaerosol,  $P_{ba}$ . This latter intrinsic parameter can be obtained once the optical calibration of the sensor is performed using a stable white source with a known emission profile (an integrating sphere for example), and assuming first, an atmospheric spectral transmission equal to 1 (short range measurements, few hundred meters) and second, an ideal spectral resolution for the spectrometer [17]:

$$P_{ba}(\lambda) = \frac{P'_{ba}(\lambda)}{\int P'_{ba}(\lambda) d\lambda}, \text{ where } P'_{ba}(\lambda) = \frac{ne_{ba}(\lambda)R_{sphere}(\lambda)}{ne_{sphere}(\lambda)}. \quad (2)$$

In this last equation,  $ne_{ba}$  and  $ne_{sphere}$  are the detected electronic signals from the bioaerosol and the calibrated integrating sphere, respectively and  $R_{sphere}$  is the integrating sphere calibrated radiance. Figure 23 presents both the sensor dependent (signature,  $s_{ba}$ ) and independent (probability distribution,  $P_{ba}$ ) spectral signature for the killed-Yp, EH and BG. The transition from the sensor dependent spectral signature to the spectral probability distribution can be made directly with the sensor optical calibration result since the transmission of the atmosphere was assumed to be equal to 1 [17]. The optical calibration used in the present case is not entirely appropriate due first to the rapidly diminishing radiance of the source when heading to the shorter wavelengths and second, to the variation of the acquired signal from the source. A source with a smoother radiance over the entire spectral window of interest and an averaging data processing over a large number of spectral acquisitions would be valuable in order to enhance the sensor characterization process. Ideally, the atmosphere transmission should also be characterized.

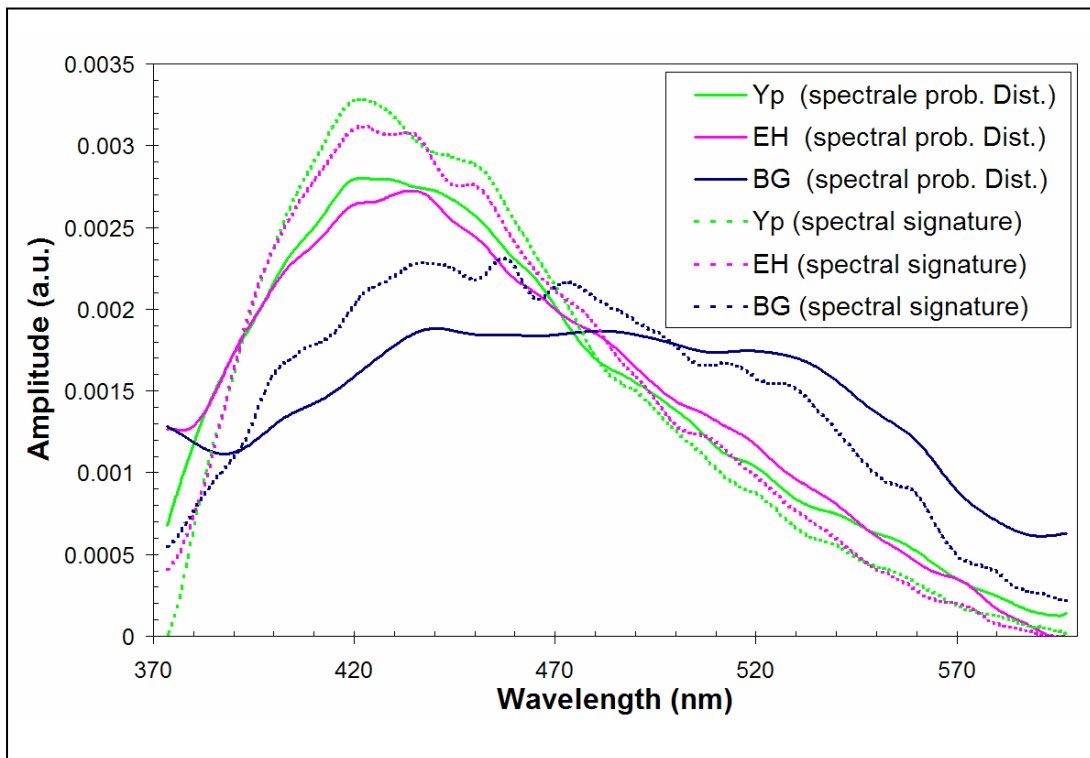


**Figure 23. Spectral probability distributions and normalized spectral signature for killed-Yp, EH and BG from one single acquisition with SINBAHD during JBSDS Demo II trial at DPG.**

## 6.2 Multivariate Analysis results

The multivariate analysis (MA) is used to separate signals associated with different inelastic scatters present in the collected spectra (section 5.3). This technique was performed on each releases data and from which the minimum possible detection limit was evaluated. Figure 24 presents SINBAHD Virtual interface introduced in section 3.2.2 [19] showing the complete result from the multivariate analysis in the Time Logged Window (lower section) for TDA015-Ba. For this example, the 'bioaerosol #1 and #2 Conc' (Figure 24) represent the amplitude of killed-Ba and background spectral signature respectively. The different results extracted from the multivariate analysis will be presented in the next section (6.3).

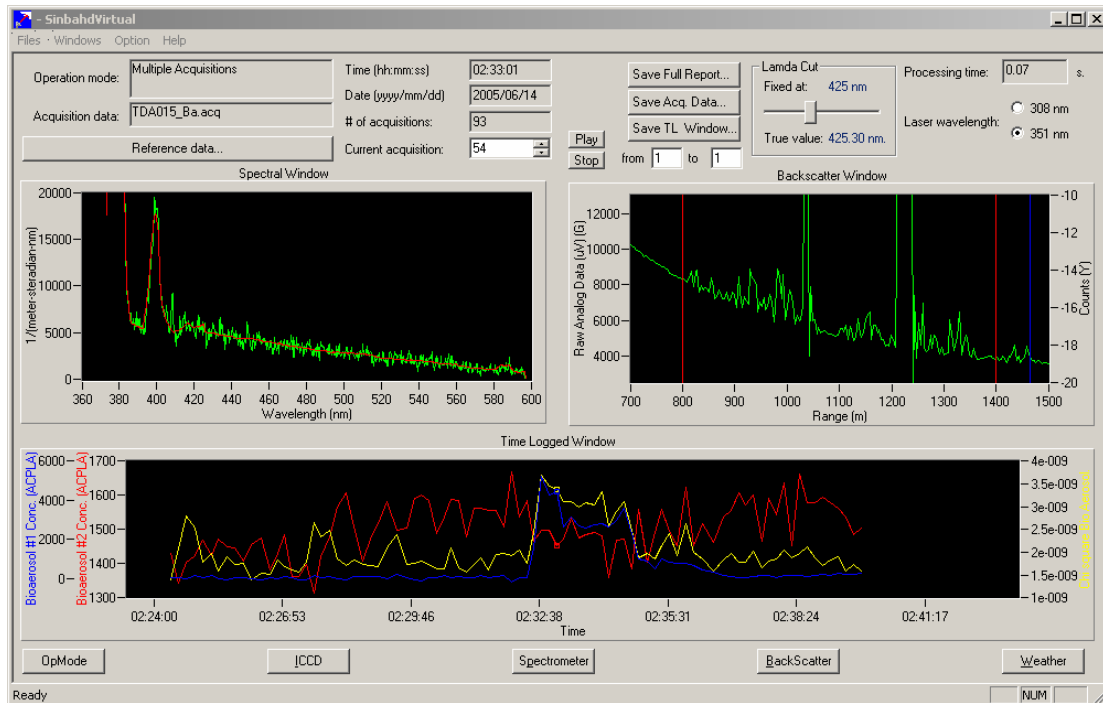


**Figure 24.** SINBAHD Virtual interface showing the multivariate analysis results for a release of killed-Ba at 1.2 km range with a gate of 600 m (June 13<sup>th</sup>, 2007, TDA015\_Ba).

## 6.3 West Desert LIDAR referee data correlation

The calibrated concentration data of Dugway West Desert LIDAR (WDL) were used to correlate SINBAHD MA results with a concentration value. This concentration calibrated WDL signals were visually correlated as best as possible. However, it must be underline that their respective line of sights through the cloud, are not exactly the same which could induce a de-correlation either temporally or spatially between the WDL and SINBAHD results. This correlation process allowed calculation of SINBAHD concentration detection limit for different simulant/interferent. The obtained results are summarized in Table 6 and presented in the present section.

The WDL referee data were previously background subtracted and smoothed with a moving average over 30 meters algorithm to remove outliers. The concentration length was obtained by integrating the concentration over the region where the cloud appeared and multiplying this later by the length of a bin. Outliers in the time series are usually the result of transient outliers in the data and should not be considered physical realizations of concentration. Probable sources include moths and other small hard targets. The WDL was either used in starring or in sweeping mode. For this later, the WDL swept the field to generate images of the cloud in lieu of simply staring at a fixed azimuth angle. In these cases, the values reported for each sweep are the maximum observed during the sweep.

*Table 6. Overview of SINBAHD/WDL correlation results during JBSDS Demo II trial.*

<b>Trial name</b>	<b>target range (km)</b>	<b>SINBAHD/WDL correlation</b>	<b>cloud depth (m)</b>	<b>4sigma kppl</b>
TDA015_Ba	1.2	good, complete	10	17.1
TDA021_Ba	2.6	fair, complete	60	6.4
TDA017_Yp	1.2	good, partial WDL	10	0.8
TDA027_Yp	1.5	good, complete	50	0.06
TDA013_BG	1.2	good, partial WDL	15	9.6
TDA019_BG	2.0	good, soil interference	60	2.3
TDA024_BG_puff	2.5	good, complete	50	4.7
TDA033_BG_aerial	3.2	low, partial WDL data	27	11.0
TDA034_BG_aerial_2	2.5	low (sweeping)	300	0.2
TDA016_EH	1.2	good, partial WDL	12	0.2
TDA025_EH	2.5-2.6	OK, complete	50	0.06
TDA026_MS2	1.6	good, complete	20	0.5
TDA011_OV	btw 0.8-1.4	OK, partial	12	1.5
TDA020_OV	2.3	low (sweeping)	50	0.4
TDA010_yellowsmoke	1.2	OK, WDL: outliers	15	0.05
TDA028_yellow_smoke	?	too partial WDL data	?	N/A
TDA032_fog_oil	1.5	no WDL data	50	N/A
TDA006_diesel	1.2	OK, complete	15	1.9
TDA018_diesel_exhaust	1.2	fair, low S/N SINBAHD	20	0.6
TDA023_diesel_exhaust	2.3-2.4	good, complete	23	0.4
TDA008_tires	1.2	fair, low S/N SINBAHD	10	10
TDA007_burningbrush	1.2	good, complete	15	3.5
TDA009_cotton	1.2	fair, low S/N SINBAHD	10	1.9
TDA005_Topsoil	1.2	fair, low S/N SINBAHD	10	10.6

The WDL concentration length data were convoluted with a 10 seconds window in order to be comparable with SINBAHD data. Once the visual correlation between WDL and SINBAHD MA result is done, the equivalent concentration of SINBAHD detection threshold can be evaluated. This latter consists in four times the standard deviation of the specie signature amplitude when the specie is not yet present. This 4sigma directly gives the detection limit of SINBAHD for that particular material at a given range and cloud depth.

**Trial:** TDA015\_Ba, June 13<sup>th</sup> 2005.

**Dissemination:** 20 g of dry killed *Bacillus anthracis* (Ba) with the point mechanism.

**SINBAHD probed volume:** 600 m wide at 800 m range.

**Target range:** 1.2 km.

The qualitative correlation between WDL calibrated concentration length and the killed-Ba normalized signature amplitude from the multivariate analysis of SINBAHD acquired data, is in the present case, quite good (Figure 25). One interesting fact to notice is that the bioaerosol (pink dashed line) is detected even at lower signal level than the background (green triangles). Once the correlation between WDL and SINBAHD MA results is made and the off-signal standard deviation of the bioaerosol is calculated (85 counts), the cloud depth must be evaluated from the backscatter response, which has a precision of a few meters, in order to determine the detection limit. In the present case, the killed-Ba signature amplitude of 5 100 counts was evaluated to correspond to 2 550kppl\*m for a cloud depth evaluated at 10 m (255kppl). The detection limit which is defined here as corresponding to 4 times the standard deviation of the killed-Ba signature amplitude while no cloud is detected is hence 340 counts (4\*85ct). This concentration length (CL) detection limit, expressed in particle per liter of air times meter (ppl\*m) with the help of the obtained correlation (340 ct\*2550kppl\*m/5 100ct = 171 kppl\*m). This gives a 17 kppl detection limit for this 10-m killed-Ba cloud at a range of 1.2 km.

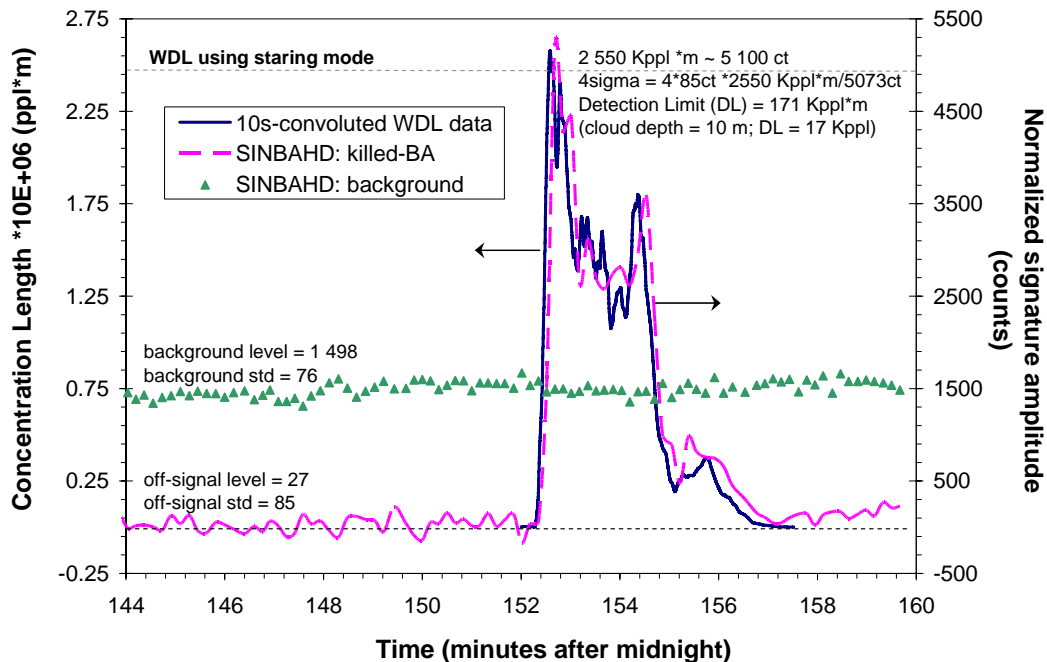


**Figure 25.** WDL calibrated concentration (solid blue line) and SINBAHD multivariate analysis results (dashed pink for Killed Ba; green triangles for background) for TDA015-Ba at 1.2 km.

**Trial:** TDA021\_Ba, June 14<sup>th</sup> 2005.

**Dissemination:** 20 g of dry killed *Bacillus anthracis* (Ba) with the point mechanism.

**SINBAHD probed volume:** 500 m wide at 2 200 m range.

**Target range:** 2.6 km.

Figure 26 presents the results obtained for a killed-Ba release at 2.6 km using a gate of 500 m wide at a range of 2 200m. The qualitative correlation is here less obvious than in the previous case due to SINBAHD low signal to noise ratio and to some extent to the fact that the WDL was used in the sweeping mode. Indeed, the WDL data are much less susceptible to correlate well with the ones of SINBAHD depending on the cloud shape, dispersion and evolution versus the interrogated spatial window from SINBAHD, which is a staring sensor. The calculated killed-Ba signature amplitude (pink line), which has a low signal to noise ratio (S/N) of around 3, is significantly lower than the one of the background (green triangles). In this particular case, this translates into a real time spectral data showing no evidence of the killed-Ba cloud (see Table 4). Once the MA is performed, a detection signal for the killed-Ba (solid pink line) can be obtained from the acquired spectral signal, which includes background LIF (green triangles).

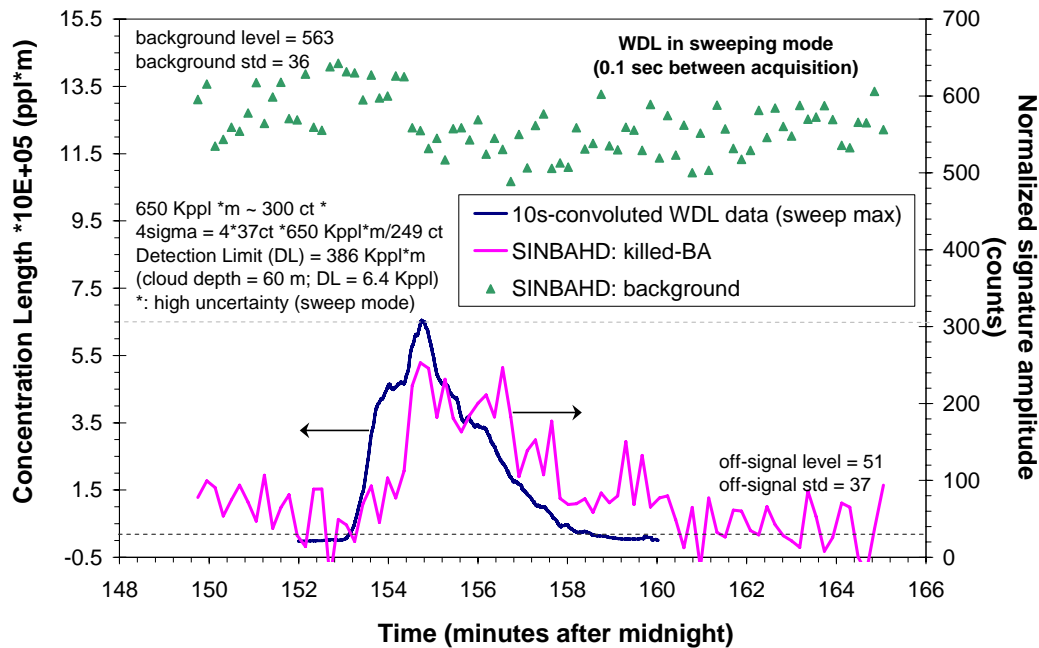


**Figure 26.** WDL calibrated concentration (solid blue line) and SINBAHD multivariate analysis results (solid pink line for Killed Ba; green triangles for background) for TDA021-Ba at 2.6 km.

**Trial:** TDA017\_Yp, June 13<sup>th</sup> 2005.

**Dissemination:** 3.5 liters of killed *Yersinia pestis* (YP) with the point mechanism.

**SINBAHD probed volume:** 600 m wide at 800 m range.

**Target range:** 1.2 km.

Figure 27 presents the obtained results for a killed-Yp release at 1.2 km using a gate of 600 m wide at a range of 800m. Correlation could be performed only over a limited section of the trial since the rest of the WDL data were not available. For each result presented in this section, all the available data from the WDL referee system are taken into account and shown in their respective figure. Even though the correlation could only be evaluated over a limited portion of the release, the obtained results show a high correlation level. The evaluation of the cloud depth was in this case, not obvious since the backscatter response from the cloud was at about the same range as a hard target return (peak in the elastic return) and was hence not clearly observable. The obtained detection limit is 0.83 kppl of killed-Yp at a range of 1.2 km for a cloud of about 10 m or a concentration-length (CL) detection limit of 8.3 kppl\*m.

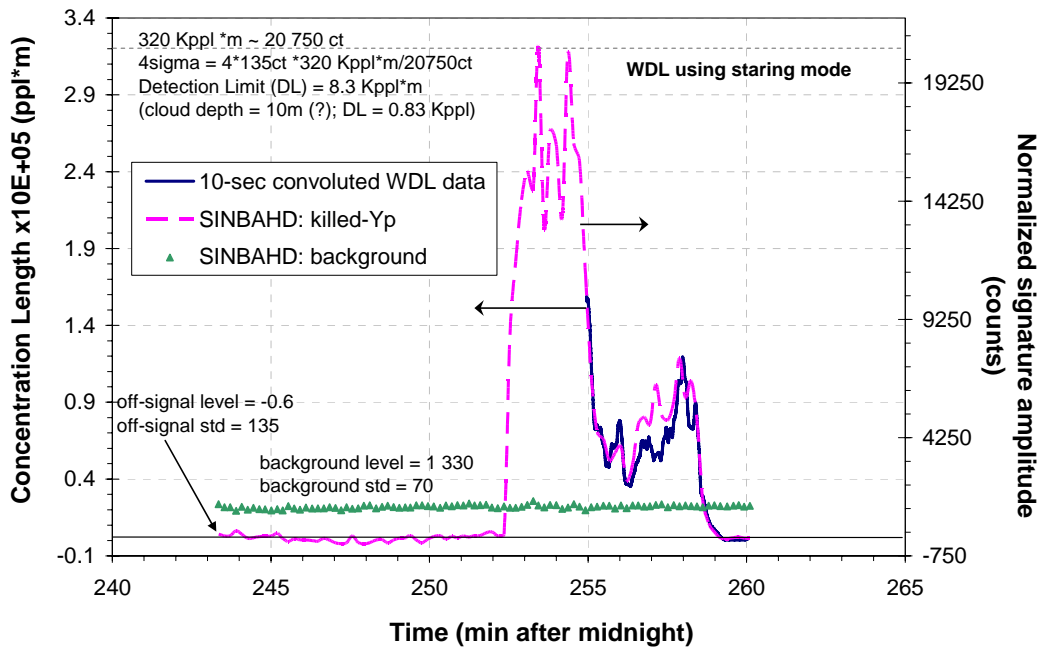


**Figure 27.** WDL calibrated concentration (solid blue line) and SINBAHD multivariate analysis results (dashed pink for Killed Yp; green triangles for background) for TDA017-Yp at 1.2 km.

**Trial:** TDA027\_Yp, June 15<sup>th</sup> 2005.

**Dissemination:** 7.0 liters of killed *Yersinia pestis* (YP) with the point mechanism.

**SINBAHD probed volume:** 400 m wide at 1 300 m range.

**Target range:** 1.45 km.

Figure 28 shows the results for a killed-Yp release at 1.45 km using a gate of 400 m wide at a range of 1 300m. The correlation is once again fairly good even though the WDL was used in the sweeping mode. The choice for SINBAHD to use a fairly large gate compared to the cloud depth, 400 versus 50 m in the present case, was to make sure that the cloud would be detected during the entire trial time without changing the gate parameters. A disadvantage of this is a higher background level (green triangles), which is however not a major issue due to the data processing technique chosen in the case where the spectral signature of the background can be easily discriminated from the one of the released material. A weakness of the multivariate analysis can be observed on the background signature amplitude signal (green triangles) while killed-Yp is detected. Indeed, as the killed-Yp normalized signature amplitude signal stays high, the one of the background is also slightly amplified due to some cross talk between the two signatures. This means that some fluorescence emitted by the released material is assumed as coming from the background, which one should have a fairly stable amplitude level during the presence and in the absence of a specific released bioaerosol.

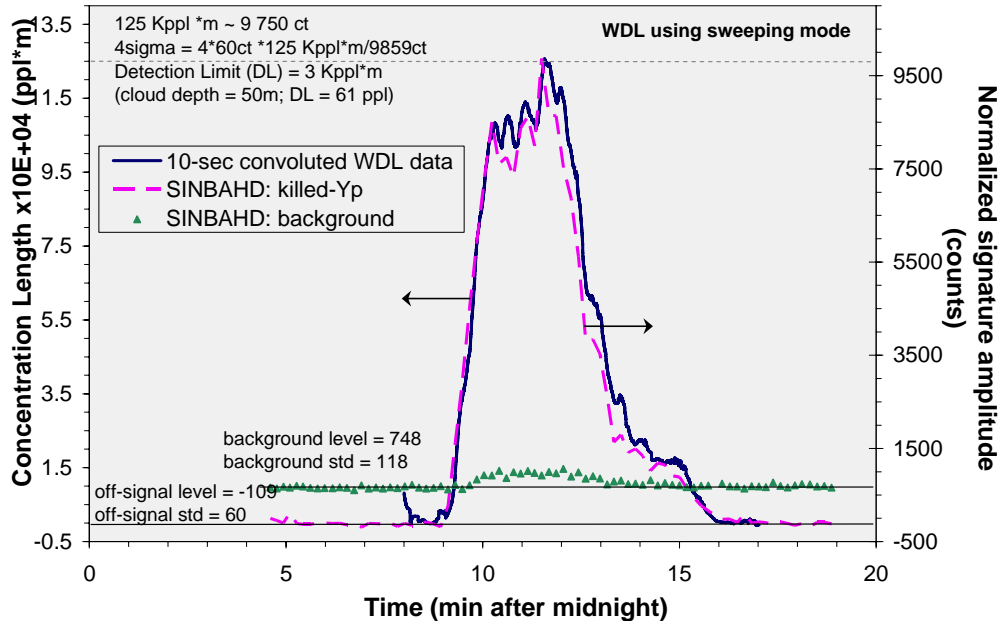


**Figure 28.** WDL calibrated concentration (solid blue line) and SINBAHD MA results (dashed pink for Killed Yp; green triangles for background) for TDA027- Yp at 1.45 km.

**Trial:** TDA013\_BG, June 13<sup>th</sup> 2005.

**Dissemination:** 77 g of dry *Bacillus subtilis* var. *niger* (BG) with the point mechanism.

**SINBAHD probed volume:** 600 m wide at 800 m range.

**Target range:** 1.2 km.

Figure 29 displays the results obtained for a BG release from the point mechanism at 1.2 km range using a gate of 600 m wide at a range of 800m. The correlation between WDL and SINBAHD MA is good but partial due to missing WDL data. Looking at the temporal evolution of the background signature amplitude (green triangles), the cross-talk between the BG and background normalized signatures seems to be negligible. This later fact implies that the multivariate analysis data processing seems to have efficiently discriminated between the released stimulant, BG, and the background aerosols present in the probed volume. The obtained detection limit is 9.6 kppl of BG at a range of 1.2 km for a cloud of about 15 m or a CL detection limit of 144 kppl\*m.

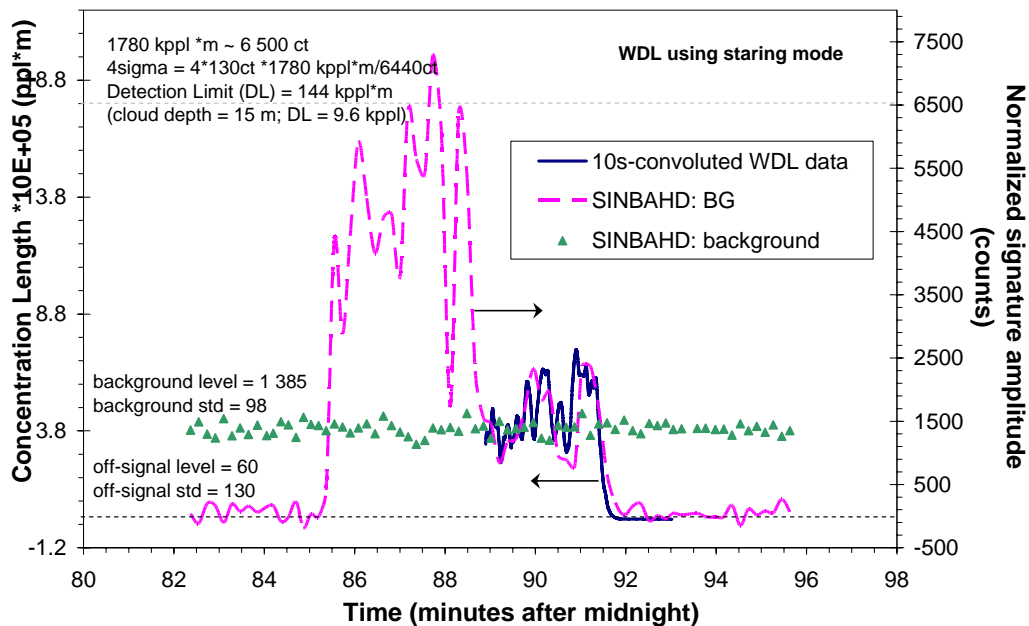


**Figure 29.** WDL calibrated concentration (solid blue line) and SINBAHD multivariate analysis results (dashed pink for BG; green triangles for background) for TDA013-BG at 1.2 km.

**Trial:** TDA019\_BG, June 14<sup>th</sup> 2005.

**Dissemination:** 85.5 g of dry *Bacillus subtilis* var. *niger* (BG) with the point mechanism.

**SINBAHD probed volume:** 1 000 m wide at 1 700 m range.

**Target range:** 2.0 km.

Figure 30 presents the obtained results during a BG release from the point mechanism at 2 km range using a 1 000 m gate at a range of 1.7 km. The obtained correlation could be qualified as good even though some interference from the soil was observed in the SINBAHD processed data. Initially, the gate was set to 400 m and shortly after the dissemination begun, the gate was stretched to 1000 m since no signal was yet observed. This change in the gate width is obvious from the change in the background (green triangles) and off-signal (pink dashed line) signature amplitude levels (indicated by vertical gray dashed line). An additional particular aspect of this trial is some period of soil interference underlined by either a cut-off of this parasitic signal and/or a vertical gray dashed oval. Indeed, the trailer and laser beam are neither perfectly stable which explains why the laser beam can hit the soil at a certain range hence creating this soil interference. This problem can be eliminated by slightly raising the laser beam elevation axe. The cloud depth was difficult to evaluate since the cloud was spread out and also due to soil interferences.

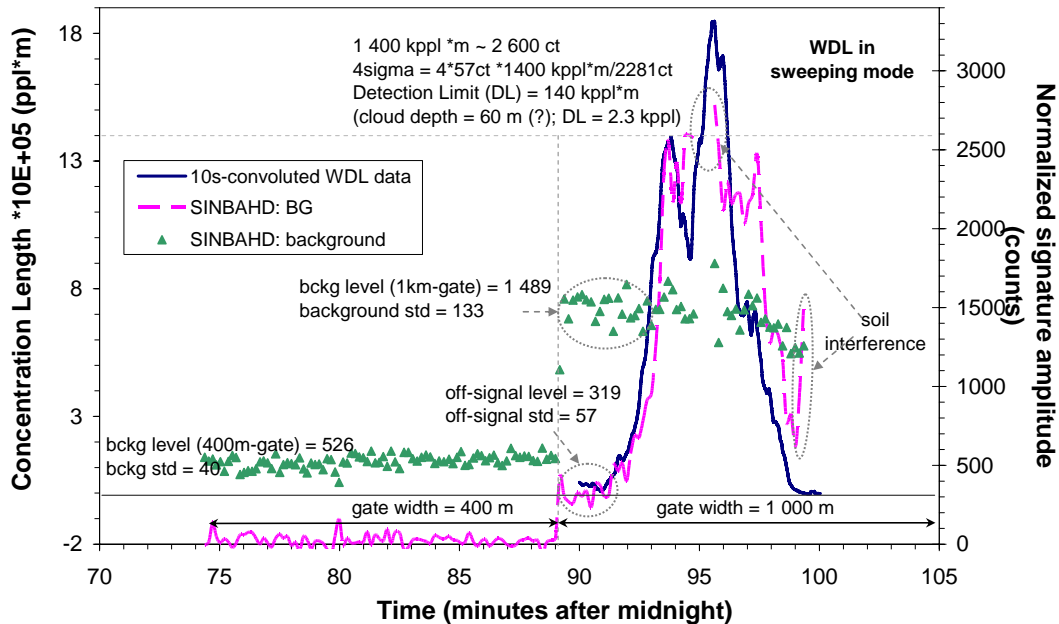


**Figure 30.** WDL calibrated concentration (solid blue line) and SINBAHD multivariate analysis results (dashed pink for BG; green triangles for background) for TDA019-BG at 2.0 km.

**Trial:** TDA024\_BG\_puff, June 14<sup>th</sup> 2005.

**Dissemination:** 400 g of dry *Bacillus subtilis* var. *niger* (BG) with the puff mechanism.

**SINBAHD probed volume:** 500 m wide at 2 200 m range.

**Target range:** 2.5 km.

Figure 31 shows the results for a BG release from the puff mechanism at 2.5 km range using a 500 m gate at a range of 2.2 km. The correlation is once again quite good even though the WDL was used in the sweeping mode. Cross-talk between BG (pink dashed line) and background (green triangles) normalized signatures is once again not observable. The detection limit obtained in this particular trial is 4.7 kppf of BG at a range of 2.5 km for a cloud of about 50 m. It must be underline that the evaluated detection limit is based on two major assumptions: 1) the cloud depth is known and constant over the release, and 2) the cloud concentration measured by the two sensors, SINBAHD and the WDL, is the same. The first assumption can be verified from the measured elastic return for most releases (table 6). The second assumption is much less obvious to validate since the releases are made in the open-air and that the two sensors line of sight are not the same, especially when the WDL is operated in the sweep mode. The ideal configuration would be to probe the cloud within a chamber, like the sABT in other to optimize cloud homogeneity. SINBAHD had a PC problem, which has led to the interruption of the acquisition.

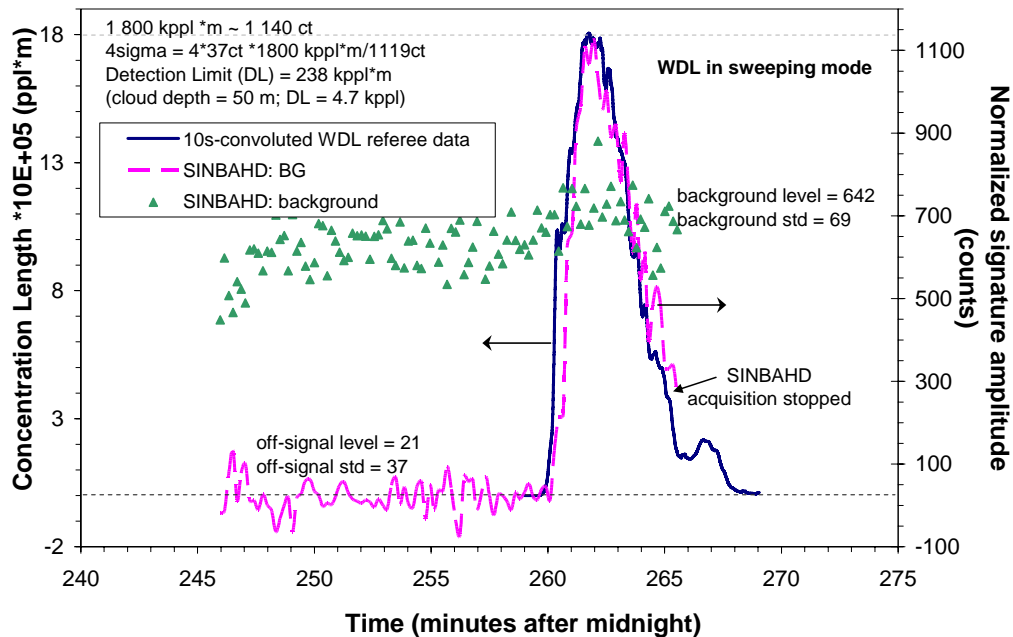


**Figure 31.** WDL calibrated concentration (solid blue line) and SINBAHD multivariate analysis results (dashed pink for BG; green triangles for background) for TDA024-BG at 2.5 km.

**Trial:** TDA033\_BG\_aerial, June 15<sup>th</sup> 2005.

**Dissemination:** 2 700 g of dry *Bacillus subtilis* var. *niger* (BG) released by an airplane.

**SINBAHD probed volume:** 400 m wide at 3 000 m range.

**Target range:** 3.2 km.

Figure 32 presents the results for a BG release from an airplane at 3.2 km range using a 400 m gate at 3 km. The WDL data available are only representing a fairly small portion of the entire trial, which is not sufficient to adequately qualify the correlation between WDL and SINBAHD MA results. But only considering the short WDL data portion, the best correlation obtained could be qualified of poor. This could be attributed once again to the sweeping mode of the WDL referee system. Indeed, since the cloud was fairly far and spread out, 27 m thick at 3.2 km, the characterization of the cloud evolution is even more susceptible to diverge when comparing the information from a static transect to the one from the complete cloud mapping. SINBAHD is a static sensor characterizing the aerosols found in a spatial window defined by the beam cross section at a certain range and the gate width. On the other hand, the WDL referee system is characterizing the entire cloud when used in the sweeping mode and then reports the maximum concentration-length observed during the complete sweep over the entire cloud. Following the above considerations, the calculated detection limit in this particular trial can not be considered as representative.

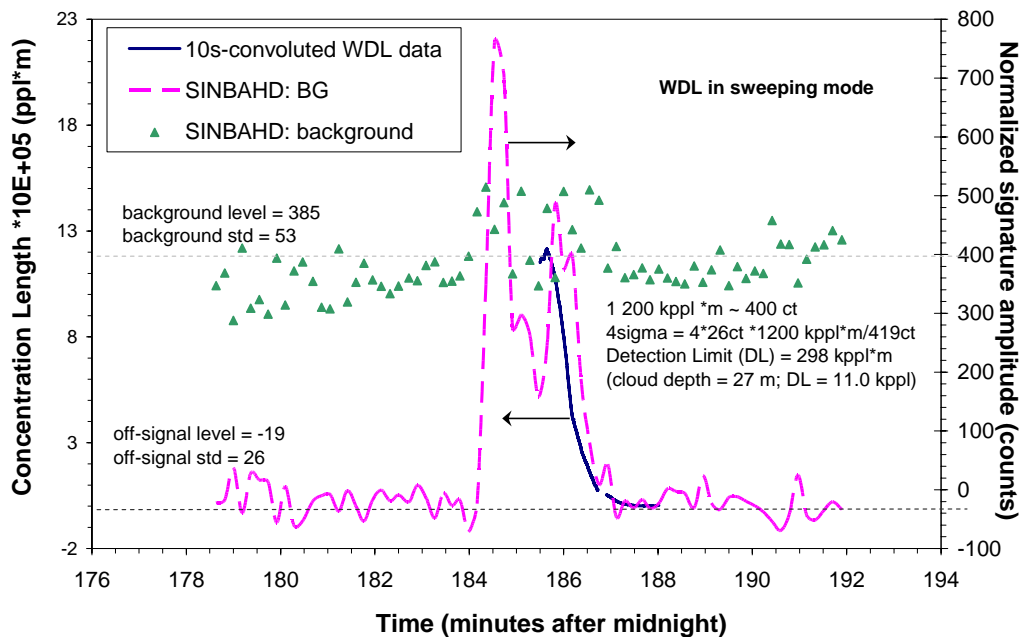


**Figure 32.** WDL calibrated concentration (solid blue line) and SINBAHD multivariate analysis results (dashed pink for BG; green triangles for background) for TDA033-BG at 3.2 km.

**Trial:** TDA034\_BG\_aerial\_2, June 14<sup>th</sup> 2005.

**Dissemination:** 2 700 g of dry *Bacillus subtilis* var. *niger* (BG) released by an airplane.

**SINBAHD probed volume:** 400 m wide at 2 200 m range.

**Target range:** 2.5 km.

Figure 33 presents the obtained results for BG released from an air plane at 2.5 km range using a 400 m gate at a range of 2.2 km. Once again, the correlation between WDL and SINBAHD MA results is quite poor due to the non similar probed atmospheric volume. For this particular case, the selected gate for SINBAHD acquisition did not enclose the entire cloud along the LIDAR beam axis, which could be observed from the bioaerosol cloud elastic returned measured by the backscatter. The gate parameters were not adjusted to enclose the entire cloud during release for consistency in background and off-signal signature amplitudes. Besides, the WDL was used in sweeping mode, hence adding one other potential source of disparity between WDL and SINBAHD MA results. These two states of fact impact on the probed volume by each sensor, explaining the high discrepancy between their respective results. The presented correlation is hence quite arbitrary and the calculated detection limit should only be considered as a range indicator.

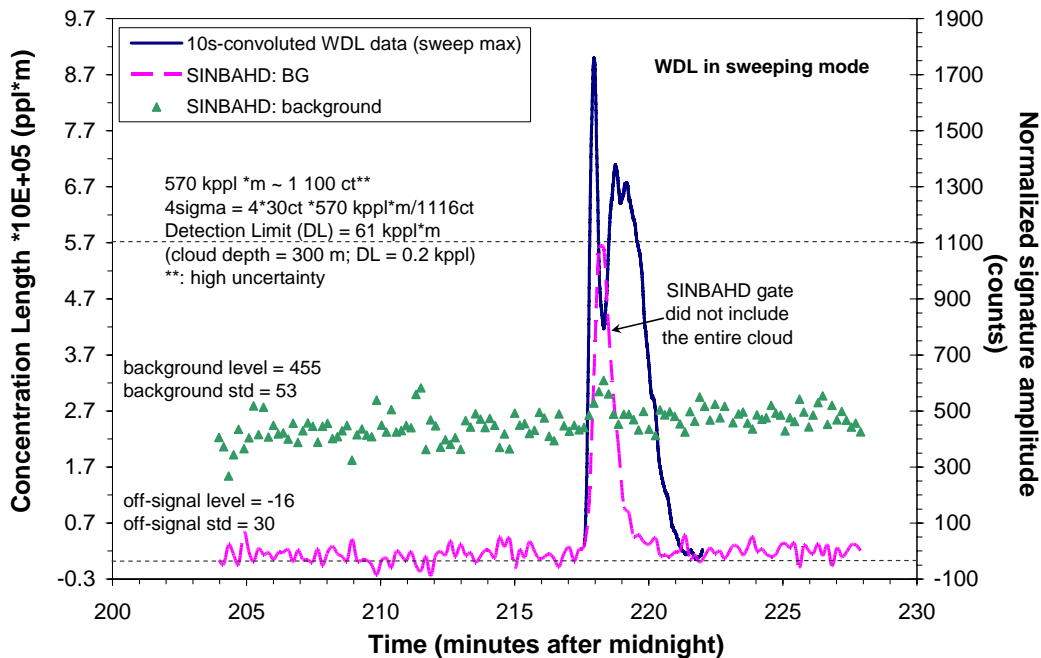


**Figure 33.** WDL calibrated concentration (solid blue line) and SINBAHD multivariate analysis results (dashed pink for BG; green triangles for background) for TDA034-BG at 2.0 km.

**Trial:** TDA016\_EH, June 13<sup>th</sup> 2005.

**Dissemination:** 7 liters of wet *Erwinia herbicola* (EH) with the point mechanism.

**SINBAHD probed volume:** 600 m wide at 800 m range.

**Target range:** 1.2 km.

Figure 35 shows the results obtained for an EH release with the point mechanism at 1.2 km, using a gate of 600 m wide at a range of 800 m. The correlation appears good even though partial. The visual correlation is based on both the detection of the cloud over time and the relative intensity during the cloud detection. The release scheme, when possible (excluding the burning material) was always to first build up a fairly high concentration cloud and then ramp down the concentration to obtain a wider range of detected concentration. Those two distinct concentration levels also allow a better evaluation of the relative intensity correlation between WDL and SINBAHD cloud detection signals. In the present case, from the partial data available from the WDL, the detection of the cloud in time is almost perfectly correlated and for the relative intensity, it is quite difficult to evaluate due to a too short time period of overlapped data and also since they are all located in one single concentration level portion of the release. Negligible cross-talk between EH and background signature is present from the multivariate analysis of the SINBAHD data. The obtained detection limit for EH at a range of 1.2 km is 2.5 kppl\*m (210 kppl x 12 m).

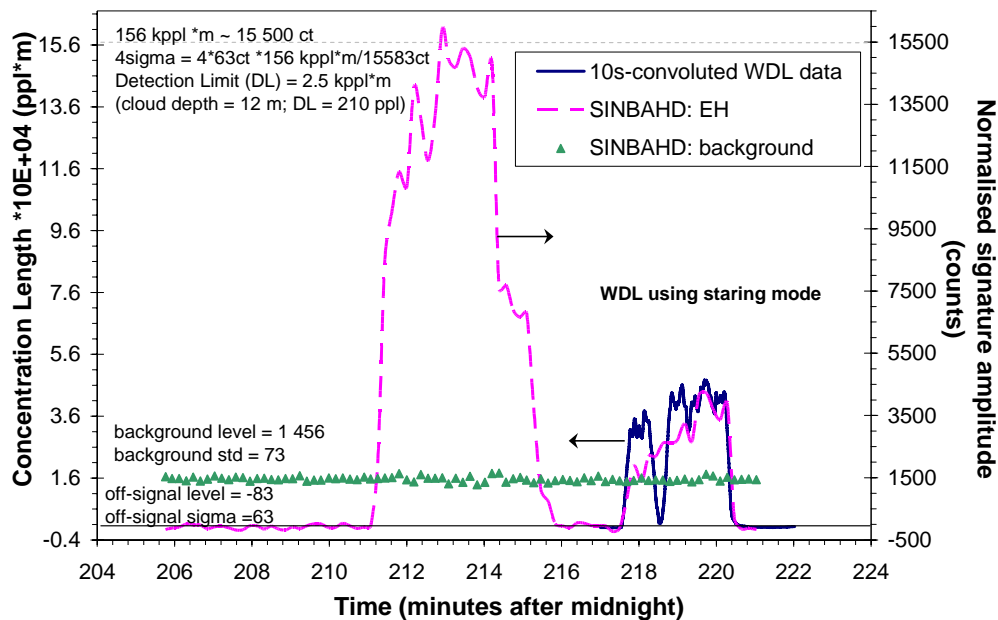


**Figure 35.** WDL calibrated concentration (solid blue line) and SINBAHD multivariate analysis results (dashed pink for EH; green triangles for background) for TDA016-EH at 1.2 km.

**Trial:** TDA025\_EH, June 14<sup>th</sup> 2005.

**Dissemination:** 5 liters of wet *Erwinia herbicola* (EH) with the point mechanism.

**SINBAHD probed volume:** 500 m wide at 2 200 m range.

**Target range:** 2.5 km.

Figure 36 presents the obtained results during an EH release with the point mechanism at 2.5 km, using a gate of 500 m wide at a range of 2.2 km. The correlation is not perfect but quite acceptable considering that the WDL referee system was used in the sweeping mode. The cloud depth could not be defined precisely (marked by the question mark in Figure 36) following the low signal to noise ratio of the elastic return from the bio-cloud measured by the backscatter PMT. The evaluation of the cloud depth is quite important in order to evaluate the concentration detection limit of the system since this latter depend. Once again, no significant cross-talk between EH and background spectral signatures was observed from the multivariate analysis of the SINBAHD data. The obtained detection limit for EH at a range of 2.5 km is 3 kpl\*m, which appears low compared to the previous results: 2.5 kpl\*m at 1.2 km range. Since the range is two times farther away, detection limit 4 times higher, around 10 kpl\*m, was expected. This later expected value is 3 higher than the one obtained (3 kpl\*m). The point is to underline the difficulty to precisely evaluate detection limits based on concentration calibrated measurement made by other sensor. In deed, with this particular methodology, everything relies on the correlation of the two sensor results.

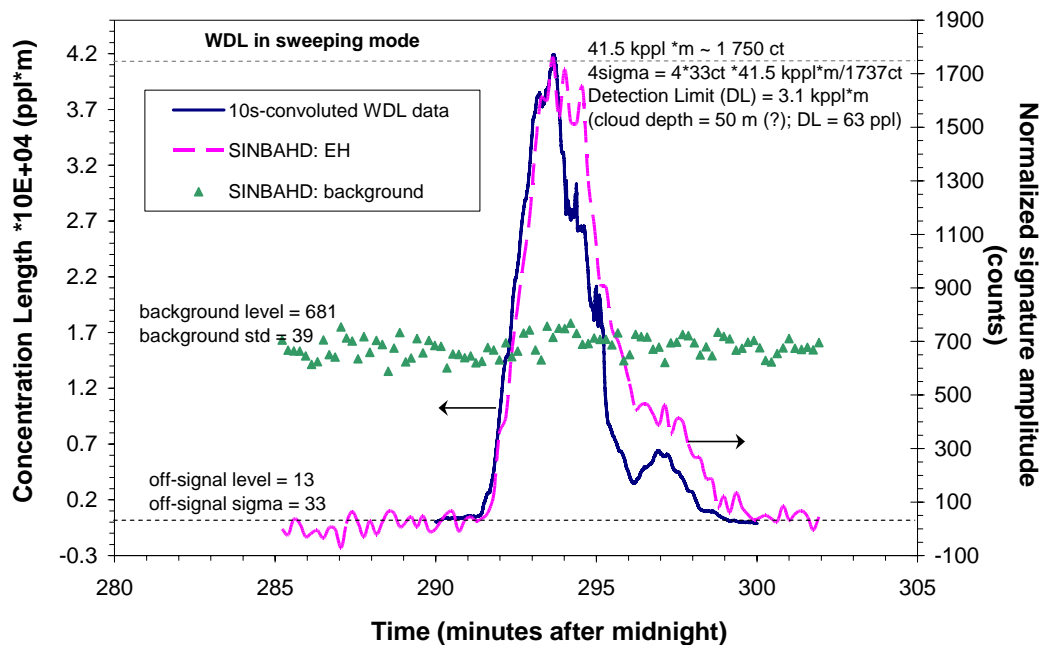


**Figure 36.** WDL calibrated concentration (solid blue line) and SINBAHD multivariate analysis results (dashed pink for EH; green triangles for background) for TDA025-EH at 2.5 km.

**Trial:** TDA026\_MS2, June 15<sup>th</sup> 2005.

**Dissemination:** 13 liters of wet bacteriophage (MS2) with the point mechanism.

**SINBAHD probed volume:** 400 m wide at 1 400 m range.

**Target range:** 1.55 km.

Figure 37 presents the results of an MS2 release with the point mechanism at 1.55 km, using a gate of 400 m wide at a range of 1.4 km. This result is particularly interesting once knowing that the collected fluorescence signal from the MS2 cloud was almost not perceptible from the one of the background in the real time pre-processed data (spectral window). Indeed, the calculated MS2 normalized signature amplitude (dashed pink line) is lower and only rarely slightly higher than the one of the background (green triangles) during most of the trial (Figure 37). The correlation between WDL and SINBAHD MA results is quite good even though the S/N of the MS2 signal is low. In deed, both the cloud detection with time and the relative intensity of the detected signal correlate almost perfectly. The obtained concentration detection limit for MS2 at a range of 1.55 km is 0.5 kppl for a cloud of about 20 m or a concentration-length detection limit of 10 kppl\*m. This particular result is a good example to show the capacity of the data exploitation method (MA) used by SINBAHD, which permits to detect the presence of the MS2 at signal level lower than the one from the background.

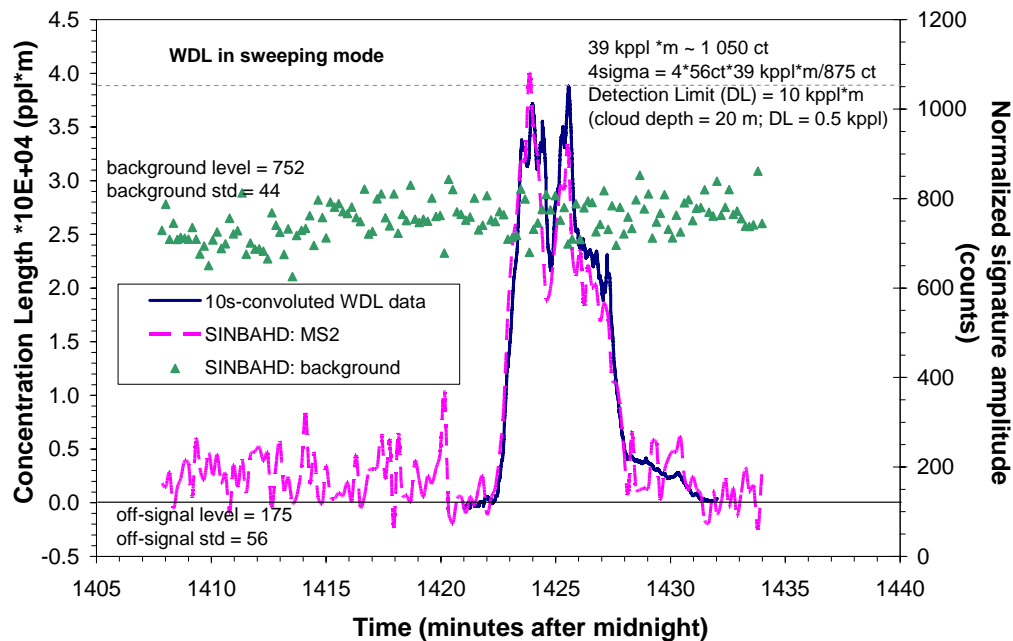


**Figure 37.** WDL calibrated concentration (solid blue line) and SINBAHD multivariate analysis results (dashed pink for MS2; green triangles for background) for TDA026-MS2 at 1.55 km.

**Trial:** TDA011\_OV, June 13<sup>th</sup> 2005.

**Dissemination:** 133 grams of dry ovalbumin (OV) with the point mechanism.

**SINBAHD probed volume:** 600 m wide at 800 m range.

**Target range:** around 1.2 km (no signal from the backscatter).

Figure 38 shows the results obtained during an OV release with the point mechanism at about 1.2 km, using a gate of 600 m wide at a range of 800 m. The OV signal from SINBAHD MA appears consistent with the WDL referee signal but the correlation between them could only be qualified of okay even though the WDL was used in the starring mode. The limited availability of WDL reference data restrains the correlation optimization. Additionally, the WDL data do not include background data, either before or after the release, which is also restraining the capacity to correlate the two sensors outputs. The cloud detection with time is not perfect but always less than a minute off-shifted and the relative intensity is also not perfect but common features can be observed on both detected signal. The obtained concentration detection limit for dry ovalbumin at a range of about 1.2 km is 1.5 kppl for a cloud of about 12 m or a concentration-length detection limit of 18 kppl\*m. The elastic return from the cloud was not recorded by the Licel PMT due to hardware/communication problem with this device, which implies that the target range and cloud depth are simply guessed based on previous release during this particular night for which stable wind conditions are assumed.

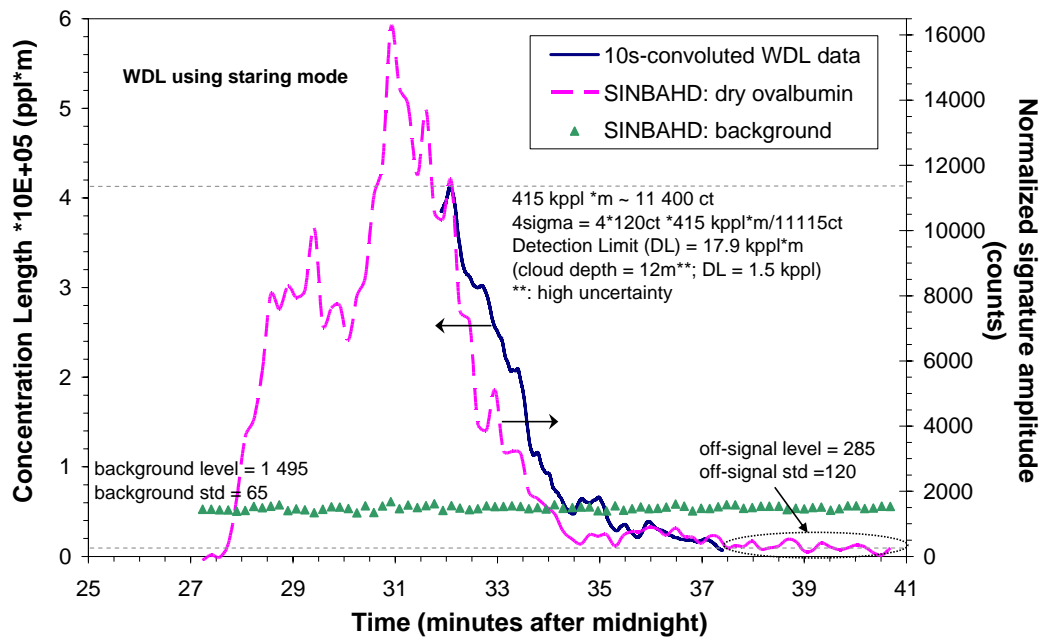


**Figure 38.** WDL calibrated concentration (solid blue line) and SINBAHD multivariate analysis results (dashed pink for OV; green triangles for background) for TDA011-OV at about 1.2 km.

**Trial:** TDA020\_OV, June 14<sup>th</sup> 2005.

**Dissemination:** 133.5 grams of dry ovalbumin (OV) with the point mechanism.

**SINBAHD probed volume:** 1 000 m wide at 1 500 m range.

**Target range:** 2.3 km.

Figure 39 presents the obtained results for an OV release made with the point mechanism at about 2.3 km, using a gate of 1 000 m wide at a range of 1.5 km. Once again, the collected fluorescence signal from the OV cloud was not perceptible from the one of the background in the real time pre-processed data (see Table 4), which can be seen by a lower amplitude for the OV signature amplitude (dashed pink) versus the one of the background (green triangles). The correlation between WDL and SINBAHD MA results was qualified of low. In deed, the cloud detection with time seems to agree at three strategic points: 1) appearance of the cloud detection signal (first signal rise), 2) concentration diminution (lowering down) and 3) end of the cloud presence in the detection signal (back to background level). The visual correlation was chosen to optimize background level versus signal level which was obtained by best matching the low concentration portion of the release rather than the higher one, explaining the 'high uncertainty' note for the CL to signature amplitude conversion. The low correlation level obtained is assumingly due to both the low S/N of the OV signal and the sweeping mode used by the WDL.

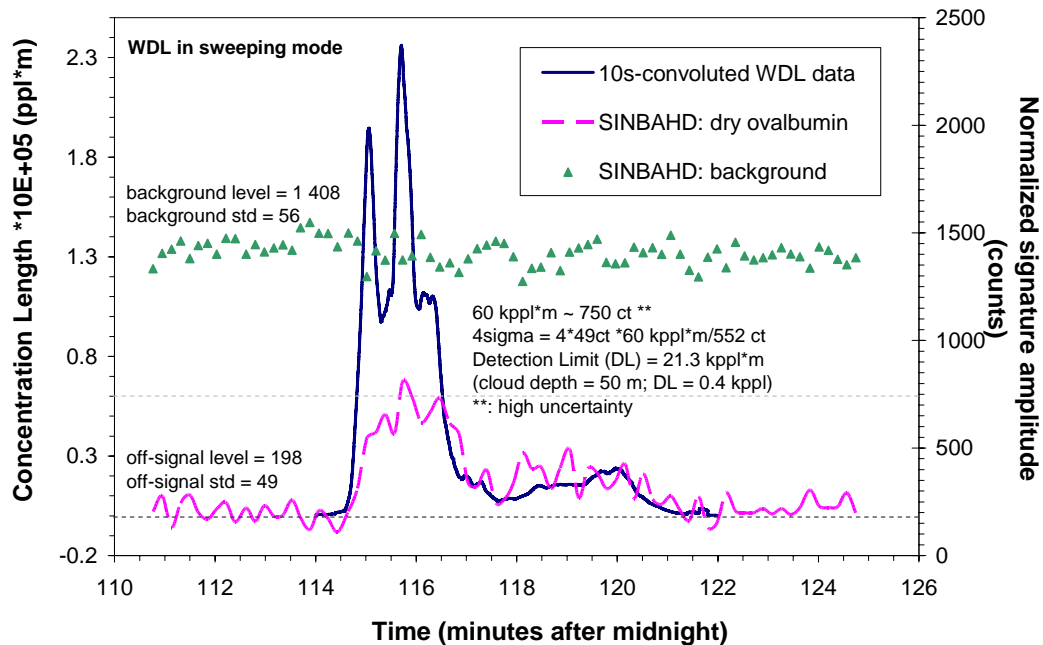


**Figure 39.** WDL calibrated concentration (solid blue line) and SINBAHD MA results (dashed pink for OV; green triangles for background) for TDA020-OV at 2.3 km.

**Trial:** TDA010\_yellowSmoke, June 12<sup>th</sup> 2005.

**Dissemination:** 2 colored smoke grenades (M18 - yellow).

**SINBAHD probed volume:** 600 m wide at 800 m range.

**Target range:** 1.2 km.

Figure 40 presents the results obtained during a yellow smoke release at about 1.2 km, using a gate of 600 m wide at a range of 800 m. First of all, it must be underline that the WDL reference data were sporadically polluted by outliers represented by two gray-shaded regions on Figure 40. A cross-talk effect between the Yellow smoke and background signatures is clearly observable on the background signature amplitude. This could be related to the fact that yellow smoke signature maxima, around 550 nm (Figure 17), is closer to the one of the background, around 520 nm (Figure 11), compared to all other material's signatures (except burning brush and BG). The correlation between SINBAHD MA and WDL results is perceptible but far from being perfect. In deed, the last portion of the trial, after 1415 minutes, shows high discrepancy between calibrated data and MA results. This could be attributed to important discrepancy in the cloud characteristics present in each probed volumes by the two sensors. Actually, the WDL referee system and SINBAHD were co-aligned but separated by about 15 meters on either side of the 101 road at DPG. This implies that even when the WDL is used in the staring mode, the cloud volume intercepted by the WDL and SINBAHD laser beams differs depending on the range of the cloud from the systems.

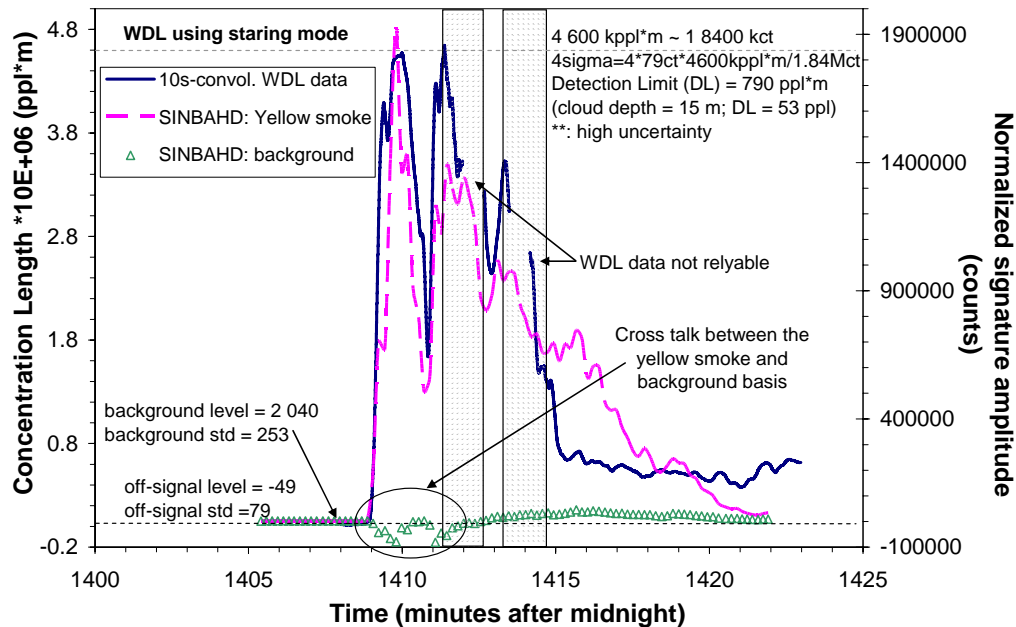


**Figure 40.** WDL calibrated concentration (solid blue line) and SINBAHD MA results (dashed pink for Yellow Smoke; green triangles for background) for TDA010-Yellow Smoke at 1.2 km.

**Trial:** TDA028\_yellow\_smoke, June 15<sup>th</sup> 2005.

**Dissemination:** 2 colored smoke grenades (M18 - yellow).

**SINBAHD probed volume:** 400 m wide at 1 300 m range.

**Target range:** between 1.3 and 1.7 km (the backscatter channel was malfunctioning).

Figure 41 shows results obtained during a yellow smoke release between 1.3 and 1.7 km, using a gate of 400 m wide at a range of 1.3 km. The available WDL reference data are covering just slightly more than three minutes of the entire release which is not enough to perform a useful correlation with SINBAHD MA results. Since no credible correlation could be made, the concentration detection limit for this yellow smoke release was not evaluated. As for the other yellow smoke release (previous page), cross talk with background spectral signature is obvious while looking at the background signature amplitude once cloud detection signal is high. The MA technique can produce impressive results but has limits like any other data exploitation techniques. The more spectral similarities there are between two signatures, the more they are susceptible to create cross-talk when used together in the Multivariate Analysis. In the case of yellow smoke grenades, the cross talk is even more apparent due to the high fluorescence level produced by this interferant.

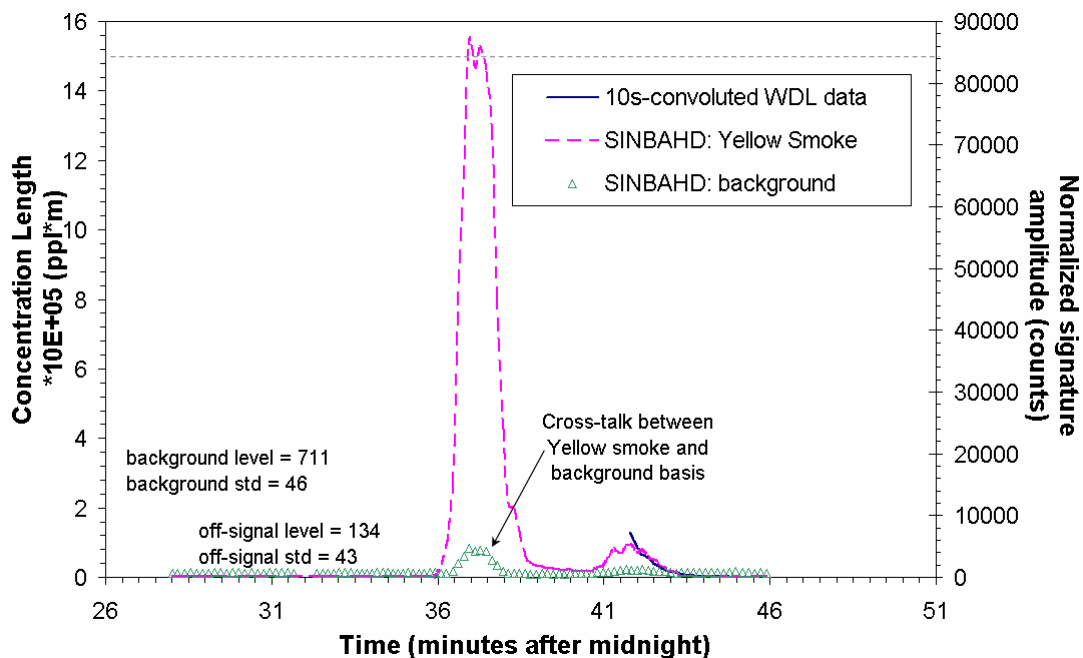


**Figure 41.** WDL calibrated concentration (solid blue line) and SINBAHD MA results (dashed pink for Yellow smoke; green triangles for background) for TDA028-Yellow Smoke at around 1.5 km.

**Trial:** TDA032\_fog\_oil, June 15<sup>th</sup> 2005.

**Dissemination:** undetermined quantity of fog oil with the point mechanism.

**SINBAHD probed volume:** 400 m wide at 1 400 m range.

**Target range:** 1.5 km.

Figure 42 presents obtained results for a fog oil release at 1.5 km, using a gate of 400 m wide at a range of 1.4 km. No data from the WDL referee system were available for this trial and hence no corresponding concentration detection limit could be extracted. The Laser Induced Fluorescence emitted by the fog oil was quite intense as seen by the much higher signature amplitude obtained for the fog oil compared to the background one. For this particular case, absolutely no cross-talk could be observed even though the high fluorescence intensity level produced by the fog oil. This later fact can be attributed to the specificity of the fog oil signature (Figure 17) related to the one used for the background (Figure 11).

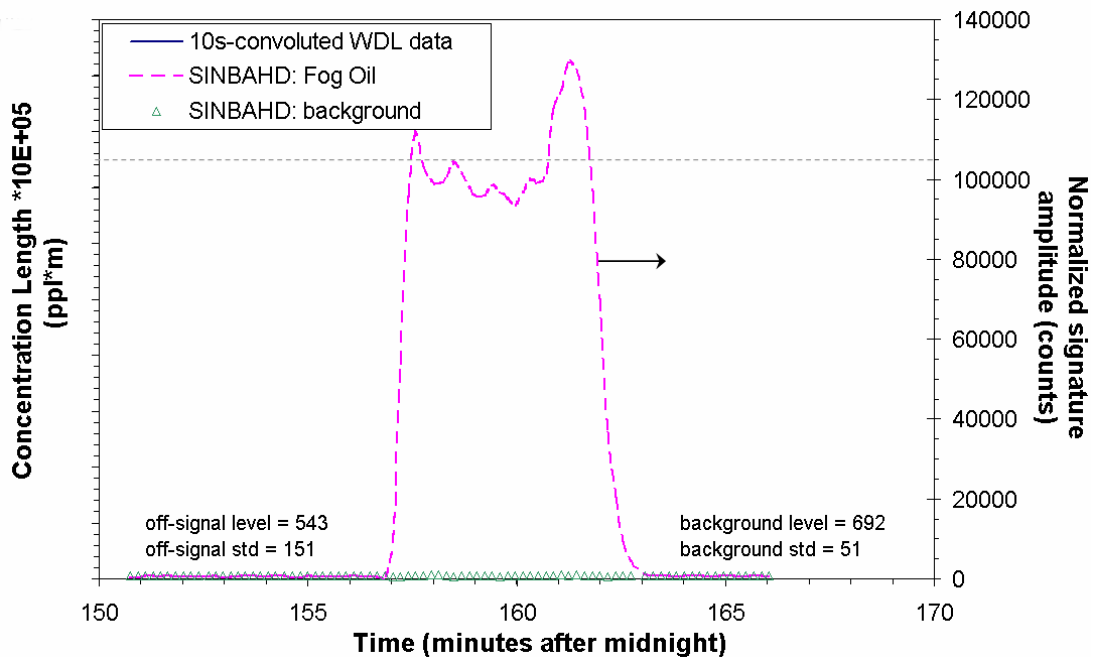


**Figure 42.** WDL calibrated concentration (solid blue line) and SINBAHD MA results (dashed pink for fog oil; green triangles for background) for TDA032-fog oil at 1.5 km.

**Trial:** TDA006\_Diesel, June 9<sup>th</sup> 2005.

**Dissemination:** diesel exhaust from a 100-KW power generator.

**SINBAHD probed volume:** 600 m wide at 800 m range.

**Target range:** 1.2 km.

Figure 43 presents the obtained results for a generator diesel exhaust at 1.2 km range using a 600 m gate at a range of 800 m. The correlation between WDL and SINBAHD MA results is fairly obvious in time but when comparing the relative signal levels, it does not appear systematically consistent. This is probably due to the different location of the two systems relatively to the cloud, hence implying probing not the same cloud volume. Depending on the homogeneity of the cloud characteristics, this difference in the cloud probed volume by the two sensors, will more or less impact on the ability to correlate their relative signal intensity. Cross-talk between the diesel and background signatures in the MA data exploitation process is again perceptible by looking at the unstable background signature amplitude (green triangles) during diesel detection portion (pink dashed line). The obtained concentration detection limit for diesel exhausted from a generator at a range of about 1.2 km is 1.9 kppl for a cloud of about 15 m or a concentration-length detection limit of 29 kppl\*m.

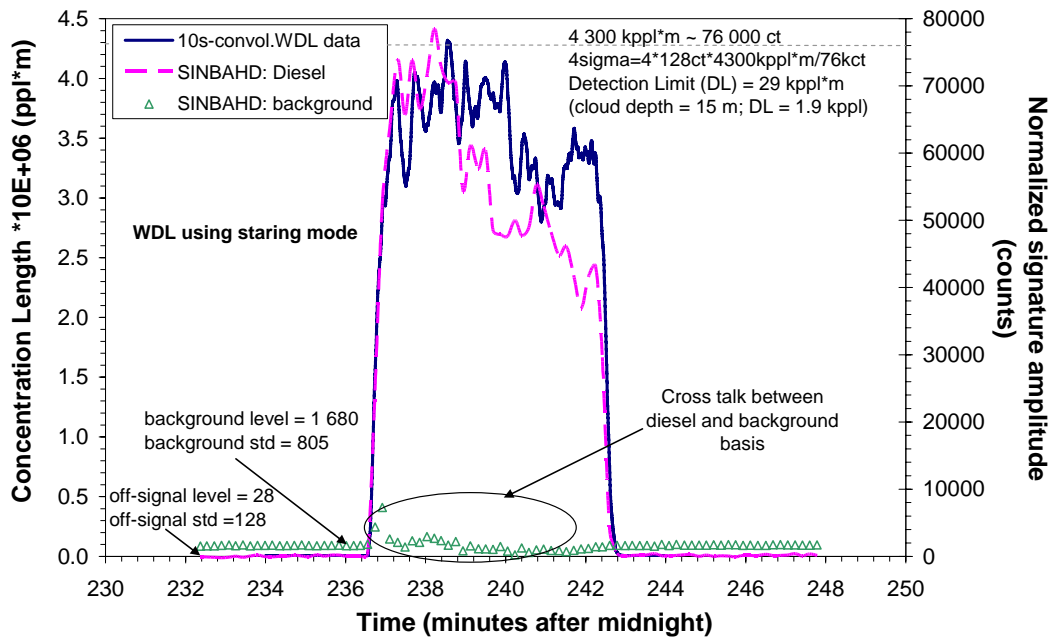


**Figure 43.** WDL calibrated concentration (solid blue line) and SINBAHD multivariate analysis results (dashed pink for diesel; green triangles for background) for TDA006-diesel at 1.2 km.

**Trial:** TDA018\_Diesel, June 13<sup>th</sup> 2005.

**Dissemination:** diesel exhaust from a HMMWV.

**SINBAHD probed volume:** 600 m wide at 800 m range.

**Target range:** 1.2 km.

Figure 44 presents the obtained results from a HMMWV diesel exhaust at about 1.2 km, using a gate of 600 m wide at a range of 800 m. The collected fluorescence signal from the exhaust of the HMMWV (diesel) could not be discriminated from the one of the background in the real time pre-processed data (see Table 4). This latter fact is demonstrated by lower diesel signature amplitude (dashed pink) versus the one of the background (green triangles). The correlation between WDL and SINBAHD MA results is fair considering the low S/N (around 3) of the diesel signal. Actually, the cloud detection signals with respect with time are not absolutely corresponding but are off-shifted by about 1 minute. The relative intensity of the two detection signals is, for its part, globally consistent with one another when considering SINBAHD low S/N. The obtained concentration detection limit for diesel exhausted from a HMMWV at a range of about 1.2 km is 0.6 kpl for a cloud of about 20 m or a concentration-length detection limit of 11.4 kpl\*m, which is about a factor of two lower and hence the same order of magnitude than the previous diesel exhaust result (Figure 43).

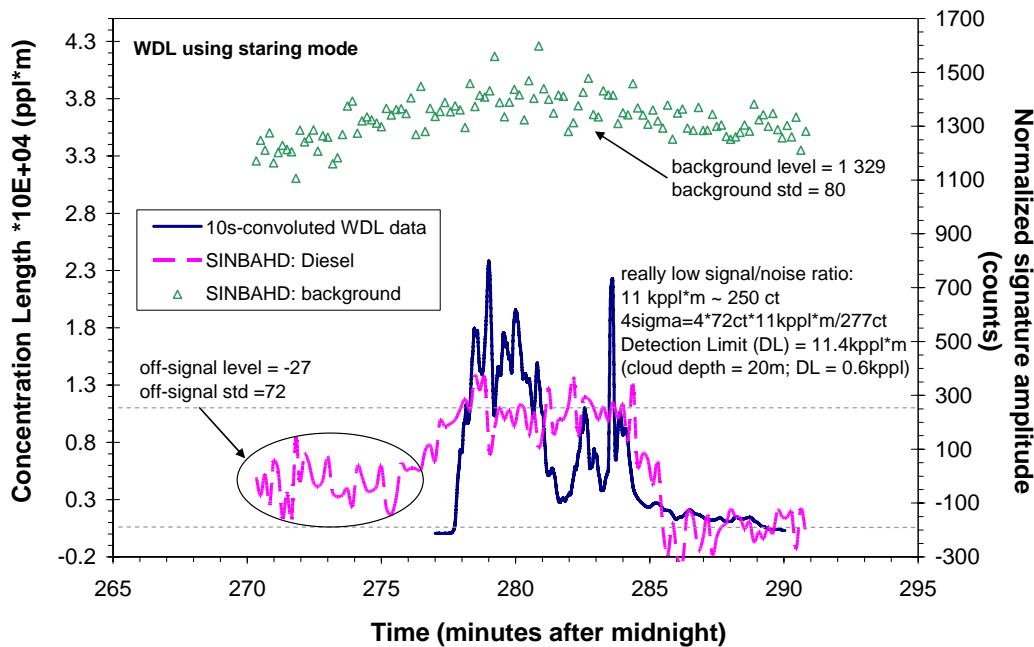


**Figure 44.** WDL calibrated concentration (solid blue line) and SINBAHD multivariate analysis results (dashed pink for diesel; green triangles for background) for TDA018-Diesel at 1.2 km.

**Trial:** TDA023\_Diesel, June 14<sup>th</sup> 2005.

**Dissemination:** diesel exhaust from a HMMWV.

**SINBAHD probed volume:** 500 m wide at 2 100 m range.

**Target range:** 2.35 km.

Figure 45 shows an additional result obtained from a HMMWV diesel exhaust this time at about 2.35 km, using a gate of 500 m wide at a range of 2.1 km. The correlation between WDL and SINBAHD MA result is good but slightly off-shifted in time by about 1 minute probably due to either or both the different position of the systems relative to the cloud and the WDL sweeping mode. The obtained concentration detection limit for diesel exhausted from a HMMWV at a range of about 2.35 km is 0.4 kppm for a cloud of about 23 m or a concentration-length detection limit of 10.2 kppm\*m, which is about the same concentration detection limit as the previous results (Figure 44) but at twice the distance which should imply a detection limit 4 times higher. This result, once again demonstrate the limit of this concentration detection limit evaluation based on the correlation of SINBAHD MA result with a concentration calibrated measurement made an other LIDAR system. All detection limit obtained by the preset approach must hence be looked at as a general evaluation of the order of magnitude of the concentration detection limit and not a precise evaluation of this important parameter.

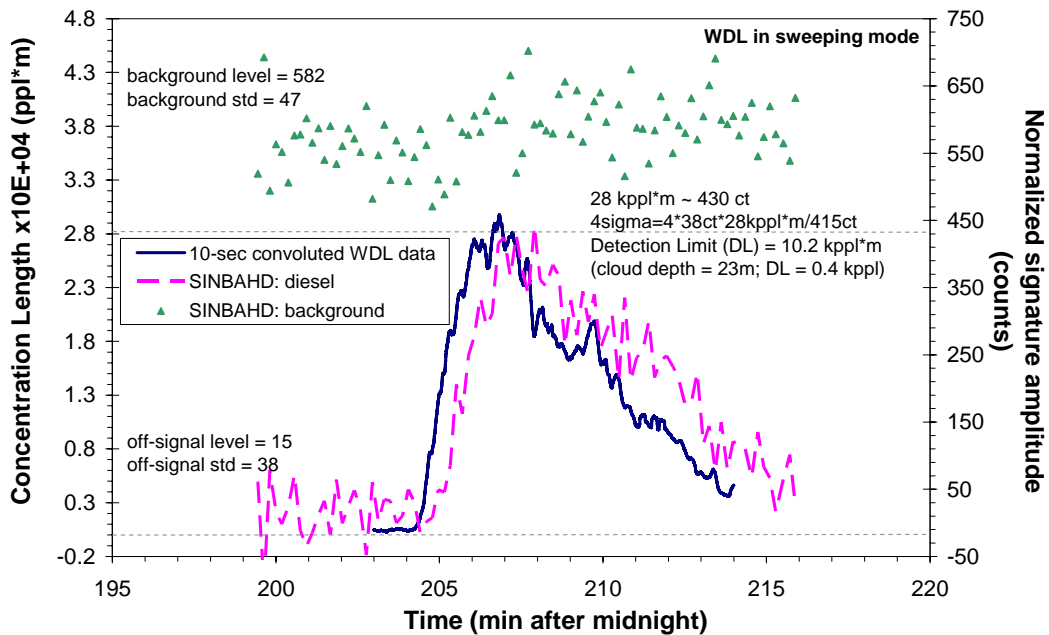


**Figure 45.** WDL calibrated concentration (solid blue line) and SINBAHD multivariate analysis results (dashed pink for diesel; green triangles for background) for TDA023-diesel at 2.35 km.

**Trial:** TDA008\_tires, June 9<sup>th</sup> 2005.

**Dissemination:** burning tires.

**SINBAHD probed volume:** 600 m wide at 800 m range.

**Target range:** 1.2 km.

Figure 46 presents a result obtained from a burning tire release at about 1.2 km, using a gate of 600 m wide at a range of 800 m. No valuable signature could be extracted from the burning tires trial due to too low fluorescence signal intensity collected by SINBAHD (Table 4). The multivariate analysis was hence performed with a bioaerosol normalized signature not corresponding to the interrogated cloud, the diesel signature was arbitrarily chosen. The detection signal obtained from the MA while not using the appropriate signature will still be reliable but the signature amplitude values are much less significant. This means that any signature could be use to detect a given particular cloud but if the concentration or cross-section of the released material needs to be evaluated, the proper signature needs to be used [17]. The WDL and SINBAHD MA results show many similar features along the trial evolution even though the diesel spectral signature was used rather than the one of the un-existing burning tires one. The correlation is poor but the main features are present in both output results. The negative values for the diesel signature amplitude (297-299 minutes) is probably related to the fact that this signature is not representing well the burning tire spectral features and hence producing awkward results from the MA process.

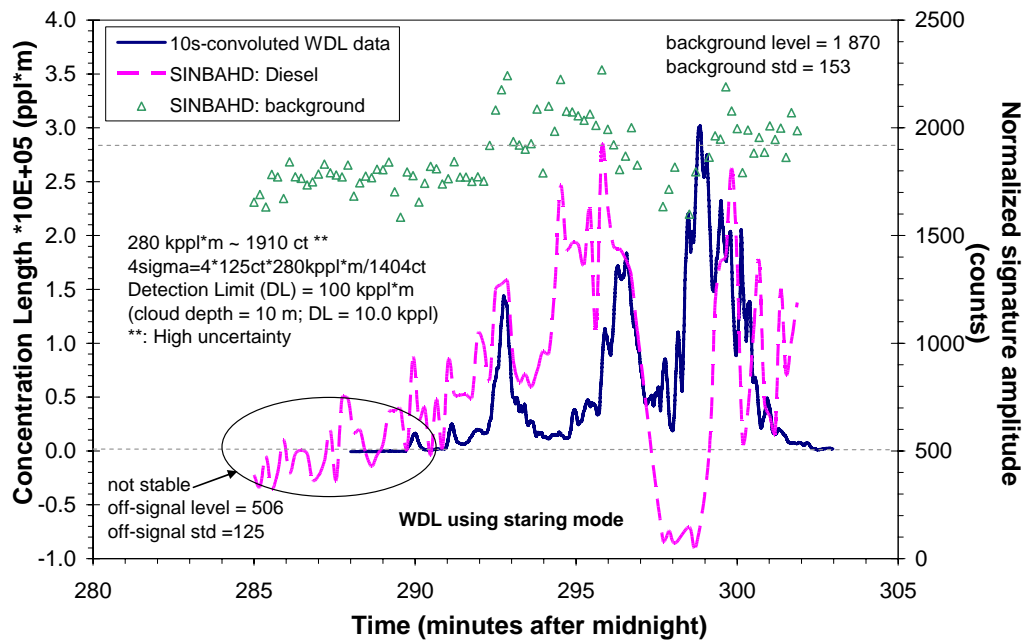


**Figure 46.** WDL calibrated concentration (solid blue line) and SINBAHD MA results (dashed pink for diesel; green triangles for background) for TDA008-tires at 1.2 km.

**Trial:** TDA007\_burningbrush, June 9<sup>th</sup> 2005.

**Dissemination:** burning brush.

**SINBAHD probed volume:** 600 m wide at 800 m range.

**Target range:** 1.2 km.

Figure 47 presents a result obtained from a burning brush release at about 1.2 km, using a gate of 600 m wide at a range of 800 m. From the evolution of background signature amplitude (green triangles) calculated by the MA, the presence of cross-talk between the burning brush and background spectral signatures, is noticeable (lower oval). The impact of this cross-talk on the burning brush signature amplitude signal is unknown (higher oval + question mark) but there is definitely one. If this latter portion of the release is not considered, the obtain correlation between WDL and SINBAHD MA result is quite good. SINBAHD acquisition stopped in the middle of the release due to a PC problem. The obtained concentration detection limit for burning brushes at a range of about 1.2 km is 3.5 kppl for a cloud of about 15 m or a concentration-length detection limit of 53 kppl\*m.

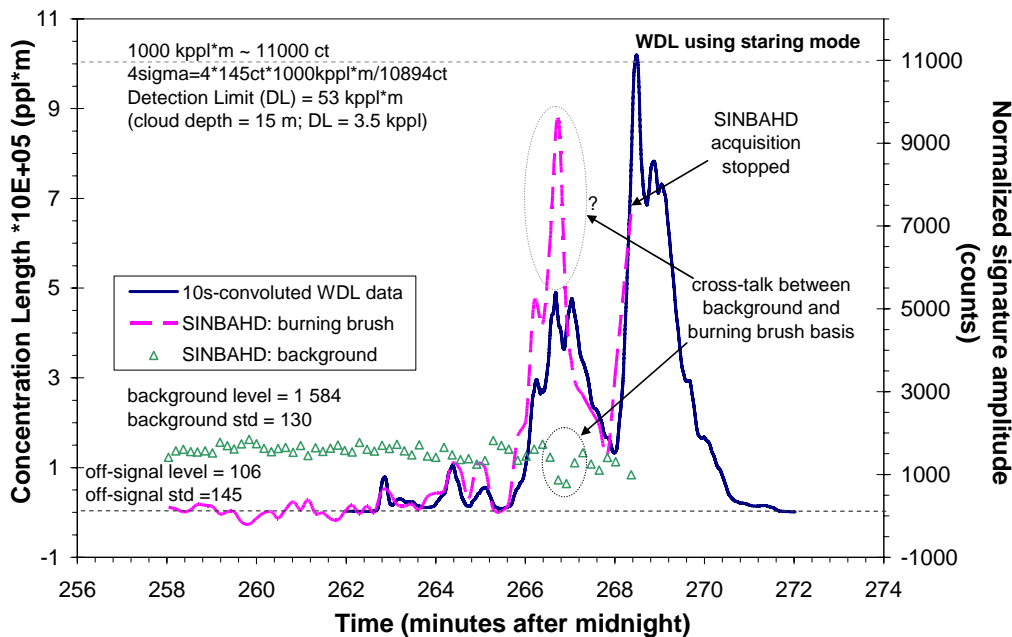


**Figure 47.** WDL calibrated concentration (solid blue line) and SINBAHD MA results (dashed pink for burning brush; green triangles for background) for TDA007-burning brush at 1.2 km.

**Trial:** TDA009\_cotton, June 12<sup>th</sup> 2005.

**Dissemination:** burning cotton.

**SINBAHD probed volume:** 600 m wide at 800 m range.

**Target range:** 1.2 km.

Figure 48 shows the obtained result for a burning cotton release at about 1.2 km, using a gate of 600 m wide at a range of 800 m. The WDL and SINBAHD MA result show many similar features along the trial evolution and their correlation could be qualified of fair considering the low S/N of the fluorescence signal acquired by SINBAHD during most of the release. The signal maxima obtained from the two systems are absolutely not correlated in time; indeed they are occurring at about 5 minutes apart. This mismatch could once again be related to the different probed volumes by the two sensors related to their different position relatively to the interrogated cloud. The visual correlation was based on the general signal level during the entire release and left aside the highest peak detected by each sensor. The obtained concentration detection limit for burning cotton at a range of about 1.2 km is 1.9 kppl for a cloud of about 10 m or a concentration-length detection limit of 19 kppl\*m.

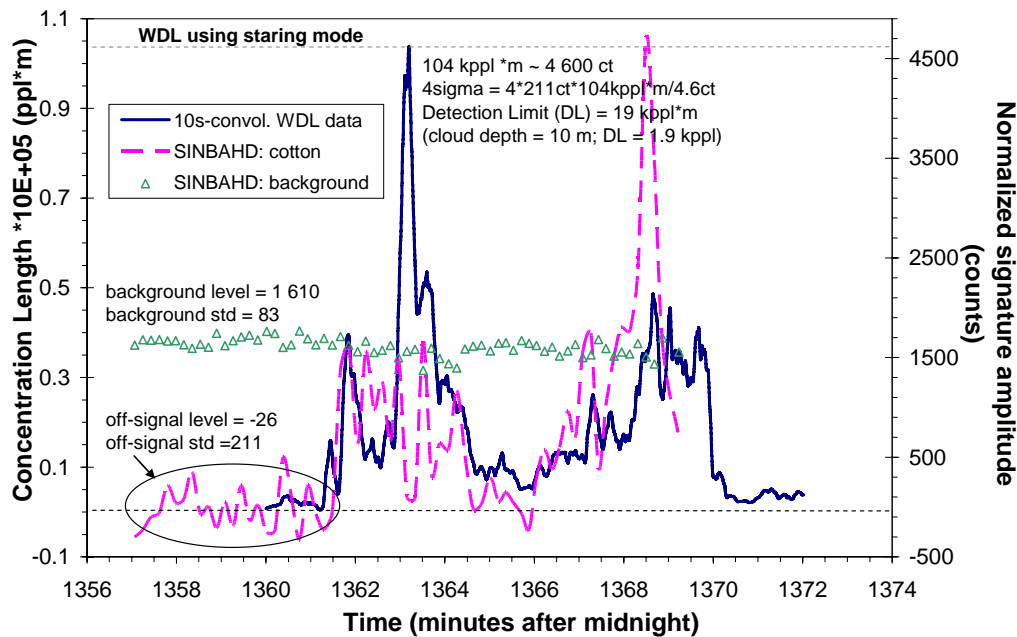


**Figure 48.** WDL calibrated concentration (solid blue line) and SINBAHD MA results (dashed pink for burning cotton; green triangles for background) for TDA007-burning brush at 1.2 km.

**Trial:** TDA005\_Topsoil, June 9<sup>th</sup> 2005.

**Dissemination:** 178 g of dry top soil with the point mechanism.

**SINBAHD probed volume:** 600 m wide at 800 m range.

**Target range:** 1.2 km.

Figure 49 presents the results obtained from a top soil release made by the point mechanism at about 1.2 km, using a gate of 600 m wide at a range of 800 m. The correlation between the WDL and SINBAHD MA results can, once again, be qualified of fair considering the low S/N of the fluorescence signal acquired by SINBAHD. The difference in the obtained amplitudes could be related to their relative position versus the interrogated cloud. The obtained concentration detection limit for this top soil release at a range of about 1.2 km is 1.9 kppl for a cloud of about 10 m or a concentration-length detection limit of 19 kppl\*m.

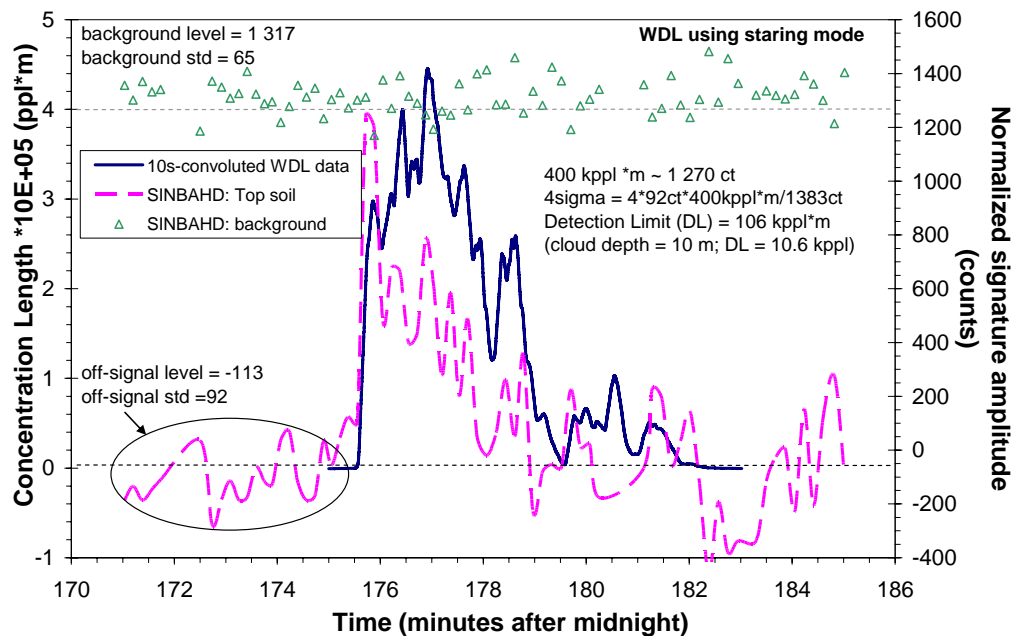


**Figure 49.** WDL calibrated concentration (solid blue line) and SINBAHD multivariate analysis results (dashed pink for top soil; green triangles for background) for TDA005-top soil at 1.2 km.

## 7 Bug and Issues

---

Different problems and issues appeared along the trial, some of which will be briefly described in the present section. In fact during the entire trial, only three types of problems were experienced: interrupted acquisition due to the visibility sensor (section 7.1); major PC crash (section 7.2) and the last is related to the power stability of the laser (section 7.3).

### 7.1 Weather monitoring

A weather station (WS-2000 from RainWise) and a visibility monitor (6100 from Belfort) are installed on the roof of SINBAHD trailer for atmospheric characterization. Between each acquisition, these two sensors are interrogated and the outputs recorded by SINBAHD software. This latter program includes a pop-up information window whenever a communication problem appears with the visibility sensor. This window can be deactivated by clicking an OK button, until which the acquisition is halted.

The first test with SINBAHD at JBSDS Demo II trial after unpacking and assembling, clearly showed a systematic communication problem with the visibility sensor. The sensor connector was tested but no sign of malfunction were present. The visibility sensor was then brought into the trailer and directly connected into the computer, which resolved the systematic communication problem. The problematic segment was hence the connector going from inside the trailer to outside, on the roof. Since the atmospheric correction is not yet included in the processing unit, the information from the visibility sensor is therefore not needed and the sensor can hence be located inside the trailer without any problem.

The communication with the visibility sensor has always been sporadically but sparsely problematic and the bypass of the troubled connection did overcome the systematic problem but not the sporadic one. The constant presence of an operator behind the main computer is hence needed, which is anyhow the case. This software particularity will be modified in the near future.

### 7.2 PC Bug

The main computer, on which the SINBAHD control software is running, experienced three major crashes during the entire trial. In these cases, the SINBAHD application froze suddenly and nothing could be made to restart the acquisition run. SINBAHD software had to be interrupted from the Windows task manager tool. The acquired data of the aborted acquisition are not yet lost but they need to be restored before any new acquisition is re-started. Indeed, as an acquisition run goes along, the acquired data are always saved in a file entitled *sinbahd.restore*, which one will be overwritten as soon as a new acquisition is started. The first time this type of bug occurred, the data were not saved under another name or restored before the acquisition was re-started and all the data for this trial were lost (TDA004\_BG, Table 4).

### 7.3 Laser power stability

SINBAHD excimer laser has an option called StabiLASE, which can maintain constant the output energy over long periods of time. This option compensate for the long-term degradation of the laser gas mixture and keep the output energy constant by increasing the charge voltage of the high voltage power supply. Indeed, the energy of the laser pulse varies with the discharge voltage on the electrodes inside the laser vessel. However, in order to break down the gas between the laser electrodes, the discharge voltage must be within a certain range. For SINBAHD laser (PM-848), using the XeF laser transition, this voltage should range between 26 and 35 kV and ideally 28 to 35 kV. When the StabiLASE option is turn on, the control seeks the correct voltage for the laser to deliver the requested energy until the discharge voltage reaches the limit set. The laser will then either stop or the StabiLASE option will turn off and the laser will continue to operate at a reduced energy, depending on the chosen setting (STOP or CONT.).

During the JBSDS Demo II trial, the laser was always used with the StabiLASE option on and with its end action set to STOP. In the case where the laser stops and an acquisition was running, a conflict is created within the software. When this particular scenario occurred (about three times), the acquisition had to be interrupted (stop), saved and the SINBAHD software had to be closed down and re-started. In order to overcome this problem, the discharge voltage was periodically checked to make sure that it was located within the comfortable range and if not, the energy level was modified in consequences. In most cases, when the energy level was modified on the laser, the corresponding input in SINBAHD software (*OPMode*) was adjusted. As the energy level setting has to be lowered down, comes a limit around 90-100 mJ, where gases change is needed.

## 8 Conclusion

---

SINBAHD was one of the 12 systems participating to the Joint Biological Standoff Detection System increment II field demonstration trial (JBSDS Demo II) at Dugway Proving Ground (DPG), Utah, USA, in June 2005. The first purpose of this field demonstration was to determine the benchmark sensitivity of the participant systems to various biosimulants/interferents.

SINBAHD participation in this field Demo trial made it possible to assess further its detection potential and also to obtain new spectral signatures to be added to its pattern set (library). SINBAHD participated in 34 test releases at Target S for cross wind open air releases. From these acquisitions, 19 signatures could be extracted, nine did not have any fluorescence signal and one was lost due to a PC crash. The five other acquisitions, from which no fluorescence signal could be visually observed in real time, were processed with SINBAHD virtual multivariate analysis tool. In all these five cases, a detection signal could be extracted, but with a fairly low signal-to-noise ratio. Many significant outcomes were obtained from these results. The bioaerosol signature is fairly robust all along the dissemination as long as the signal level intensity is sufficient. Ideally, the spectral signature should be obtained during a high concentration release at short range in order to optimize the signal-to-noise ratio and at the same time, maximizing the robustness of the obtained spectral signature. The signature discrepancy was fairly obvious between most materials but not between the two vegetative cells, irradiated-Yp and EH. Indeed, the killed vaccine strain of *Yersinia pestis* had about the exact same signature as *Erwinia herbicola* even though the first has been irradiated but not the last. There was, however, obvious spectral differences between irradiated-Ba and BG, which are two species of *Bacillus* bacteria spores. The impact of the gamma illumination process performed on the Ba spores and the Yp vegetative cell on their LIF signature was not evaluated or measured but is expected to be present. The signature of ovalbumin and MS2, which are respectively toxin and virus simulants, showed spectral features much closer to killed-Ba than BG did. The robustness of BG and EH having different origins, preparation or dissemination methods was demonstrated by comparing the results previously obtained at Suffield in 2001 and the actual ones from the JBSDS Demo II, 2005.

All the results, once processed with the SINBAHD multivariate analysis tool, were correlated with the data of DPG West Desert LIDAR (WDL) reference system. The obtained correlation from the 24 trials having obvious (19) or weak (5) specific specie fluorescence was either good (10), OK (4), fair (5) or low (3) and could not be obtained in two cases due to missing reference data. From these correlations, the 4 sigma sensitivity was evaluated for a given cloud depth and range. Indeed, this 4 sigma parameter represents the minimal detection limit possible since the performed MA only used the proper signatures to represent the detected specie and background (except for the burning tires trial). These different results demonstrate the optimum sensitivity that SINBAHD can reach when using SINBAHD multivariate analysis tool in conjunction with the proper signatures.

## 9 Recommendations

Following the JBSDS Demo II trial and in the light of the data processing period, some trial procedures are recommended for future trial:

- 1) Perform a background acquisition at the beginning and the end of each trial's session (each day and/or night) with the appropriate gate width and range. Perform different background acquisition if many gate widths/ranges are used.
- 2) Ideally, choose a unique gate width over all the measurement during a given trial.
- 3) When the dissemination is far and the range is not well known, use a larger gate width and enlarge the range of the 'Backscatter window' X-axis. Once the target is located reduce the gate width to its usual size.
- 4) Note the general conditions: Temperature, barometric pressure, wind, presence of cloud, moon phase, presence of glow, etc.
- 5) Note the general characteristics of the measurement while it is being acquired (see Table 7):

*Table 7. Suggested trial data sheet.*

<b>Date:</b>				
<b>Trial name (file name):</b>				
<b>Time</b>	<b>Release evolution</b>	<b>Acq. #</b>	<b>Notes (suggested)</b>	<b>Conditions</b>
	Start background		Background acq = # - ;# -	Temp. = Wind = Humidity = Target range = Gate width = Gate range =
	Start dissemination		Backscatter = to #	
	Ramp down.		Max fluo = acq # , counts =	
	Stop dissemination		Fluorescence acq. = # to #	
	Stop background		Total number of acq. =	
<b>Results:</b>				

## 10 References

---

1. J. K. Li, E. C. Asali, A. E. Humphrey and J. J. Horvath, *Monitoring Cell Concentration and Activity by Multiple Excitation Fluorometry*, Biotechnol. Prog., Vol. 7, pp. 21-27, 1991.
2. G. W. Faris, R. A. Copeland, K. Mortelmans and B. V. Bronk, *Spectrally resolved absolute fluorescence cross sections for bacillus spores*, Applied Optics, Vol. 36, No. 4, p.958-967, February 1997.
3. P. P. Hairston, J. Ho and F. R. Quant, *Design of an Instrument for Real-Time Detection of Bioaerosols using Simultaneous Measurement of Particle Aerodynamic Size and Intrinsic Fluorescence*, J. Aerosol Sci., Vol. 28, No. 3, pp. 471-482, 1997.
4. S. D. Christesen and K. K. Ong, *Fluorescence spectroscopy of biological agents: I. Bacillus Anthracis*”, Edgewood Research, Development & Engineering Contractor Report No. ERDEC-TR-466, April 1998.
5. N.F. Fell Jr, R. G. Pinnick, S. C. Hill, G. Videen, S. Niles, R. K. Chang, S. Holler, Y. Pan, J. R. Bottiger, and B. V. Bronk, *Concentration, Size, and Excitation Power Effects on Fluorescence from Microdroplets and Microparticles Containing Tryptophan and Bacteria*, Proceedings of the Conference on Air Monitoring and Detection of Chemical and Biological Agents, SPIE Vol. 3533, Boston, p.52-63, November 1998.
6. J. Gelbwachs and M. Birnbaum, *Fluorescence of Atmospheric Aerosols and Lidar Implications*, Applied Optics, Vol.12, No. 10, p. 2442, October 1973.
7. W. B. Grant, *Optical Bases for Remote Biological Aerosol Detection*, Edgewood Arsenal Contractor Report No. ED-CR-77025, Stanford Research Institute, March 1977.
8. P. J. Hargis, Jr., A. R. Lang, R. L. Schmitt, T. D. Henson, J. W. Daniels, J. D. Jordan, K. L. Shroder and I. R. Shokair, *Sandia Multispectral Airborne Lidar for UAV Deployment*, Proceeding of the 4<sup>th</sup> Joint Workshop on Standoff Detection for Chemical and Biological Defense, 26-30 October 1998.
9. J.R. Simard, G. Roy, P. Mathieu, V. Larochelle, J. McFee, J. Ho, *Standoff sensing of bioaerosols using intensified range-gated spectral analysis of laser-induced fluorescence*, IEEE Trans. on Geoscience and Remote Sensing, Vol. 42, No. 4, April 2004.
10. G. Roy, L. Bissonnette, C. Bastille, and G. Vallée, *Retrieval of droplet-size density distribution from multiple-field-of-view cross-polarized lidar signals: theory and experimental validation*, Applied Optics, Vol. 38, No. 24, p. 5202-5211, August 1999.
11. J. D. Houston and B. T. N. Evans, *Monitoring Aerosols Optically*, Photonic Spectra, p. 93, July 1987.

12. L. A. Condatore, Jr., R. B. Guthrie, B. J. Bradshaw, K. E. Logan, L. S. Lingvay, T. H. Smith, T. S. Kaffenberger, B. W. Jezek, V. J. Cannaliato, W. J. Ginley and W. S. Hungate, *U.S. Army Chemical and Biological Defense Command Counter-Proliferation Long-Range Biological Standoff Detection System*, Proceeding of the 4<sup>th</sup> Joint Workshop on Standoff Detection for Chemical and Biological Defense, 26-30 October 1998.
13. D. L. Hutt, L. R. Bissonnette and L. Durand, *Multiple Field of View Lidar Returns from Atmospheric Aerosols*, *Applied Optics*, 33, 2338-2348, 1994.
14. R. R. Karl, Jr., *Lidar Detection of Biologicals by Fluorescence*, Proceedings of Seminar on Stand-off Detection of Pollutants, Centre d'Études du Bouchet, France, p. 131, December 1992.
15. C. L. Chen, D. L. Heglund, M. D. Ray, D. Harder, R. Dobert, K. P. Leung, M. Wu and A. J. Sedlacek III, *Application of Resonance Raman Lidar for Chemical Species Identification*, SPIE Vol. 3065, p.279, 1997.
16. M. D. Ray and A. J. Sedlacek III, *Mini Raman Laser-Radar System for In Situ, Stand-Off Interrogation of Surface Contamination*, 19<sup>th</sup> International Laser Radar Conference, p. 677, July 1998.
17. J.-R. Simard, G. Roy, P. Mathieu, V. Larochelle, J. E. McFee and J. Ho, *Standoff Integrated Bioaerosol Active Hyperspectral Detection (SINBAHD): Final report*, DREV TR 2002-125, 118 pages, UNCLASSIFIED, April 2003.
18. Y. Painchaud, J.-F. Cormier, J.-F. Hébert, M. Deladurantaye, D. Antov, B. Bélanger and S. Bernier, *SINBAHD project: Integration of a laser-induced fluorescence LIDAR for the detection and characterisation of threatening biological clouds*. Final report, INO 99-5217SP RF N/A, 66 pages, November 2000.
19. J.-F. Hébert, *SINBAHD project: Software user manual*. Final report, INO 99-5217SM R N/A, 22 pages, May 2001.

## Annex A: Crosswind tests during JBSDS Demo II, 2005

Date	Release ID	Time		Agent	Quantity g or L	Concentration (kppL)	Release		Wind		Temp	Humidity	WDL	Comments
		Local Start Release	Stop Release				Location	Type	Direction	Speed (m/s)			APD Gain	
06-09-05	TDA001	23:52:00	23:57:00	road dust	----	----		Line	0	0	8.1	62.8	240	
		23:54:00												
	TDA002	0:18:00	00:18:40	kaolin	19.5	2mil		Line	140	1.1	7.8	62	240	
		0:20:00												
	TDA003	0:47:00	0:53:00	kaolin	96	3mil		Point	112	0.9	7.5	66	120	75% 18 tooth
		0:50:00												
	TDA004	1:10:00	1:17:00	BG	106	1mil		Point	125	0.9	6	73	120	50%
		1:14:00												
	TDA005	2:55:00	3:01:00	top soil	178	500		Point	135	1.1	4.4	75	120	50%
		2:58:00												
	TDA006	3:56:00	4:02:00	diesel	----	360		Point	135	6	3	84	120	on
	TDA007	4:22:00	4:29:30	burning brush	----	100		Point	110	1	2.6	85	120	burning
	TDA008	4:49:00	5:00:00	burning tire	----	200		Point	139	0.8	2.9	85	120	burning

2005 06/12	TDA009	22:41:00	22:49:45	cotton	----	16		Point	0	0.9	14	44	120	
	TDA010	23:28:00	23:33:00	yellow smoke	2	750		Point	161	1.4	12	52	120	
	ambient 1													Active Systems Collecting Background
														background collected without lasers firing
2005 06/13	TDA011	0:27:00	0:31:30	OV	133g	45		Point	137	0.4	11.6	54.6	120	off the BB, looking at Dugway Range
		0:30:00												change to 10%
	TDA012	0:54:00	0:59:15	Kaolin(H )	56g	750		Point	137	0.4	11.6	53	120	Hydrosil
		0:57:00				25								ramp down to 10%
	TDA013	1:25:00	1:31:00	BG	77g	no data		Point	110.5	2.3	12.3	57.7	120	
		1:28:00												ramp down to 10%
	TDA014	1:51:00	1:57:00	Kaolin(G )	24g	500		Point	181.5	0.9	12	58.3	120	GloMax
		1:54:00				100								ramp down to 10%
	TDA015	2:32:00	2:35:30	Ba	20	200		Point	137.2	0.8	8.9	65	120	20g @ 50%

		2:24:30				25								10%
	TDA016	3:31:00	3:36:00	EH	7L	>8		Point	122	0.8	8.1	67.1	120	3 machines on initially; on the BB
		3:34:00				4								Dissem. Machines started up at 03:29
		3:37:30	3:40:00											Ramp down 03:34; re-started dissem.
	TDA017	4:12:00	4:18:00	Yp	3.5L	60		Point	144.4	1.2	8.2	66	120	WDL using ND filter of 1
		4:15:00				15								start dissem machines at 04:10
														ramp down at 04:15
														04:13:30 two machines running
	TDA018	4:37:00	4:43:00	Diesel	n/a			Point	109.9	0.8	7.8	67.4	120	Release from HMMWV
2005 06/14														
	TDA019	1:25:00	1:31:00	BG	85.5g	7		Point	197	1.7	18.5	37	220	42 tooth wheel
		1:28:00				39								ramp down to 10%
	TDA020	1:51:00	1:57:00	OV	133.5	6		Point	164.4	1.6	17.4	40.4	220	For the passive systems there might have been a BG cloud at approx 3 km
		1:54:00												ramp down to 10%
	TDA021	2:30:00	2:34:00	Ba	20	10		Point	94.7	2.2	15.9	47.6	220	20 g, release until gone
		2:32:00				15								
	TDA022	2:57:00	3:03:00	Kaolin(G )	33	26		Point	108	1.1	14.2	53.4	220	GloMax

		3:00:00				35								ramp down at 10%
	TDA023	3:22:00	3:28:00	Diesel	n/a			Point	148.5	2	13.9	52.9		
	TDA024	4:16:00	4:16:05	BG	400	75		Puff	128	1.5	11.7	62	220	
	TDA025	4:48:00	4:54:00	EH	5L	0.8		Point	78	1.8	11.2	62	220	
		4:51:00												ramp down to 1 machine
2005 06/15														
	TDA026	23:41:00	23:49:00	MS2	13L	2		Point	116	3.2	20.4	30.7	220	
		23:46:00				0.5								ramp down to 1 machine
	TDA027	0:07:00	0:13:00	Yp	7L	5		Point	170	2.4	20.1	32.4	220	3" High
		0:10:00												3" Low
	TDA028	0:33:00	0:36:09	Yellow Smoke	2ea	na		Smoke	180	1.5	20.2	31.7	220	Switched from Fog to Smoke Grenade 2 canisters cloud height 17 meters
	TDA029	1:02:00	1:02:10	Kaolin(G)	3.5lbs	300	101	Air	277	1	19.8	32.6	240	Aircraft release along range road 945 100m cloud depth, 3.2 K from CP
						150								
	TDA030	1:36:03	1:36:15	Kaolin(G)	3.5lbs	90	101	Air	240	1	18.8	35.8	240	Aircraft release along range road 945 cloud height 40m, cloud depth 600m, 3.2 K from CP

	TDA031	2:08:00	2:13:26	HC Smoke	2ea	na		Smoke	130	2	20.3	30.7	240	smoke grenade, 1.6 K from highway 101
														cloud height 15 meters, 150 meters deep
	TDA032	2:36:00	2:40:00	Fog Oil		na		Fog	142	3.6	19.8	32.4	240	1.6 K from Hwy 101
														cloud height 25 m
	TDA033	3:04:00	3:04:14	Bg	5.4lbs	50	Fox Trot	Air	140	3.3	19.6	32.7	240	Aircraft release along range road 945, 3.2 K from CP
	TDA034	3:35:31	3:35:45	Bg	5.4lbs	10	Fox Trot	Air	140	4	20.7	30	240	gusts at 6.5, Range to release 2.5-3 K
														2.3- 3.1 K distant, 500m deep
	TDA035	4:27:00	4:30:00	Cabosil	.5g	na		Point	147	4	19	33.3		Range, 1.2K
	TDA036	4:46:00	4:50:00	Cabosil	51g	50		Point	137	4.2	19.8	31.5		Range, 1.2K
		4:49:00												

## **Annex B: SINBAHD general alignment procedure**

---

- 1) A target was installed on the back of a truck and positioned at a few hundred meters from SINBAHD
- 2) Verify that the emission and collection channel are co-aligned, in which case the pointing camera image corresponds with the one of the ICCD (See document Alignment procedure for SINBAHD part A)
- 3) Optimize the collection channel focus by adjusting the position of the spectrometer/ICCD block with respect to focused image plane.
- 4) Obtain an image of the incident beam on the target with the intensified CCD with the spectrometer slit wide open. (document: Alignment procedure for SINBAHD part B)
- 5) Optimize the emission channel focus by adjusting the lens position of the beam expander, which is mounted on a one-axis micrometric displacement mount. The intensity of the beam must be maximized in the same as minimizing its spreading.
- 6) Adjust the position of the laser spot right in the middle of the slit at mid-height of the ICCD 128 pixel vertical axis by modifying the inclination in both axes of the folding mirror.
- 7) Adjust the spectrometer slit to the proper width (200  $\mu\text{m}$  in the present case).
- 8) Position the laser beam on the target.

Once SINBAHD set up was unpacked and re-assembled, all 8 steps were performed once. The two subsequent trial-nights, only step 4 to 8 were performed. For all the following trial-night, only step 8, consisting in positioning the beam on the target, was performed.

## Annex C: Normalized signature construction (1 acq)

---

```
function [lambda, base] = nsignature2
%function nsignature2

close;
cd('D:\My documents\SINBAHD\data\Dugway2005\')

% Get the filename with the MathLab browser
[SPECTRAFILENAME,SPECTRAPATHNAME] = uigetfile('*.txt','Select an acquisition of fluorescence');
cd(SPECTRAPATHNAME);
[BACKGROUNDFILENAME,BACKGROUNDPATHNAME] = uigetfile('*.txt','Select an acquisition of background');
signalfilename = strcat(SPECTRAPATHNAME, SPECTRAFILENAME);
bckfilename = strcat(BACKGROUNDPATHNAME, BACKGROUNDFILENAME);

% Read the file
spectradata = dlmread(signalfilename);
backgrounddata = dlmread(bckfilename);

% extract the array of data
lambda = spectradata(2:676,1);
radiance = spectradata(2:676,2);
background = backgrounddata(2:676,2);

% Correct the spectra for the background contribution
Bcorr_radiance = radiance - background;

% N2 pic Correction
[p,S,mu] = polyfit([lambda(1:2); lambda(35:50)],...
    [Bcorr_radiance(1:2) ; Bcorr_radiance(35:50)], 2);
fit_segment = polyval(p,lambda(3:34),[],mu);
RBcorr_radiance = [Bcorr_radiance(1:2); fit_segment; Bcorr_radiance(35:675)];

% H2O pic Correction
[p,S,mu] = polyfit([lambda(40:60); lambda(100:120)],...
    [RBcorr_radiance(40:60) ; RBcorr_radiance(100:120)], 2);
fit_segment = polyval(p,lambda(61:99),[],mu);
RRBcorr_radiance = [RBcorr_radiance(1:60); fit_segment; RBcorr_radiance(100:675)];

% Smooth the collected spectra (moyenne glissante)
smooth_corr_radiancel = sliding_mean(RRBcorr_radiance, 21);
smooth_corr_radiance2 = sliding_mean(smooth_corr_radiancel, 21);
smooth_corr_radiance = sliding_mean(smooth_corr_radiance2, 21);

% Normalise the smoothed spectra which creates the signature (Sij)
base = smooth_corr_radiance/sum(smooth_corr_radiance);
```

## Annex D: Normalized signature construction (many acq)

```
function [lambda, sum_base] = nsum_signatureb

% Get the filename with the MathLab browser
[sfilename, spathname] = uigetfile('*.acq', 'Select a file');
signalfilename = strcat(spathname, sfilename);

% Read the file
lambdadata = dlmread('D:\My documents\SINBAHD\data\Dugway2005\lambda.txt');
[signalConfig , signalAcqui] = ReadSNEDVersion2File(signalfilename);

% Get the acquisition number to sum (bck and fluo)
prompt = {'Background start:', 'Background end:', 'Fluorescence start:', 'Fluorescence end:'};
dlg_title = 'Enter the acquisition number selected';
num_lines= 1;
def = {'55', '75', '15', '35'};
answer = inputdlg(prompt,dlg_title,num_lines,def);
bckS = str2num(char(answer(1)));
bckE = str2num(char(answer(2)));
fluoS = str2num(char(answer(3)));
fluoE = str2num(char(answer(4)));
Number_acq = fluoE-fluoS+1;
Number_acq_bck = bckE-bckS+1;

% extract the array of data
lambda = lambdadata(2:676,1);
signalall = zeros(675, Number_acq);
backgroundall = zeros(675, Number_acq_bck);
signalUVback = zeros(675, Number_acq);
backgroundUVback = zeros(675, Number_acq_bck);

for( ii = 1:Number_acq )
    signalall(:,ii) = signalAcqui(fluoS+ii-1).ICCDSumLaserPulseData(166:840);
    signalUVback(:,ii) = signalAcqui(fluoS+ii-1).ICCDSumBackGroundData(166:840);
end
for( ii = 1:Number_acq_bck)
    backgroundall(:,ii) = signalAcqui(bckS+ii-1).ICCDSumLaserPulseData(166:840);
    backgroundUVback(:,ii) = signalAcqui(bckS+ii-1).ICCDSumBackGroundData(166:840);
end

% Subtract the radiance background (acquisition between two laser shot) from the signal file
signal = zeros(675, Number_acq);
background = zeros(675, Number_acq_bck);
for( ii = 1:Number_acq)
    signal(:,ii) = signalall(:,ii) - signalUVback(:,ii);
end
for( ii = 1:Number_acq_bck)
    background(:,ii) = backgroundall(:,ii) - backgroundUVback(:,ii);
end
```

```

% Calculate the mean of the background
mean_background = mean(background,2);

% Smooth the background spectra (hyperspectral filter)
dimen = 575;
filter_1 = zeros(dimen,dimen);
xx = 1:dimen;
for( ii = 1:dimen);
    filter_1(ii,:) = exp(-((xx-xx(ii)).^2)/400);
    filter_1(ii,:) = filter_1(ii,+)/sum(filter_1(ii,:));
end
smooth_mean_background =mean_background;
smooth_mean_background(101:675) = filter_1 * mean_background(101:675);

for( ii = 1:Number_acq)
    % Correct the spectra for the background contribution
    Bcorr_signal = signal(:,ii) - smooth_mean_background;

    % N2 pic Correction
    [p,S,mu] = polyfit([lambda(1:2); lambda(35:50)],...
        [Bcorr_signal(1:2) ; Bcorr_signal(35:50)], 2);
    fit_segment = polyval(p,lambda(3:34),[],mu);
    RBcorr_signal = [Bcorr_signal(1:2); fit_segment; Bcorr_signal(35:675)];

    % H2O pic Correction
    [p,S,mu] = polyfit([lambda(40:60); lambda(100:120)],...
        [RBcorr_signal(40:60) ; RBcorr_signal(100:120)], 2);
    fit_segment = polyval(p,lambda(61:99),[],mu);
    RRBcorr_signal = [RBcorr_signal(1:60); fit_segment; RRBcorr_signal(100:675)];

    % detector pic Correction (585nm)
    [p,S,mu] = polyfit([lambda(605:625); lambda(654:674)],...
        [RRBcorr_signal(605:625) ; RRBcorr_signal(654:674)], 2);
    fit_segment = polyval(p,lambda(626:653),[],mu);
    DRRBcorr_signal = [RRBcorr_signal(1:625); fit_segment; RRBcorr_signal(654:675)];

    % Smooth the collected spectra (moyenne glissante)
    smooth_corr_signal1 = sliding_mean(DRRBcorr_signal, 21);
    smooth_corr_signal2 = sliding_mean(smooth_corr_signal1, 21);
    smooth_corr_signal = sliding_mean(smooth_corr_signal2, 21);

    % Creates the unnormalised signatures matrice
    signature(:,ii) = smooth_corr_signal;
end

% calculate the sum
sum_signature = zeros(675,1);
sum_signature = sum(signature,2);

% Normalise the summed signatures (Sij)
sum_base = sum_signature / sum (sum_signature );

```

## List of symbols/abbreviations/acronyms/initialisms

---

ACPLA	Agent Containing Particles per Liter of Air
APS	Aerosol Particle Seizer
AR	Anti-reflective
ATCC	American Type Culture Collection
Ba	Bacillus anthracis
BG	Bacillus subtilis var globiggi
CANUKUS	Canada + Union Kingdom + United State
CBR	Chemical, Biological, Radiological
CCD	Charged Couple Device
DNBCD	Directorate of Nuclear, Biological and Chemical Defense
DRDC	Defence Research and Development Canada
DPG	Dugway Proving Ground
EH	Erwinia herbicola
FF	Fluorescence Filters
FM	Folding Mirror
FOV	Field Of View
ICCD	Intensified Charged Couple Device
JBSDS	Joint Biological Standoff Detection System
JHU-APL	Johns Hopkins University Applied Physics Laboratory
LIDAR	Light Detection And Ranging
LIF	Laser Induced Fluorescence
MA	Multivariate Analysis
MOU	Memorandum Of Understanding

OV	Ovalbumin
sABT	Standoff Ambient Breeze Tunnel
SBS	Scatter Beam Splitter
SBWG	Standoff Biodetection Working Group
SF	Scatter Filters
SINBAHD	Stand-off INtegrated Bioaerosol Active Hyperspectral Detection
S/N	Signal to Noise Ratio (S/N or SNR)
SRB	Senior Review Board
TDP	Technology Demonstration Program
UV	Ultra-Violet
VBS	Visual Beam Splitter
WDL	West Desert LIDAR
Yp	Yersinia pestis

## Distribution list

---

### INTERNAL

- 1- Director General
- 3- Document Library
- 1- Hd/SOP
- 1- Hd/EOW
- 1- Sylvie Buteau (author)
- 1- J.-R. Simard (co-author)
- 1- P. Lahaie (co-author)
- 1- G. Roy (co-author)
- 1- P. Mathieu (co-author)
- 1- P. Lacasse (AEREX)
- 1- H. Lavoie
- 1- B. Déry
- 1- J. Tremblay
- 1- V. Larochelle
- 1- D. Nadeau

## EXTERNAL DISTRIBUTION

- 1- DRDKIM (PDF File)
- 2- John McFee, DRDC – Suffield (co-author)  
Jim Ho, DRDC – Suffield (co-author)
- 1- Walter Dyck  
DSTHP  
National Defence Headquarters  
101 Colonel By Drive  
Ottawa, Ontario, K1A 0K2
- 2- LCol. Rick Barker  
LCmd. Kevin Johnston  
  
DJCP-5  
National Defence Headquarters  
101 Colonel By Drive  
Ottawa, Ontario, K1A 0K2
- 1- Susan Rowsell, M.E.Des., M.Sc.  
Counter Terrorism Technology Centre  
DRDC Suffield  
PO Box 4000  
Medicine Hat, AB T1A 8K6
- 1- John Strawbridge  
Joint Program Manager BioDefense  
Attn: SFAE-CBD-BD-DS /J. Strawbridge  
BLDG E4470  
Aberdeen Proving Ground, MD 21010-5424  
USA
- 1- Michael Castle  
Virginia Foot  
Dstl  
Porton Down  
Salisbury, Wiltshire SP4 OJQ  
United Kingdom



UNCLASSIFIED  
 SECURITY CLASSIFICATION OF FORM  
 (Highest Classification of Title, Abstract, Keywords)

<b>DOCUMENT CONTROL DATA</b>		
1. ORIGINATOR (name and address) Defence R&D Valcartier 2459 Pie-XI Blvd. North Québec, Qc G3J 1X8	2. SECURITY CLASSIFICATION (Including special warning terms if applicable) Unclassified	
3. TITLE (Its classification should be indicated by the appropriate abbreviation (S, C, R or U)) Joint Biological Standoff Detection System increment II: Field demonstration - SINBAHD performances (U)		
4. AUTHORS (Last name, first name, middle initial. If military, show rank, e.g. Doe, Maj. John E.) S. Buteau, J.-R. Simard, J. McFee, J. Ho, P. Lahaie, G. Roy and P. Mathieu		
5. DATE OF PUBLICATION (month and year) 2007	6a. NO. OF PAGES 79	6b. NO. OF REFERENCES 19
7. DESCRIPTIVE NOTES (the category of the document, e.g. technical report, technical note or memorandum. Give the inclusive dates when a specific reporting period is covered.) Technical memorandum		
8. SPONSORING ACTIVITY (name and address) TDP programm		
9a. PROJECT OR GRANT NO. (Please specify whether project or grant) BioSense (16q1)	9b. CONTRACT NO.	
10a. ORIGINATOR'S DOCUMENT NUMBER TM 2006-140	10b. OTHER DOCUMENT NOS  N/A	
11. DOCUMENT AVAILABILITY (any limitations on further dissemination of the document, other than those imposed by security classification) <ul style="list-style-type: none"> <li><input checked="" type="checkbox"/> Unlimited distribution</li> <li><input type="checkbox"/> Restricted to contractors in approved countries (specify)</li> <li><input type="checkbox"/> Restricted to Canadian contractors (with need-to-know)</li> <li><input type="checkbox"/> Restricted to Government (with need-to-know)</li> <li><input type="checkbox"/> Restricted to Defense departments</li> <li><input type="checkbox"/> Others</li> </ul>		
12. DOCUMENT ANNOUNCEMENT (any limitation to the bibliographic announcement of this document. This will normally correspond to the Document Availability (11). However, where further distribution (beyond the audience specified in 11) is possible, a wider announcement audience may be selected.)		

UNCLASSIFIED  
 SECURITY CLASSIFICATION OF FORM  
 (Highest Classification of Title, Abstract, Keywords)

UNCLASSIFIED  
SECURITY CLASSIFICATION OF FORM  
(Highest Classification of Title, Abstract, Keywords)

13. ABSTRACT (a brief and factual summary of the document. It may also appear elsewhere in the body of the document itself. It is highly desirable that the abstract of classified documents be unclassified. Each paragraph of the abstract shall begin with an indication of the security classification of the information in the paragraph (unless the document itself is unclassified) represented as (S), (C), (R), or (U). It is not necessary to include here abstracts in both official languages unless the text is bilingual).

By the end of the 90s, Defence Research and Development Canada (DRDC) initiated the investigation of a novel LIDAR concept which open the possibility of collecting all at once the detailed spectral information contained in the return signals. This 3-year project called SINBAHD (Stand-off INtegrated Bioaerosol Active Hyperspectral Detection) aimed at evaluating the capability of using UV LIF with intensified range-gated spectrometry to detect and characterize bioaerosol from stand-off position. Essentially, the LIDAR system monitors atmospheric volumes in which specific spectrally wide fluorescence signal can be generated from inelastic interactions with complex molecules forming the building blocks of most bioaerosols. This LIF signal is collected by the combination of a dispersive element and a range-gated ICCD that limits the spectral information within the selected volume. This technique has showed an important potential of detecting and discriminating different bioaerosol agent simulants in real time. Through the Standoff Biodetection Working Group (SBWG) under the CANUKUS CBR MOU, SINBAHD was invited to participate in the Joint Biological Standoff Detection System (JBSDS) increment II field demonstration trial. The purpose of this international trial, which took place at Dugway Proving Ground (DPG), Utah in June 2005, was to determine the benchmark sensitivity of different technologies to various biological simulants and interferents. SINBAHD demonstrated its high level of performance and the results made it possible to obtain new spectral signatures.

14. KEYWORDS, DESCRIPTORS or IDENTIFIERS (technically meaningful terms or short phrases that characterize a document and could be helpful in cataloguing the document. They should be selected so that no security classification is required. Identifiers, such as equipment model designation, trade name, military project code name, geographic location may also be included. If possible keywords should be selected from a published thesaurus, e.g. Thesaurus of Engineering and Scientific Terms (TEST) and that thesaurus-identified. If it is not possible to select indexing terms which are Unclassified, the classification of each should be indicated as with the title.)

Bioaerosol, Standoff detection, LIDAR, LIF, spectral signature.

UNCLASSIFIED  
SECURITY CLASSIFICATION OF FORM  
(Highest Classification of Title, Abstract, Keywords)



## **Defence R&D Canada**

Canada's Leader in Defence  
and National Security  
Science and Technology

## **R & D pour la défense Canada**

Chef de file au Canada en matière  
de science et de technologie pour  
la défense et la sécurité nationale



[www.drdc-rddc.gc.ca](http://www.drdc-rddc.gc.ca)

